INFORMATION TO USERS

This manuscript has been reproduced from the microfilm master. UMI films the text directly from the original or copy submitted. Thus, some thesis and dissertation copies are in typewriter face, while others may be from any type of computer printer.

The quality of this reproduction is dependent upon the quality of the copy submitted. Broken or indistinct print, colored or poor quality illustrations and photographs, print bleedthrough, substandard margins, and improper alignment can adversely affect reproduction.

In the unlikely event that the author did not send UMI a complete manuscript and there are missing pages, these will be noted. Also, if unauthorized copyright material had to be removed, a note will indicate the deletion.

Oversize materials (e.g., maps, drawings, charts) are reproduced by sectioning the original, beginning at the upper left-hand corner and continuing from left to right in equal sections with small overlaps.

ProQuest Information and Learning
300 North Zeeb Road, Ann Arbor, MI 48106-1346 USA
800-521-0600

Modeling of Dynamic Friction in Vibration Environment for Heavy Vehicle Load Security

Zhaohui Shen

A Thesis
in
The Department
of
Mechanical and Industrial Engineering

Presented in Partial Fulfilment of the Requirements
For the Degree of Master of Applied Science in Mechanical Engineering at
Concordia University
Montreal, Quebec
Canada

February 2003

ABSTRACT

Modeling of Dynamic Friction in Vibration Environment for Heavy Vehicle Load Security

Zhaohui Shen

Heavy vehicle load security is a very important factor for all road users, and the friction forces arising within the cargo layer and between the cargo and the trailer bed are known to offer definite resistance to the dynamic forces and moments induced by the directional maneuvers, which would affect the load security significantly. A simple load-platform friction model is proposed to study the relationship between the friction coefficients and vertical vibration, and validated with the experimental record from the tests conducted at CONCAVE research center. The dynamic friction coefficient is observed to be a function of the acceleration of vertical vibration and horizontal movement. The vertical vibration has significant influence on the magnitude of friction forces between the mating surfaces. The model further incorporates the load-deck interface friction and vertical trailer vibration, by establishing the vehicle model with dynamic friction model. The dynamic response characteristics of the friction coefficients are evaluated in terms of sinusoidal excitation and random road input. The model is utilized to study the longitudinal cargo movement under breaking maneuvers. The results of the analysis revealed the strong influences of vibration amplitude and frequency as well as deceleration rate on the potential cargo movement. The vehicle parameters are also found to influence the dynamic friction coefficients and resulting cargo dynamics.

Acknowledgments

The author wishes to express his sincere appreciation to his thesis supervisor, Dr. A.K.W.Ahmed and Dr. I. Stiharu for their constant guidance and dedication throughout the realization of this thesis.

Thanks are due to the colleagues, faculty members and students of CONCAVE Research Center, and the Department of Mechanical Engineering for their contribution during the course of this work.

The author also would like to express his special thanks to Dr. Subhash Rakheja and Arlene Zimmerman for their kindly advice and helpful suggestion during the past two years.

Finally, the author wishes to thank his wife, Lanzi, and his mother, Qiugu Li. They have been taking most of his responsibility to the family to support his work during these years.

Table of Contents

LIST OF FIGURES

LIST OF TABLES

NOMENCLATURE

a_L	Lateral acceleration
θ	Pitch angle
λ	Wavelength of sinusoidal road input
δ_{TR}	Static deflection of tire
a_t	Tangential component of lateral acceleration
δ_{TF}	Static deflection of suspension
Ψ	Deck Roll Angle
Φ	Unsprung mass roll angle
y_0	Displacement of Deck Vibration
μ_v	Dynamic Friction Coefficient
$\ddot{x}$	Horizontal Acceleration
$\dot{x}$	Horizontal Velocity
$\ddot{y}_0$	Acceleration of deck vibration
ω	Vibration frequency
σ	Stiffness coefficient
σ_0	Stiffness of Bristles
τ_y	Shear Strength
μ_k	Kinetic Friction Coefficient
μ_s	Static Friction Coefficient

α_i	Unit contact area
μ	Friction coefficient
A	Magnitude of vertical vibration acceleration
A_R	Total contact area
C_s	Equivalent damping coefficient of suspension
C_{SF}	Damping coefficient of front suspension
C_{SR}	Damping coefficient of rear suspension
C_t	Equivalent damping coefficient of suspension
C_{TF}	Damping coefficient of front tire
C_{TR}	Damping coefficient of rear tire
F	Friction force
F_a	Breakaway friction force
F_b	Kinetic friction force
F_C	Coulomb friction force
F_e	External force
f_{n-t}	Natural frequency of unsprung mass
f_i	Unit normal load
F_N	Normal load
f_{n-s}	Natural frequency of sprung mass
F_{SC}	Suspension damping force
F_{SF}	Front suspension force
F_{SF}	Static friction force
F_{SK}	Suspension spring force

F_{SR}	Rear suspension force
F_{TC}	Tire damping force
F_{TK}	Tire spring Force
F_v	Viscous friction force
H_P	Center of gravity height of platform
H_T	Center of gravity height of deck
I	Pitch mass moment
K_s	Equivalent stiffness of suspension
K_{SF}	Stiffness of front suspension
K_{SR}	Stiffness of rear suspension
K_t	Equivalent stiffness of tire
K_{TF}	Stiffness of front tire
K_{TR}	Stiffness of rear tire
L_F	Distance from front axle to CG
L_R	Distance from rear axle to CG
M_C	Cargo mass
M_D	Deck mass
M_s	Sprung mass
M_{SC}	Moment acting on deck by suspension force F_{SC}
M_{SK}	Moment acting on deck by suspension force F_{SK}
M_{TC}	Moment acting on unsprung mass by suspension force F_{TC}
M_{TF}	Front tire mass
M_{TK}	Moment acting on unsprung mass by suspension force F_{TK}

M_{TR}	Rear tire mass
M_u	Unsprung mass
N	Normal load
V	Horizontal velocity
V_{max}	Maximum horizontal velocity
Y	Magnitude of displacement of deck vibration
Z_0	Elevation of ground surface profile
Z_{0F}	Road profile input on front wheel
Z_{0R}	Road profile input on Rear wheel
Z_1	Unsprung mass displacement along Z axis direction
Z_2	Sprung mass displacement along Z axis direction
Z_{left}	Road profile input on left wheel
Z_{right}	Road profile input on right wheel
Z_s	Sprung mass displacement along the Z axis direction
Z_u	Unsprung mass displacement along the Z axis direction

CHAPTER 1

INTRODUCTION AND LITERATURE REVIEW

1.1 Introduction

Highways in US and Canada are widely used by heavy-duty commercial vehicles. The number of trucks on highway has been steadily increasing from year to year. Trucking is at this time the largest and most important means of product transportation in North America. Accidents involving heavy trucks usually lead to serious consequences. While statistics shows a notable reduction in the number of victims over the years, the incidence of the accidents with fatalities remains quite steady over past years. Despite the awareness and security measure imposed by the traffic authority, fatal accidents are mainly attributed to the steady increase in traffic in general, the large number of heavy vehicles on the roads, the lack of understanding of the heavy vehicle maneuverability, the lack of correlation between the road condition and the speed or the type of maneuver.

On average, each year in Canada there are 43,000 collisions involving heavy trucks that kill or injure 12,000 people. Truck safety is particularly important because these large and heavy vehicles share public roads and streets with more vulnerable road users -- pedestrians, cyclists, motorcyclists, bus riders and motorists [1]. Moreover, from the commercial and environmental points of view, any accident with the trucks often involves cargo damage apart from the potential fatalities.

There are many causes that yield to such accidents. Loss of directional stability and controll due to load shift is one of them. The dynamic forces and moments developed

during various directional maneuvers can lead to movement of the certain type of cargo relative to the trailer bed. The dynamic relative movements of the cargo might lead to reduced handling and control limits of vehicle and thus the potential load spills situations. A study by Kusters [2, 3] reported that the majority of rollover accidents in The Netherlands involve articulated heavy vehicles (typically tractor semi-trailer and tractor full-trailer combinations) and occur on highways. These accidents have been attributed to three main causes: sudden path deviation, often in combination with braking from high initial speed; excessive speed on curves; and shift of load under vibration environment. The first two causes also often imply the load shift, which may thus be an important factor that contributes to the loss of stability of the vehicle.

Heavy vehicle designers have implemented many types of load securement mechanisms to minimize the occurrences of load movement or spills. Most of these mechanisms are basically built to resist the dynamic cargo motion and are based on enhancing the friction force at the cargo-deck interface. The friction forces arising within the cargo layers and between the cargo and the trail bed are known to offer definite resistance to the dynamic forces and moments induced by the directional maneuvers [4]. Friction is always present between tiedowns and load, and between the load and truck deck. It is not considered reliable [5, 6], as the presence of water, oil or ice between the load and the deck can all significantly affect the friction. Vertical vibration of the truck deck as a vehicle travels along a road affects the force between the load and the deck as it is likely to effect the available friction force.

When an object is placed in an environment where it is subjected to a steady acceleration, the weight of the object, as expressed by the force between the object and its

support, appears to change. If the acceleration is directed upwards, its weight apparently increases, and so would the total force needed just to move the object. The reverse is true when the acceleration is directed downwards. When the object is in a vibrating environment, it experiences rapid reversals of vertical acceleration. Under such condition, its tendency to slide is not uniform as that under the static loading situation.

While experiments were carried out in some laboratories to fill the lack of reliable database on the friction forces between typical loads and trailer decks, specifically under dynamic vehicular environment, few attempts were made to model the dynamic friction force subject to the vertical vibration. The basic concept of this issue is the correlation between horizontal acceleration and vertical acceleration. Whether an object will slide when exposed to a vibrating environment depends on the probability that the horizontal acceleration will be large enough to exceed the maximum friction force, which is instantaneously modified by the vertical vibration. Any directional maneuver or braking will introduce horizontal acceleration to the vehicle and the load, and the road roughness will produce and transmit vertical vibration to the vehicle deck through tire and suspension. It seems that these two kinds of acceleration appear inherently un-correlated. However, when the vehicle encounters a significant bump, such as a bridge expansion joint or roadway construction joint, or a repair, that is on a curve or in some location, a correlation between the horizontal acceleration and vertical acceleration arise from the roughness of the road may exist. This research thesis is therefore directed towards the modeling of dynamic friction force under vibration environment in application to heavy vehicle load security. The developed friction model is validated utilizing available experimental data. A pitch-plane vehicle model incorporation cargo friction characteristic

is then developed to investigate load security issue under vibration environment. Vehicle-cargo intersections and responses are examined under sinusoidal and random road excitations in the presence of braking deceleration.

1.2 Literature Review on Friction

Relevant literature are reviewed in the following subsections in order to develop the scope of the present investigation.

1.2.1 Friction

From the fundamental characteristics of frictional processes, the great generality of these phenomena is readily conceivable. Indeed, it is hard to imagine any process, whether in nature or in industry, that is entirely free of friction. It appears that only processes of the largest and the smallest dimensions, namely astronomical and intra-atomic motions, can be described without the involvement of friction. However, even this situation might change with a better understanding of the universe on the one hand and of the elementary particles in an atom on the other [7].

The most familiar name in the friction area should be Charles Augustin Coulomb. All students who had their high school physics class know the friction law and friction phenomena connected with this name. G. Amontons, the first scientist who brought the concept of friction in literature through the pioneering work: " De la resistance causée dans les machines" [50], in which for the first time he identifies the problem of friction. Further Coulomb made the most comprehensive contribution to the modern

understanding of friction phenomenon. He established the basic laws of friction and made an attempt to quantify it in a very familiar form $\mu=F/N$ in his work "Théorie des machines simples". He considered that the major factor involved in friction was the interaction of surface roughness. He presented the roughness as though they were like brushes, the bristle on one brush dragging their way through those on the other. Further, he suggested that sliding involved the riding asperities on one surface over the other. It is still customary nowadays to refer to frictional surfaces as rough, and frictionless surface as smooth, which was proved to be false and out of date by J. Desaguliers in his interfacial adhesion theory in 1725. Later, L. Euler assumed that the asperities on one surface could jump part of the way over the gap between the asperities on the other to explain the fact that the friction during sliding is often smaller than the static friction, similar reason can explain the lubrication that reduce the friction by filling the hollows and reducing the effective roughness.

In late 19th century, Hertz developed a contact model that was universally accepted and is still used in modern tribology through study of the contact between two smooth elastic spheres and cylinders. However, there is no smooth surface under microscopy. Bowden and Tabor [13] noted that the real area of contact for rough surface is much smaller than the area predicted by Hertz. They also stated that the majority of contacting asperities deform plastically under the load. Early models assumed that the asperities were located only on one surface. Yamada et al. investigated the case where asperities were located on both surfaces. Chang et al. [63] stated that in contact region some asperities will deform elastically and others plastically.

In 1724, the English scientist Desaguliers proposed the theory on which friction could be explained by the molecular attraction forces between solids. This fruitful idea was confirmed and quantified much later in the works of William Hardy and Tomlinson, but showed its greatest development in the works of B.V. Deryagin. In 1804, J. Leslie, in criticizing the inclined surface idea, suggested that at the contact zones the asperities form "rolls" in front of themselves, which are displaced on relative sliding of the solids. [8]

The pros and cons of the mechanical and molecular theories were discussed for many years. In 1939 Kragelsky combined the two points of view and proposed a theory [8] [9] according to which surface friction has a dual nature and is determined by the overcoming of molecular interaction forces between surfaces and mechanical resistance associated with profile changes in the surface layer.

Bowden and Tabor proposed the concept of the dual nature of friction independently in 1943, but further discarded the mechanical (deformational) component, since in the case of metals it apperas to be too small to be worth considering. They revised the dual nature of friction in 1957 in connection with polymers.

Allowance for the discrete contact between two solids, which is determined by the roughness and waviness found on the contacting surfaces of any solids, lies at the basis of the molecular-mechanical theory of dry and boundary friction and wear.

Low speed friction has long been recognized to play a dominant role in the complex but very important phenomenon of "stick-slip", a name coined by Bowden and Leben in 1940. To describe it, two different coefficients of friction were postulated, the static and the kinetic friction coefficients. Coulomb friction is an example of the latter

and is widely used in mathematical analysis. Although Bowden and Leben gave a thermal explanation of what came to be known as "stick-slip", it was Blok in 1940 who presented the first systematic study of frictional oscillations and established a quantitative criterion for their appearance. Morgan et al. and Sampson et al in 1941 introduced popular technique for frictional oscillation analysis – substitution of assumed characteristics for the damping into the differential equation of motion.

The most known model of stick-slip vibratory motion at present is attributed to B. Derjaguin at al.. He stated that when the static friction force between the two contacting bodies is overcame by the restoring force at the deformed elastic member, relative sliding motion between the two bodies will occur. If relative motion is accompanied by a reduction in the friction force, the sliding body will accelerate until the point where the elastic restoring force and the friction force between the sliding bodies balance each other and deceleration takes place until a new period of stick occurs. The regimes of stick and slip constitute the complete vibration cycle. The explanation of stick-slip motion was based on the instantaneous drop from a constant static friction force to a constant kinetic friction force, which in turn was explained by the difference between the values of static and dynamic coefficient of friction, wherein the static coefficient (μ_s) is larger on account of adhesive bonding, Rabinovicz, [62].

Friction is associated with majority of moving mechanical components. In some cases, such as gears, bearings, seals, etc., friction can be cause of trouble and efforts are made to minimize it. In other cases, such as belt drives, brakes and clutches, joints, etc., it may be desirable and efforts are made to maximize the friction force. For the present research topic, friction can be classified as desirable, and must be modeled accurately to

investigate the load security issue. The following subsection presents a review of literature pertaining to friction models.

1.2.2 Friction Model

Friction models are used in the simulation and design of many dynamic and control system. Surveys by Armstrong-Helouvry [10] and Armstrong-Helouvry et al. [11], addressed most relevant modeling issues. H. Olsson et al. in [12] also summarized many latest friction models in view of friction compensation in control system.

All friction models attempt to capture the essence of the complicated friction phenomena with models of reasonable complexity. The nature of each of the model is quite different. They are either static or dynamic models. They can be described by differential equations, differential algebraic equations or hybrid models that include specific events. There are many different mechanisms that apply to different situation. Construction of a general friction model based on the fundamental physical principles only is not possible at this time. However, approximate models with limited applicability could be applied to certain configurations under specific friction conditions.

In dry sliding, contacts between flat surfaces can be modeled as elastic and plastic deformation forces of microscopical asperities in contact. The asperities each carry a part of normal load N designated by N_i. Assuming plastic deformation until the contact area of each junction has grown large enough to carry its part of the normal load, the contact area of each asperity junction is $a_i = \frac{N_i}{H}$, where H is the hardness of weakest bulk material of

the bodies in contact. The total real contact area can thus be written as $A_R = N/H$. This relation holds even with elastic junction area growth, provided that H is adjusted properly. For each asperity in contact, the tangential deformation is elastic until the applied shear pressure exceeds the shear strength τ_y of the surface materials, after which it becomes plastic. In sliding, the friction force is thus $F_T = \tau_y A_R$, and the friction coefficient becomes $\mu = F_T/N = \tau_y/H$. The friction coefficient is not dependent on the normal load or the velocity in this case. Consequently, it is possible to manipulate friction characteristics by deploying surface films of suitable materials on the bodies in contact. These films can also be the result of contaminations or oxidation at the surface of the material [13].

The friction-velocity relation is application dependent and varies with material properties, contact surface condition, temperature, wear etc. The classical friction model consists of different independent components, such that each one corresponds to certain aspect of the friction force. The main idea is that friction force opposes motion and that its magnitude is independent of velocity and contact area. It can therefore be described as

$$F = F_C \operatorname{sgn}(v) \qquad (1.1)$$

where the friction force F_C is proportional to the normal load, i.e. $F_C = \mu N$. The sign function ($sgn(v)$) is assigned either +1 or −1, depending on the sign of the velocity. This description of friction is termed *Coulomb friction*, as showed in Figure 1.1 (a). The Coulomb friction model does not specify the friction force for zero velocity. It maybe zero or it can take any value in the interval between $-F_C$ and F_C, depending on how the

sign function is defined. The Coulomb friction model has been widely used due to its simplicity.

The theory of hydrodynamics developed in 19th century brought the idea of viscous friction to the friction models through expression for the friction force caused by the viscosity of lubricants [14]. The term viscous friction F_v is used for this force component, which is normally described as:

$$F = F_v v \tag{1.2}$$

Viscous friction combined with Coulomb friction will be dependent on the speed and it could be generally represented as in Figure 1.1(b). An analytical expression obtained from experimental data assuming a nonlinear dependence on velocity yields from an exponential relation and is written as:

$$F = F_v |v|^{\delta_v} \operatorname{sgn}(v) \tag{1.3}$$

where δ_v depends on the geometry of the contact [44].

The fact that the friction force at rest is higher than the Coulomb friction level further revealed that friction at rest cannot be described as a function of velocity only. The concept of that static friction counteracts external forces below a certain level and thus keeps an object from moving was brought into the model [45]. Model involving external force F_e can be expressed in following manner:

$$F = \begin{cases} F_e & \text{if } v = 0 \text{ and } |F_e| < F_S \\ F_S \operatorname{sgn}(F_e) & \text{if } v = 0 \text{ and } |F_e| \geq F_S \end{cases} \tag{1.4}$$

where F_S is the static friction force.

The friction force for zero velocity is a function of the external force and not of the velocity. The classic friction components can be combined in different ways, like

shown in Figure 1.1(c), and any such combination is referred to as a classical model. These models have components that are either linear in velocity or constant. Stribeck [17] experimentally established that friction does not decrease discontinuously as in Figure 1.1(c), but that the velocity dependence is continuous as shown in Figure 1.1(d). The friction force as a function of velocity for constant load is called the Stribeck curve after the work of Stribeck [12]. In particular, the dip in the force at lower velocity is known as the Stribeck effect, as shown in Figure 1.1 (d). A more general description of friction than the classical model is, therefore,

$$F = \begin{cases} F_{(v)} & \text{if } v \neq 0 \\ F_e & \text{if } v = 0 \text{ and } |F_e| < |F_S| \\ F_S \operatorname{sgn}(F_e) & \text{otherwise} \end{cases} \tag{1.5}$$

where $F_{(v)}$ is an arbitrary function, which may look as in Figure 1.1(d). A number of parameterizations of $F_{(v)}$ have been proposed [11].

While static friction models were studied by scientists from different area, a significant interest in dynamic friction model was expressed by the researches.

Dahl [18] developed a dynamic model through several experiments on friction in servo system with ball bearings. He found that the bearing friction behaved very similar to solid friction. Starting from the stress-strain curve in classical solid mechanics, and subject to stress the friction force increases gradually until rupture occurs, Dahl modeled the stress-strain curve by a differential equation. If x be the displacement, F the friction force, and F_C the Coulomb friction force, then the Dahl's model could be written in the form

$$\frac{dF}{dx} = \sigma\left(1 - \frac{F}{F_C}\operatorname{sgn} v\right)^{\alpha} \tag{1.6}$$

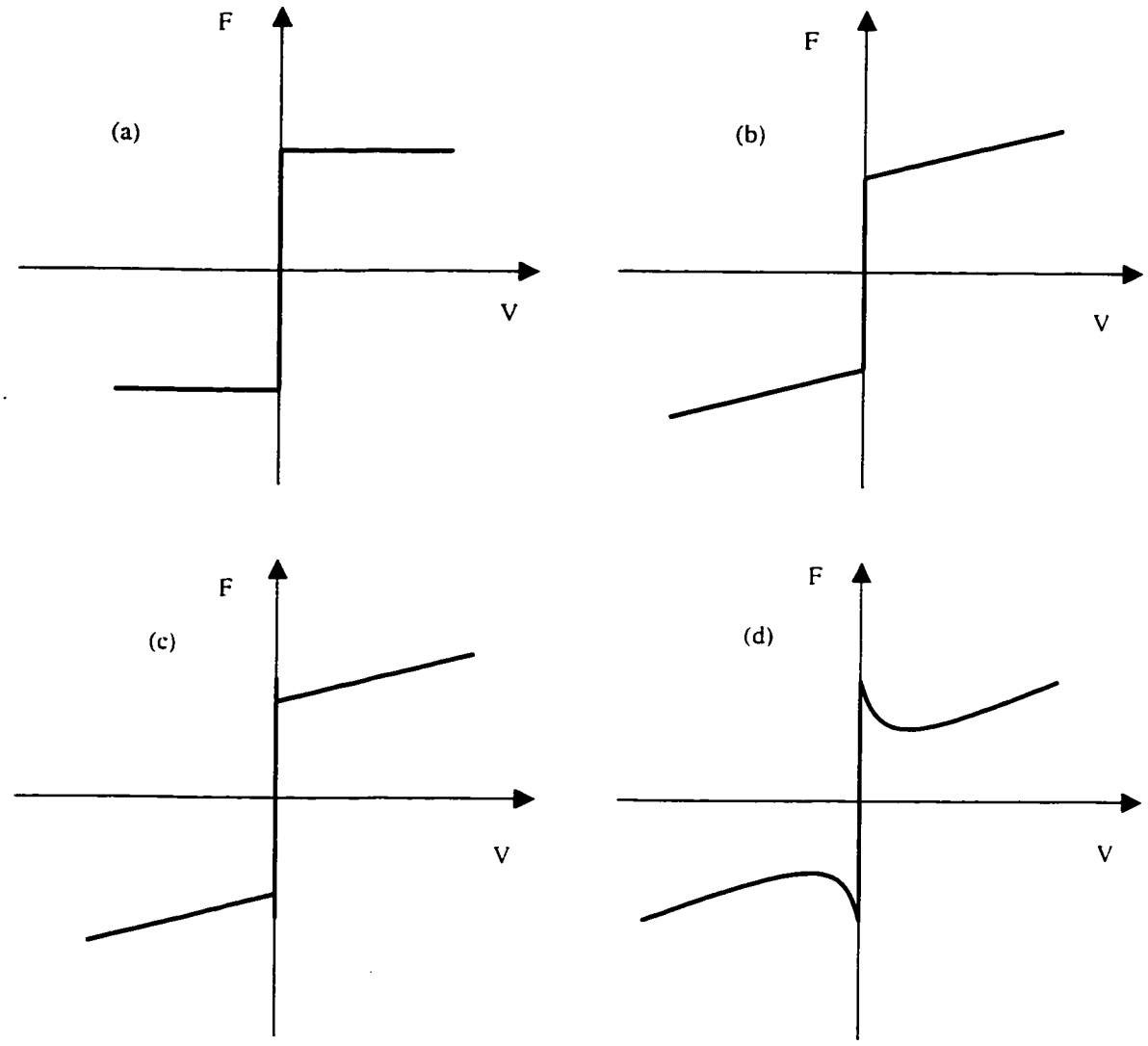

Figure 1.1 Examples of static friction models: (a) Coulomb friction; (b)Coulomb plus viscous friction; (c) Stiction plus Coulomb and viscous friction; (d) friction force with continues velocity dependence [12]

where σ is the stiffness coefficient and α is a parameter that determines the shape of the stress-strain curve. The value α=1 is most commonly used, although $\alpha \neq 1$ may be used to fine tune the analytical results to match experimental data. In this model, the friction force is only a function of the displacement and dependent on the sign of the velocity. This implies that the friction force is only position dependent. To obtain a time domain model, Dahl observed that:

$$\frac{dF}{dt} = \frac{dF}{dx}\frac{dx}{dt} = \frac{dF}{dx}v = \sigma(1 - \frac{F}{F_C}\text{sgn}\, v)^{\alpha} v \qquad (1.7)$$

The model is a generalization of the ordinary Coulomb friction. For the case α=1, the Dahl model (1.7) becomes

$$\frac{dF}{dt} = \sigma v - \frac{F}{F_C}|v|$$

Introducing $F = \sigma z$, the model can be written as

$$\frac{dz}{dt} = v - \frac{\sigma|v|}{F_C} z \qquad (1.8)$$

The "bristle" model is another approach to dynamic modeling introduced by Haessig and Friedland in [48], which attempted to capture the behavior of the microscopical contact points between two surfaces. The number of contact points and their location are random due to the irregularities in the surface. Each point of contact is thought of as a bond between flexible bristles. As the surfaces move relative to each other the strain in the bond increases and the bristles act as springs producing a rise in the friction force. The friction force is then given by:

$$F = \sum_{i=1}^{N} \sigma_0 (x_i - b_i) \qquad (1.9)$$

where N is the number of bristles, σ_0 the stiffness of the bristles, x_i the relative position of the bristles, and b_i the location where the bond was found. When $|x_i - b_i|$ equal δ_s, the bond snaps and a new one is formed at a random location relative to the previous location. The interesting property of the model is that it captures the random nature of friction. The randomness depends on the number of bristles.

Similar to the "bristles" model, the LuGre model is related to the bristles interpretation of friction as in [19]. Friction is modeled as the average deflection force of elastic spring. The bristles will deflect like springs when a tangential force is applied to the bristles. If the deflection is sufficiently large the bristles start to slip. The average bristle deflection for a steady state motion is determined by the velocity. Thus the deflection is lower at low velocities, which implies that the steady state deflection decreases with increased velocity. This model is able to capture the phenomenon through which the surfaces are pushed apart by the lubricant, and confirms the Stribeck's effect. The model also includes rate dependent friction phenomena such as varying breakaway force and frictional lag. The model could be formulated in the following manner:

$$\frac{dz}{dt} = v - \sigma_0 \frac{|v|}{g(v)} z,$$
$$F = \sigma_0 z + \sigma_1(v)\frac{dz}{dt} + f(v) \qquad (1.10)$$

where z represents the average bristle deflection. The model behaves like a spring under small displacement. Further derivation and modification to the model lead the steady state friction force, which has following form for a constant velocity v:

$$F = g(v)\mathrm{sgn}(v) + f(v) \qquad (1.11)$$

The function $g(v)$ models the Stribeck effect, and $f(v)$ is the viscous friction. A reasonable choice of $g(v)$ which gives a good approximation of the Stribeck's effect is:

$$g(v) = \alpha_0 + \alpha_1 e^{-(v/v_0)^2} \tag{1.12}$$

The sum $\alpha_0 + \alpha_1$ corresponds to stiction force and α_0 to Coulomb friction force. The parameter v_0 determines how $g(v)$ vary within its bounds $\alpha_0 < g(v) \leq \alpha_0 + \alpha_1$. A common choice of $f(v)$ is linear viscous friction $f(v) = \alpha_2 v$ as in (1.2), see also (1.3).

The following special case of the model given by (1.10) and (1.12), which includes linear viscous friction and constant σ_1, is called the *standard parameterization*

$$\begin{aligned} \frac{dz}{dt} &= v - \sigma_0 \frac{|v|}{g(v)} z \\ g(v) &= \alpha_0 + \alpha_1 e^{-(v/v_0)^2} \\ F &= \sigma_0 z + \sigma_1 \dot{z} + \alpha_2 v \end{aligned} \tag{1.13}$$

Andreas A. Polycarpou and Andres Soom combined the friction model with dynamics of the sliding system to develop two-dimensional quasi-steady friction models that explicitly include the normal separation of sliding bodies [20, 21]. They used a fifth-order linearized model of sliding system operating in boundary and mixed lubricated regimes to describe the normal dynamic motions of the system. With their model, they obtained accurate estimates of the time-varying friction coefficient (or force) under some specific condition. They found that good results could be obtained when system is excited at other frequencies, away from system resonance. If the system is excited at a frequency near one of the system resonances, the behavior becomes more complex, since system nonlinearities and coupling among motions can result in nonlinear resonances and larger

amplitude dynamic motions that are difficult to describe. The complexity of dynamics of the entire system is likely to limit the applicability of the modeling effort.

The last model introduced above focuses on the relationship between the friction coefficient and vibration. A review of the investigations on friction and vibration will be presented in following subsection.

1.2.3 Friction and Vibration

Historically, efforts to explain friction phenomenon and its relationship with the friction coefficient had driven scientists on the path which inevitably brought them to consider the relationship between the friction and vibration. While more of these studies were focusing on the phenomenon of friction-induced vibration, some other studies were directed towards estimation of the amount of friction force under vibration environment.

A reduction in friction due to normal contact motions during sliding has been observed by Tolstoi et al [22, 23]. They modeled the contact regime between two surfaces as a non-linear spring, using an empirical stiffness relation. Both the model and measurements showed that the friction reduction due to normal vibration could be as large as 30% for various steel surfaces. The friction will induce self-excited vibration, which represented the core of his work. The experimental results of his research proved the existence of natural normal microvibrations whose frequency is determined by the contact stiffness and mass of the slider. He addressed that these microvibrations strongly affect both the magnitude of the frictional force and the stability of sliding and suggested

that low-power forced vibrations at the resonance frequency may sharply reduce the friction.

Godfrey [23] and Sakamoto [24] presented experimental evidence of the reduction in friction for Hertzian contact. Sakamoto also related the instantaneous normal contact deflection to the instantaneous friction coefficient during start-up, under the assumption that the friction force is proportional to the real area of contact. In the later research, Sakamoto et al [25] quantitatively studied the relationship between the friction change and vibration frequency. Their experimental results showed that when the deformation of frictional contact zone is proper elastic, the friction at the vibratory load above 0.1 Hz is lower than at the corresponding static load. When the plastic deformation occurred in the frictional contact zone the friction force gradually approached that of the static load with the increase of the vibratory load frequency and then the effect of reduction of friction by the vibratory load was not any more observed. At any type of frictional contact a vibratory load of extremely low frequency of below 0.01 Hz result in an increase of frictional force. When the deformation in the frictional contact zone is only elastic, a noticeable reduction of friction occurs when the vibration load in conjunction with a frequency above 0.1 Hz is applied. They further found that the extent of friction reduction was determined not only by the amplitude and the frequency of the vibratory load, but also significantly depended on the vibration characteristics of the friction system along the loading direction. Thus, the friction reduction around the resonant frequency is significant [26].

Nayak [27] modeled a dynamic system incorporating a Hertzian contact as a non-linear mass-spring-damper system subjected to broadband random excitation. This work

emphasized the probability of plastic deformation, without examining in detail the change in the mean contact deflection, the contact area or friction reduction under excitation.

Hess and Soom [28, 29] analyzed resonant non-linear normal vibrations as well as the associated instantaneous contact area or friction force under harmonic loads applied to both Hertzian contacts and rough planar contacts using a non-linear mass-spring-damper model. A decrease in the average contact deflection under loading was predicted in each case. Thus, an average of 11% reduction in the overall friction force for Hertzian contacts when the normal vibration amplitude was just below that required to produce momentary loss of contact was recorded. Moreover, Hess, Soom and Kim also studied this phenomenon under the random excitation [30]. They concluded that the decrease of the friction occurs in the mean contact compression under external random loading. When the internal rough surface excitation can be quantified, it will yield to the conclusion that a reduction in the mean value of the contact area and is associated to a decrease in the friction force. Thus it implies that the instantaneous friction force is proportional to the instantaneous area of contact.

Richardson and Nolle [64] studied the static friction coefficients resulting from time-variable tests and variable loading rate through a dynamic loading system. They carried out a series of experiments that concluded that the static friction coefficients at constant high loading rates are constant and independent of contact time. Further, the study suggested that the rate of tangential loading is a major variable affecting static friction in other situations involving time-dependent forces.

1.2.4 Friction on Load Security

Security of loads on heavy trucks is a matter of public safety; as a consequence it has drawn attention both from industry practice and government regulators. A government sponsored project carried out by Billing and Mercer [31] considered that the load security system might be composed of three parts:

1) Friction, which acts between the load and the vehicle, and may also act between the load and other elements of the load security system;

2) Blocking, which prevents movement of the load; and

3) Tiedown assemblies and anchor points, which together secure the load to the vehicle.

In the view of movement of the load, the second and third parts are also connected with the first part. The basic concept of the load movement come from the external force applied to the load overcoming the friction force between the cargo and trailer deck.

Friction is always available when the load is placed on a clean, dry surface, and is tightly tied down to the vehicle. However, these conditions cannot practically be maintained at all time. When load is placed on an icy or snowy surface; if it is placed on a surface contaminated with oil or grease; if it is placed on un-braked rollers, or would be free to roll, or in some other number of possible conditions, the load security depending on friction cannot be guaranteed. [31].

It should be noted that the real function of tiedown assemblies on the load security is realized through increasing the pressure of the load on the vehicle to enhance the friction force between them. Tiredown and friction are therefore not completely independent of each other.

Billing and Lam of MTO (Ministry of Transport Ontario) conducted a series of test to determine the friction coefficients of static and sliding friction between typical truck decks and typical load material for various deck conditions with a steady still deck [32], which belong to a CCMTA (Canadian Council of Motor Transport Administrators) load security research project. The test rig they had used provided a flat bed, to which the test deck was attached. The load was represented by a sled, to which various skidder materials could be attached. The test results shows peak friction coefficients ranged from 0.18 for the machine feet skid to 0.56 for the rubber skid and the corresponding sliding coefficients of 0.15 and 0.54 for the machine feet and rubber skids respectively. One of the parameters examined in their test program was to study the effect of vertical load on the frictional characteristics at the skid-sled interface, and they concluded that the effect of vertical load on the frictional characteristics was insignificant.

The experiment performed by Rakheja et al at CONCAVE were undertaken to characterize the friction forces under vertical vibrations [4]. They used the same contact material combination as MTO did in a series of tests to characterize the breakaway and sliding friction coefficients between loads and deck surface under sinusoidal vertical vibration. The study considered different magnitude and frequency of vibration, normal load and properties of the interface. Unlike the conclusion drawn by MTO test, their results showed that the variation in friction coefficients with changes in the normal load were observed to be strongly dependent upon the relative flexibility of the skid and deck materials. However, the most important conclusion they had is that the minimum value of friction coefficients occurs under the condition of vertical vibration. Their results clearly demonstrated that the minimum values of friction coefficients were observed to be up to

80% lower than the mean values under high normal loads and high magnitude of vertical vibration, and were dependent upon the flexibility of the deck and skid materials. Moreover, the measurement performed under measured trailer vibration, synthesized in the laboratory revealed that the coefficient of friction falls below 75% of the mean value for duration as high as 25% of the total test duration. The results presented in [4] provide useful trends that can be readily used for validation of analytical models. A meaningful load security study should however, include a representation of vehicle system and its dynymics.

1.3 Vehicle Dynamics

The load security of vehicle is concerned with the security of load when the vehicle is in motion, such that the dynamics of vehicle is also very important for the study of load security. The dynamics of vehicle could be defined as the behavior and performance of the vehicle under different road and operating conditions, for example: performance at different velocities under road irregularities and side winds; performance at different velocity under a steering input; as well as performance under braking and acceleration. The analytical study of the vehicle dynamics is based on mathematical model, which effectively represents the vehicle system, identification of performance indices and solution of the mathematical model using an appropriate and suitable tool. The model considered vary widely dependency on the aspect of dynamics and investigation, such as ride, handling, roll, stability, etc.

1.3.1 Vehicle Models

To formulate an adequate mathematical model of a vehicle one must study the mechanicals of tires, suspension and steering since they play the role of intermediate between the vehicle and the road. Validity of a model largely depends on validity of the component characteristics used in the model.

Leonard Segel created the modern automobile control and stability theory by stating that aircraft dynamic stability and control theory was best suited for analyzing automobile behavior, and that previously developed vehicle equations of motion were not as comprehensively effective [33]. He defined handling as the vehicle's yaw, rolling and side-slipping motions resulting from road irregularities, aerodynamics, and driver-applied inputs. The basic feature of handling deals with the driver's evaluation of ease and precision with which a vehicle can be steered into and maintained on a desired path. Segel's vehicle model was a three degree-of-freedom linear dynamic system, which represents the fixed control automobile where the dynamics of tires was neglected. A vehicle-fixed coordinate system was used. Particular road test configuration verified that the analytical solution has excellent match with the experiment.

Okada et al. solved a 7-DOF vehicle model with 63 design parameters by using a polynomial-type empirical tire model in his study of the vehicle response during skidpad and slalom maneuvers, as well as during straight-running motion with wind and steering input [34]. Their reports indicated that the results for the skidpad test above 0.6g were limited by inaccuracies in the tire model and the representation of roll characteristics.

As the most complicated part of the vehicle, tire behavior has been studied for a long time and is still extensively being studied. Ellis introduced different tire model for

the study of cornering forces, which modeled the tire as the stretched string retained by lateral springs while as another model the tread band is treated as equivalent beam supported by an elastic foundation [35]. In general studies of vertical and ride dynamics, tire is often considered as a parallel combination of a linear spring and damper. The cornering properties of the tire depend on the lateral force developed at road-tire interface, which is a function of many factors, such as lateral force, rolling resistance and self-aligning moment. Wong [36] presents simple empirical approach, which can be incorporated in the tire model for simulation of cornering performance.

Another important component that dictates the ride quality and handling performance of the vehicle is the suspension. There are also many different suspension model corresponding to different designs. However, they can be divided into two distinctive categories. The first is the axle suspension where the left and the right wheels are connected by a rigid axle, and the second is the independent suspension in which the left and right wheels are independent. Both of these two suspension model categories always require the evaluation of the equivalent spring stiffness, equivalent damping coefficient, equivalent roll stiffness and the roll center location [35, 37]. While the suspension equivalent stiffness and damping characteristics are often considered to be linear in modeling, nonlinear elements are used in reality to achieve a compromise between ride and handling performances [38, 39].

The mathematical model of a vehicle under steering input could vary from very simple like the three DOF model formulated by Ellis [35] and Wong [36], to very complex ones. The simplest vehicle model for the analysis of the directional dynamics is referred to as a bicycle model where the vehicle mass is situated between the front and

the rear tires. Such model is effectively used to evaluate steady state curving performance of a vehicle, but cannot simulate the roll performance of the vehicle under a steering input. Load security study under handling thus must include a 3-D model or a roll plane model with lateral, roll and yaw dynamics capability. Separate model are commonly utilized for study of ride and longitudinal dynamics. Ride and suspension studies often consider a simple 2 DOF quarter-vehicle model and are inadequate for the study of load security under longitudinal dynamics. In this case, bounce-pitch model with longitudinal dynamics is appropriate and can be utilized to simulate load security under braking while traveling over a rough road.

1.3.2 Bounce and Pitch Dynamics

To study the ride quality of ground vehicle, different ride models have been developed. Figure 1.2 shows a commonly used seven-degree-of-freedom model, which the pitch, bounce and roll of the vehicle body, as well as the bounce of the two front wheels, and the bounce and roll (tramp) of the solid rear axle are taken into consideration. A vehicle represents a complex vibration system with many degree of freedom [36]. It is possible, however, to simplify the system by considering only some of the major motions of the vehicle.

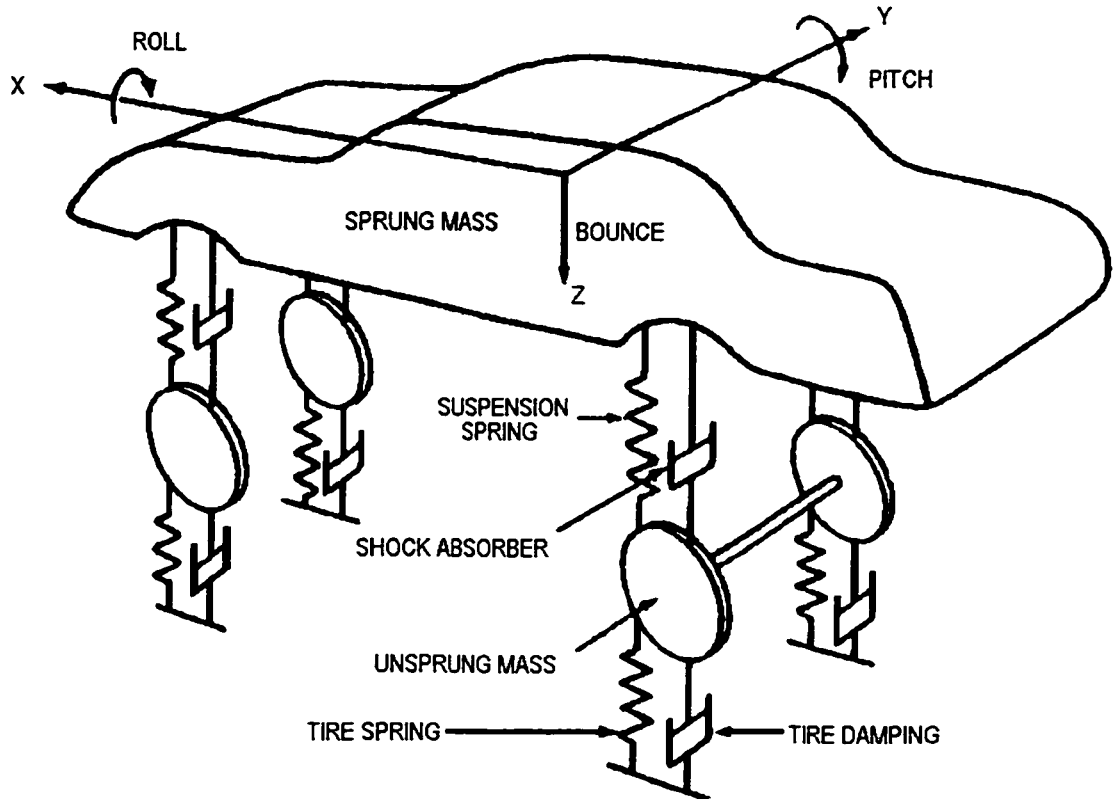

Figure 1.2 A Seven–Degree-of-Freedom Ride Model for a Passenger Car [36]

Many vehicle models ranging from linear quarter vehicle models with two degrees-of-freedom to complex three-dimensional models with as many as 19 DOF have been reported in the literature. Simple one and two DOF of linear vehicle models have been used by several investigators to study the dynamic interaction of the heavy vehicle with the pavement [40]. These models permit the analysis of either bounce or pitch motion under uncoupled vertical motion in a highly convenient manner. Nevertheless, for most vehicles there is a coupling of motions in the vertical and pitch directions, such that there are no "pure" bounce and pitch modes [41]. Since the simple one-dimensional vehicle model cannot be used to predict the complex dynamics associated with heavy

vehicle, a number of comprehensive two and three-dimensional vehicle models have been developed to study the tire force and the ride quality of the vehicle. Analytical models with limited number of DOF, but realistic enough to provide reasonable accurate estimate of the dynamic characteristics are desirable for design and analysis [41] [42]. Many analytical and experiments studies, related to dynamic pavement-vehicle interactions and ride quality, have concluded that the contributions of the roll-plane dynamics of highway vehicles are relatively insignificant [43]. The four DOF in-plane model of a single unit have been demonstrated to effectively yield vehicle's behavior pertaining to dynamic tire loads and ride quality [40] [42].

An appropriate vehicle model for load security study under excitation will depend on the dynamic maneuver to be considered. Since the objective here is to investigate the influence of road excitation on the availability of dynamic friction for load security, a simple bounce-pitch model may be considered. Such model is the most appropriate simple model that can predict the dynamic of load under any combination of longitudinal and vertical excitation.

1.4 Load Security Study

The motorization of the highway system was introduced without any formal consideration of either how the motor vehicle might serve the transportation needs of the people or what effect a change from animal to mechanical power might have on the economy [44]. As automobile accidents increased, manufacturers expanded their support of and influence in the highway safety movement with its emphasis on driver responsibility. Government regulation also has kept on working to ensure the safety of

transportation. While trends in freight transportation are providing increasing pressure on the exceeding minimum regulatory requirements for load security, there are sufficient loads lost each year that enables that this issue still remains a concern to the public, highway safety agencies, truckers and shippers [5] [31].

In 1993, The Ministry of Transportation of Ontario (MTO) prepared a proposal for the research that was circulated to the task force on load security and its parents committee for review [31]. It quickly got wide circulation throughout North America. Many research were carried out in different research center under the guide of this proposal and suggestions for amendment based on the comments received.

In the proposal, three objectives were described, they are:

1) To determine how parts of load security systems contribute to the overall capacity of those systems;

2) To demonstrate the adequacy of parts, and the overall capacity, of load security system;

3) To develop principles, based on sound engineering analysis that could contribute to a revised national standard on load security for heavy trucks.

Mercer and Billing conducted a series of tests in 1998 to determine the force and reactions experienced by vertical stakes, made from various materials with different cross sections mounted in stake pockets [45]. A bending force was applied 1m above, and parallel to the trailer deck in an outboard direction and was increased until the stake material yielded. The tests showed that wood stakes failed abruptly by cracking and splintering, metal channels failed in bending, and tubes buckled.

Billing conducted another series of tests to investigates the friction between some surfaces that are commonly in use in the trucking industry, including effects of dirt, oil, water, sand and roughness on the surfaces [5] [32]. Their purpose was to determine the coefficients of static and sliding friction between typical truck decks and typical load material for various deck conditions with the deck static. Their study assessed the role that friction plays in load security. Based on the these testes, S. Rakheja, P. Sauvé and D. Juras conducted a series of experiments to characterize the friction force between typical trailer deck and load under both static and vibrated environment [4].

Many research focus on the strength and capability of securement devices. It is clear from other evidence that the problem of inadequate cargo securement goes far beyond failure of trailer securement devices and consequent release of massive, dangerous cargo. Many crashes of commercial vehicles can be traced directly to shifting cargo, which dramatically changes vehicle rollover threshold, for example. Although in some instances these crashes are due to either poor maintenance and/or improper deployment of securement devices, in other instances they directly result from the failure of securement devices themselves because of inadequate strength, especially under the elevated dynamic loads created by crash deceleration [46]. Romerot et al presented a simple model in [47] to study the load –securement properties of indirect tiedowns under a longitudinal deceleration. He expressed the elasiticty of the tiedown with an equivalent stiffness as a function of the material properties, tiedown angle, initial tension and cargo geometry. A further study incorporating the model and the effect of load-deck interface friction and vertical trailer vibration revealed that the strong influence of cargo-deck friction is dictated by the vibration amplitude, tiedown material and tiedown angle on the

potential cargo movement. The initial tension is also found to influence the effectiveness of the restraints.

1.5 Scope of the Thesis

The overall objective of this dissertation research is to create a dynamical friction coefficient model for the study of load security of heavy vehicle. The specific objective of the dissertation research is to integrate the friction model with the vehicle model, and analyze the friction response under vertical vibration condition. A simulation connecting the dynamic friction coefficient response and the vertical vibration input is established to study the performance, where friction force is considered as the primary load security contribution for a specific loaded truck. The detail objectives of this study are:

1. Develop friction model for load on platform under vibration environment, and utilize existing database for validation of the model. Formulate the analytical friction model as function of contact material properties, acceleration of vertical vibration, and horizontal acceleration.

2. Develop appropriate vehicle model for study of load security issue under road induced vibration environment.

3. Study the response of dynamical friction model and load security during braking of the vehicle under sinusoidal road excitation.

4. Evaluate the influence of random road excitations on the load security during braking.

5. Evaluate the influence of the suspension parameters on the security of the load during braking of the vehicle under sinusoidal road excitation.

1.6 Layout of the Thesis

In Chapter 2, a load-platform dynamic friction coefficient (DFC) model was proposed, and the simulation results were compared with the experiment record for the validation. The experiment record has been collected from the laboratory tests conducted at CONCAVE center.

In Chapter 3, three kinds of vehicles model were created. The first is a bounce-roll model, which studied the combined effect of the bounce and roll motion on the vehicle deck surface. The second and third models are created in the vehicle pitch plane. The second model is a simple 2-degree-of –freedom model, while the third model is a 4-degree-of-freedom model with the pitch motion. Horizontal forces were discussed in corresponding section. A transmissibility study of the later two models was used to predicte the most dangerous area for the friction force under the vertical vibration.

In Chapter 4, the vehicle models with DFC model created in Chapter 3 were used to simulate the behaviors of the load and vehicle subjected to sinusoidal excitation to study the response of the DFC model. A simulation of braking maneuver was carried out

with the quarter vehicle-DFC model. Different deceleration rate were utilized to study DFC performance and the trend of cargo sliding. A parametric study is also carried out to examine the influence of various suspension parameters on the dynamics of cargo.

In Chapter 5, attempts are made to study the response of the quarter-vehicle DFC model under random road excitation and braking on a specific road condition. A study of the braking performance was done by simulating the same model under a specific road excitation input.

Chapter 6 presents the major contributions of the study together with the major conclusions and future recommendation.

CHAPTER 2

FRICTION MODEL AND VALIDATION

2.1 Introduction

Friction clearly plays an important role in the interaction between load and vehicle. Unsecured cargos on the deck of ground vehicle are held in position by friction while the vehicle performs smooth braking or accelerating. The cargo would rest on the deck of the vehicle as long as the inertia force induced by the maneuver at the cargo c.g. would not exceed the friction force.

Since friction is very much dependent on the surface condition at the interface of the bodies, (i.e. the surface of the load and the deck), water, oil or ice or any other third material between the two surfaces would seriously affect the maximum value of the friction force and thus the capability of the cargo to withstand the vehicle maneuvers. Further complexity is introduced as the vehicle is subjected to vibrations transmitted from the road roughness through the suspension to the deck. The vibration induces vertical inertial force to the cargo. The inertia force will modify the normal force at the deck vehicle interface and thus, the friction force.

For the two reasons above, strong views point out towards not using the friction alone as an effective load securement. It is quite apparent, however, that friction may play a major role in the effective security of many loads. It has been therefore considered necessary to understand the magnitude and role of friction in load securement. [5]

In this chapter, a Load-Platform model is proposed to analyze the friction force responses under both static and vibrated foundation, based on the classical dynamics theory. The dynamic friction coefficient model derived to study the dynamic friction performance for the load position under vibration is validated against available data obtained from experiments conducted at the CONCAVE Research Center Laboratory [4].

2.2 Load-Platform Model

The load-platform model is developed to establish an analytical tool for simulation of friction between load and platform under vibration environment. The model is established based on general friction model aspresenting in the following subsections.

2.2.1 General Friction Model

Frictional is a phenomena defined as two bodies in mutual contact with tendency for relative motion, exert retarding force on each other. These forces are called frictional forces, and phenomena involving such forces are called frictional phenomena. [7] The physical mechanism underlying the friction processes is very complex. In dynamics, the friction is the most frequently encountered case of nonconservative force, thus it cannot be represented by means of a potential function in a manner analogous to the presentation of conservative forces. If a body rests on a horizontal solid base and an external force is applied parallel to the surface of contact, the body will not move until a certain threshold of the force is reached. The cause of these phenomena is obviously friction, and it means that friction force could be encountered even if the relative velocity is zero, which is so-

called static friction. Obviously, there is no work expended against such friction force, since the relative velocity, and the relative displacement, are zero. From the equilibrium point of view, the friction force is equal to the instantaneous external force acting on the mass, till the value of maximum static friction is reached. If the external force F_e will exceed the static friction force F_{SF}, the mass m will commence moving with uniform acceleration:

$$a = \frac{F_e - F_{SF}}{m}$$

Coulomb stated that the friction is dependent on kind of material in contact and is independent on the area of contact, load or relative speed between the bodies. However, the inter dependencies between the physical quantities that intervene in friction is much more complex than the basic enouncement of Coulomb.

The merit of Coulomb friction of Coulomb friction law is in providing a non-dimensional friction coefficient that relates friction to the normal load. Two different friction coefficients are always associated to the friction phenomena:

------The static friction coefficient μ_S which indicates the ratio of the friction force by normal force when a body change the states from the rest to motion;

------The kinetic friction coefficient μ_K which relates the friction force to the normal force while the body is in motion.

The static friction coefficient is always higher than the kinetic friction coefficient. At very low speeds, alternately motion followed by short period at rest phenomena is known as stick-slip condition. The stick-slip is a complex phenomenon, which is still difficult to explain. However, simplified models of the complex physical phenomenon have been successfully attempted.

There are several study and explanation concerning about Stick-slip [48]. Karnopp defined a zero velocity interval, $|v| = DV$, in the model that he developed to overcome the problem with zero velocity detection and to avoid switching between different state equations for sticking and sliding. Depending on if $|v| < DV$ or not, the friction force is either a saturated version of the external force or an arbitrary static function of velocity. The internal $\pm DV$ can be quite coarse and promote so-called stick-slip behavior. [58]

Based on the models, the assumption that a slide-free mass M is pulled through an interposed spring K_s such that the free end of the spring moves at a constant speed V_s would yield reasonable approximation to the real phenomena. Figure 2.1 illustrates such a situation where the force developed by the spring is easily measured.

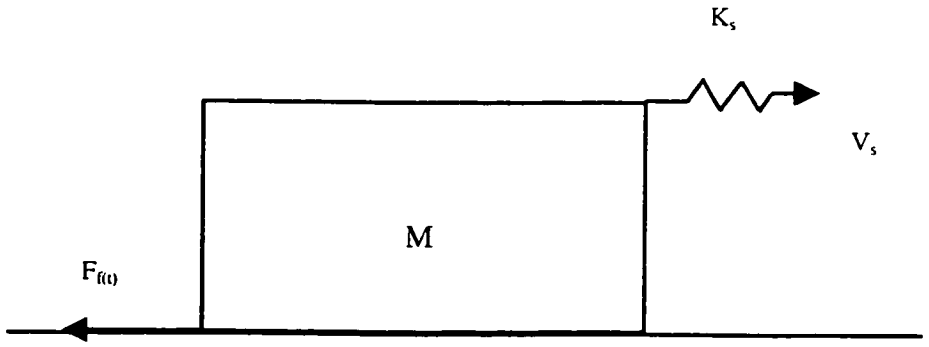

Figure 2.1 Friction model of a mass sliding on a horizontal surface, with time dependent pulling force

Assuming that sliding starts with the spring at its natural length, the spring force initially increases linearly with time while the block is stationary. When the spring force

reaches a critical value *Fa*, the so-called static friction force, the block starts to move. The motion is either of the steady type as in Figure.2.2a, in which case the spring force equals the kinetic friction force *Fb*, or else stick-slip motion occurs, where the block motion alternates between stick and slip, as illustrated in Figure 2.2b. In the latter case illustrated in Figure 2.2c, the kinetic friction force cannot be directly deduced from the stick-slip oscillations. It is experimental observation that stick-slip always disappears if the spring is stiff enough, or if the sliding velocity *Vs* is high enough, as illustrated in Figure.2.3

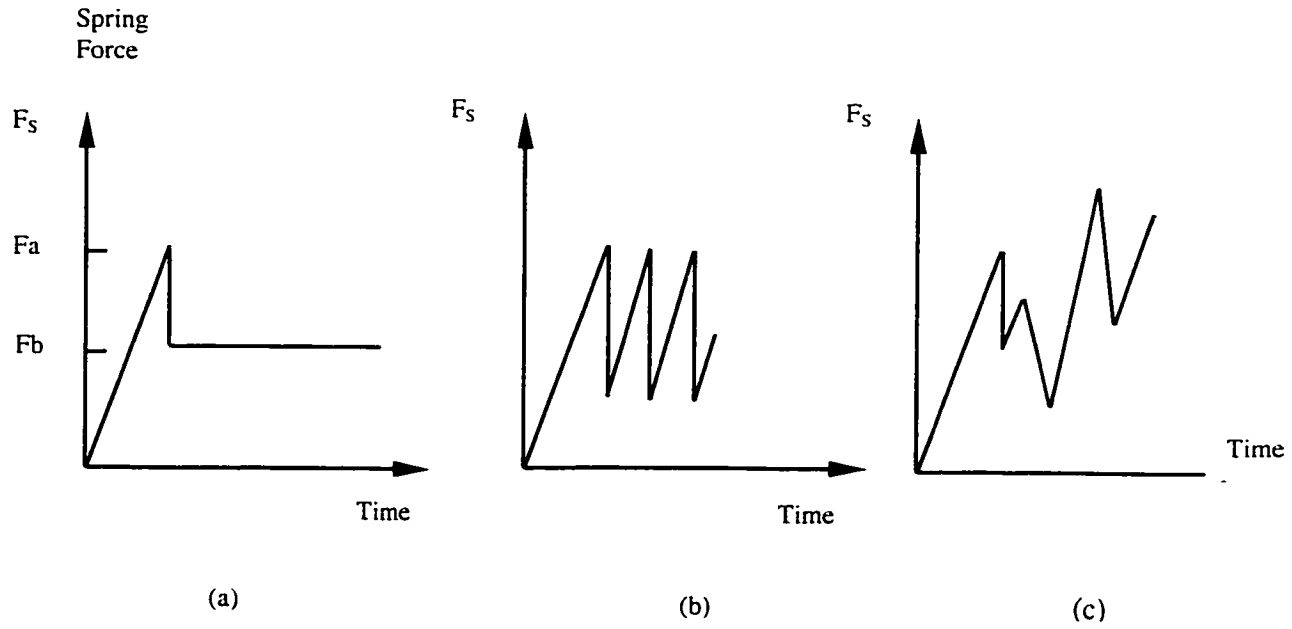

Figure 2.2 Time dependent friction force under the assumption of constant speed at the free end of the spring

Generally, the friction force as a function of time under the constant velocity sliding condition exhibit a constant friction coefficient, as show in Figure.2.4, such that most kinetic friction coefficients are derived from such kind of experiment.

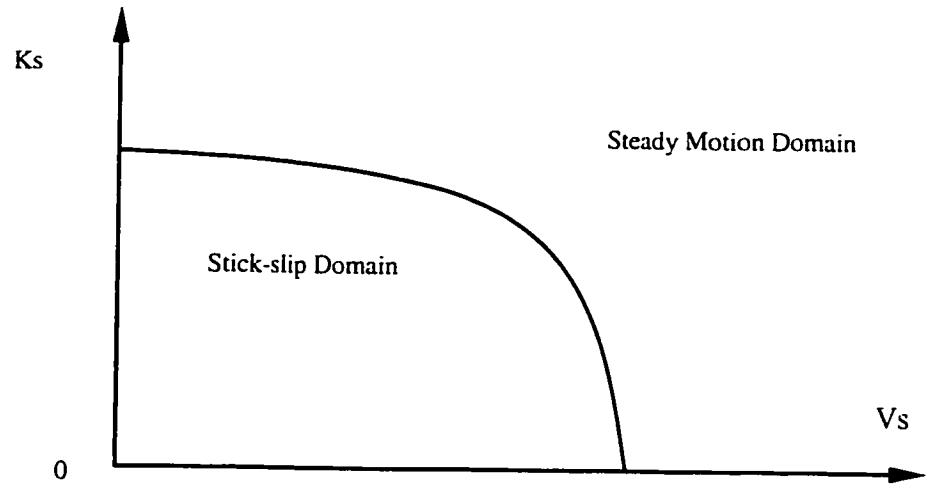

Figure 2.3 The Occurrence of the stick-slip --- For high stiffness of the spring

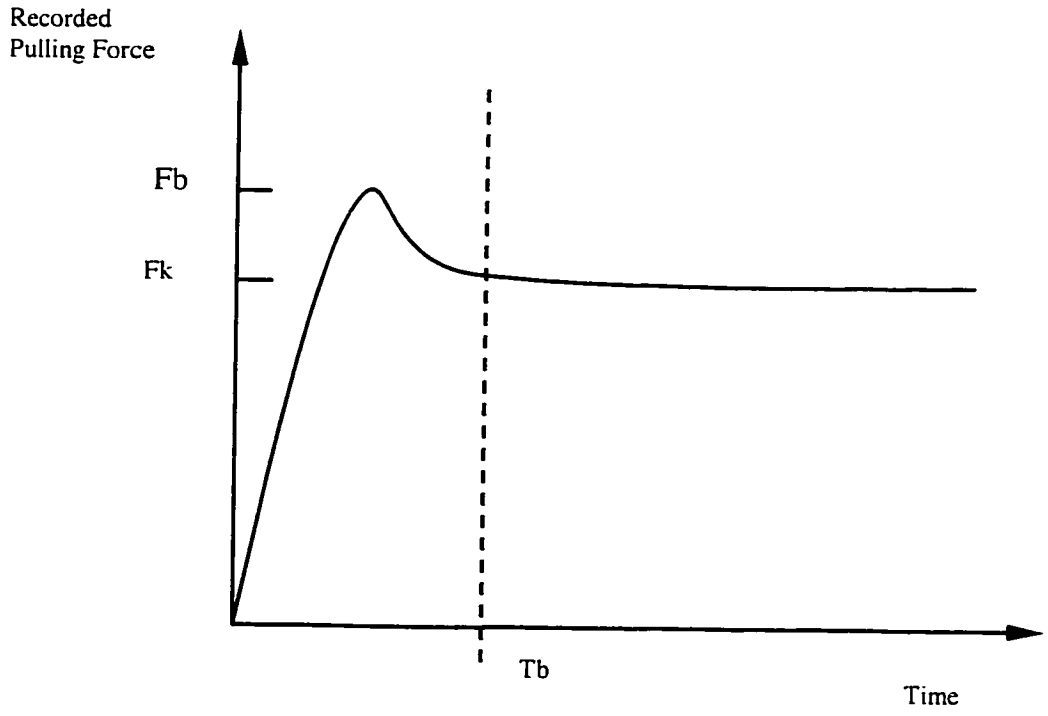

Figure 2.4 Recorded pulling force represent two friction force: Breakaway Friction and Kinetic Friction

The friction force is indirectly measured, and there is no way to measure the friction force itself directly. In most experiments, the friction force exerted on a body in uniform motion is measured by determining the value of an applied force on the body to promote the motion that is equal to and opposite in direction to the desired friction force. As illustrated in Figure.2.4, the friction force is represented by the record of the applied external force. The force after a time *Tb* becomes constant, and the friction coefficients μ_k can be determined from the value of the force and the normal component of the weight. The force before time *Tb*, reaches its maximum value, which occurs in the moment of the moving, and it is also called breakaway friction. The accuracy of the breakaway value is dependant on the sensitivity of the experiment apparatus, mainly the bandwidth of the load cell and sampling rate of the recording instrument. Based on the above considerations and taking into account the interest of assessment of friction of bodies under vertical vibration, a matching model based on the dynamic behavior of the rigid mass will be proposed to fit the experimental results obtained by the research team at CONCAVE. The cause of friction and stick-slip will not be considered in the proposed dynamic model.

2.2.2 Load-Platform Model

Figure. 2.5 illustrate the FBD (Free Body Diagram) of a rigid mass subjected to a pulling force. Assuming that during the sliding period, the horizontal velocity is constant, friction force f will be equal and heading in opposite direction with external applied force F_e.

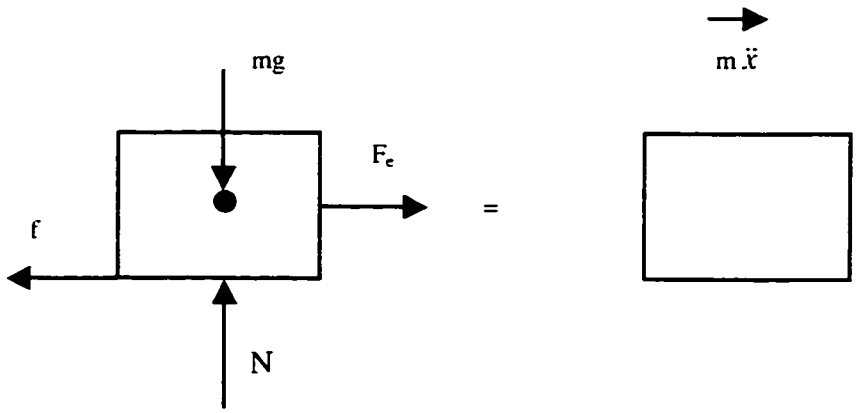

Figure 2.5 The free body diagram of a rigid mass pulled by a force *F* and subjected to a friction force *f*

Appliing Newton's second law, the equation of motion for the system is:

$$F_e - f = m\ddot{x} \qquad (2.1)$$

Where F_e is the applied force, f is the sliding friction force, which is based on the friction law and is proportional to the normal load weighted by a coefficient μ_k, and $\ddot{x}$ is horizontal acceleration of the sliding mass. Further in the friction experiment, F will be used to evaluate the friction force while the acceleration $\ddot{x}$ during the sliding period will be assume as zero. Equation (2.1) can therefore be rewritten as:

$$F = f + m\ddot{x} = \mu_k N + m\frac{d\dot{x}}{dt} \qquad (2.2)$$

If relation (2.2) is used to model the variation of the friction force during motion of the mass, from the static condition at a constant sliding speed, implies that the breakaway friction force would be the sum of the sliding friction and the inertia. Consequently, the acceleration will affect the breakaway friction. Assuming that a pulse

signal is employed to represent the speed, the setting time of the pulse signal could be adjusted to fit the measured acceleration.

If the sliding just occurs under static conditions on a horizontal surface, N in (2.2) is just equal to the weight of the mass. As mentioned before, the main point of this thesis is to develop friction model under vertical vibration environment,

It has been noticed that, the friction forces are significantly affected by the vibration environment encountered in freight vehicles. The inertial forces developed by the vibration of the load influence the magnitude of dynamic friction forces within the load layers, and between the load and the trailer bed surfaces. The influence of vertical vibration on the friction force can be demonstrated through the example of a solid sliding on a rigid surface, shown in Figure.2.6. When a solid mass "m" is subject to a periodic vertical acceleration $a(t)$, the normal force N is related to the acceleration of the following manner:

$$N=m(g-A\sin\omega t) \qquad (2.3)$$

where A is the magnitude of vertical acceleration, and ω is the frequency of vibration. The instantaneous friction force, assuming ideal friction of a constant friction coefficient μ, can then be expressed as:

$$f(t)=\mu m(g-A\sin\omega t) \qquad (2.4)$$

where $f(t)$ is the instantaneous friction force and is time dependent . From equation (2.4), it is obvious that the instantaneous friction force is different from the friction force measured under static conditions ($f_0=\mu mg$), and is dependent upon the magnitude and direction of the vertical vibration. The vehicle vibration imposing downward acceleration

on the load can lead to significantly lower instantaneous friction forces, which may influence the effectiveness of the load securement in an adverse manner [4].

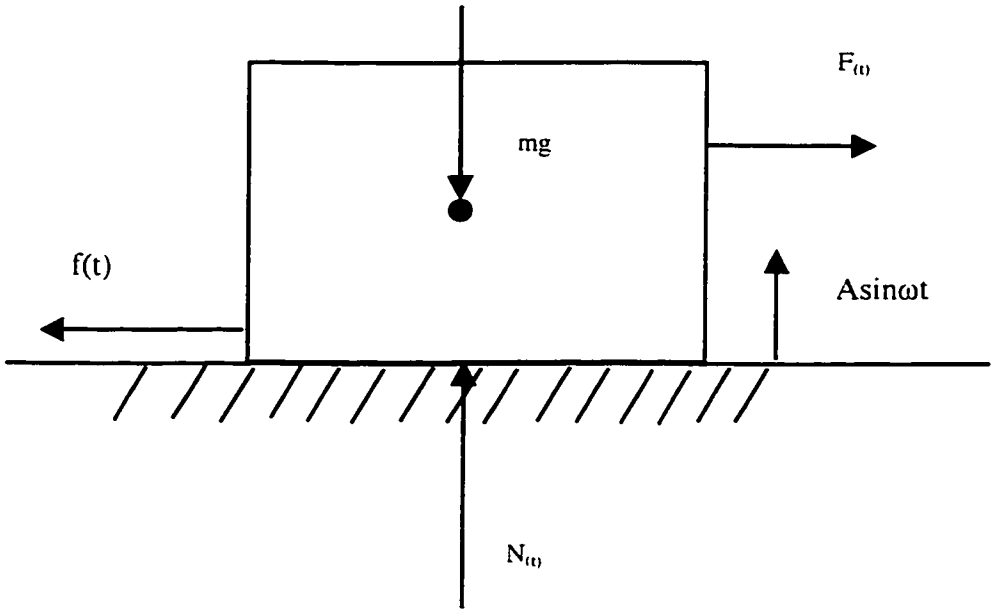

Figure 2.6 FBD of a solid mass subject to a vertical vibration

Relationships (2.2) and (2.4), set the friction model under vibration environment and can be combined to yield:

$$F = \mu_k (mg + m\ddot{z}_0) + m\frac{d\dot{x}}{dt} \qquad (2.6)$$

where $\ddot{z}_0$ is the acceleration of the vibration induced from the surface of the deck. According to the experience, the second term $m\frac{d\dot{x}}{dt}$ is effective only during initial period of the motion when the longitudinal acceleration $\frac{d\dot{x}}{dt}$ is not zero. After the mass gained certain speed, the only factors that affect the friction force is the sliding friction coefficient and the normal load.

The friction model can be readily compared with experimental results obtained at CONCAVE. For this, however, it is essential to first formulate the analytical model to match the input and response that are similar to that of the experiment.

2.2.3 Friction Model for Validation

A model of the friction phenomena will be developed to study the performance of the above friction model. The correctness of the model will be validated against the results of the test carried out at CONCAVE laboratory.

The test fixture of the CONCAVE experiment is as showed in Figure 2.7. A large mass was resting on a rigid support that was fixed to two synchronized hydraulic actuators that could induce a vibratory input with frequencies ranging from 0.3 to 150 Hz. The instantaneous load on the deck can be measured and recorded through load cells. Another hydraulic actuator articulated on the support of the load could pull the load on the deck. LVDT is used to build a position feed back in the hydraulic system of the horizontal actuator. The load is instantaneously measured and recorded. The friction force is measured as the pulling force at constant speed controlled through LVDT. The ratio of the friction force to the load is treated as the instantaneous friction coefficient μ_K. The constant speed in the experiment is obtained the application of pseudo-rectangular wave pulse of finite rising time.

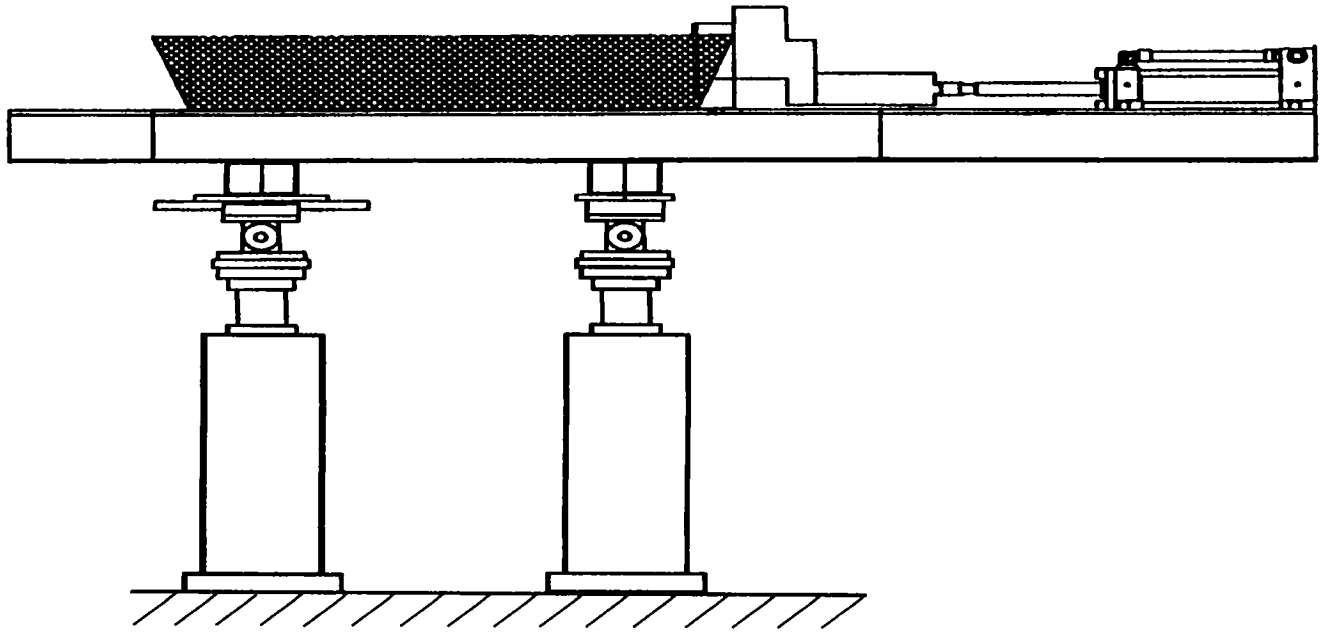

Figure 2.7 Test fixture of CONCAVE laboratory [4]

A rounded step displacement input is thus adapted to model the rectangular pulse for the simulations. Convenient way to express the rounded step is through a general function expressed as: [49]:

$$x(t) = X_{max}[1 - e^{-\gamma\omega_0 t}(1 + \gamma\omega_0 t)], \quad t > 0 \qquad (2.7)$$

where e=2.71828, X_{max} is the maximum input displacement and γ is the severity parameter, defined by

$$\gamma = \frac{\pi}{\omega_0 \tau_l}$$

and τ_l is the time required for the displacement to reach its maximum value. Figure.2.8 illustrates several rounded step signal for different severity factor values.

The function presented in Equation (2.7) can be easily adapted to simulate the rounded pulse input for the model. A rounded pulse velocity input that will provide a constant speed of 1 inch/sec for a period of 2 seconds with rest period of 2 seconds between pulse can be expressed as :

$$V = \begin{cases} V_{max}[1 - e^{-\gamma\omega_0 t}(1 + \gamma\omega_0 t)] & 0 < t < 1 \\ V_{max}\{[1 - e^{-\gamma\omega_0 (2-t)}[1 + \gamma\omega_0 (2 - t)]\} & 1 < t < 2 \\ 0 & 2 < t < 4 \end{cases} \qquad (2.8)$$

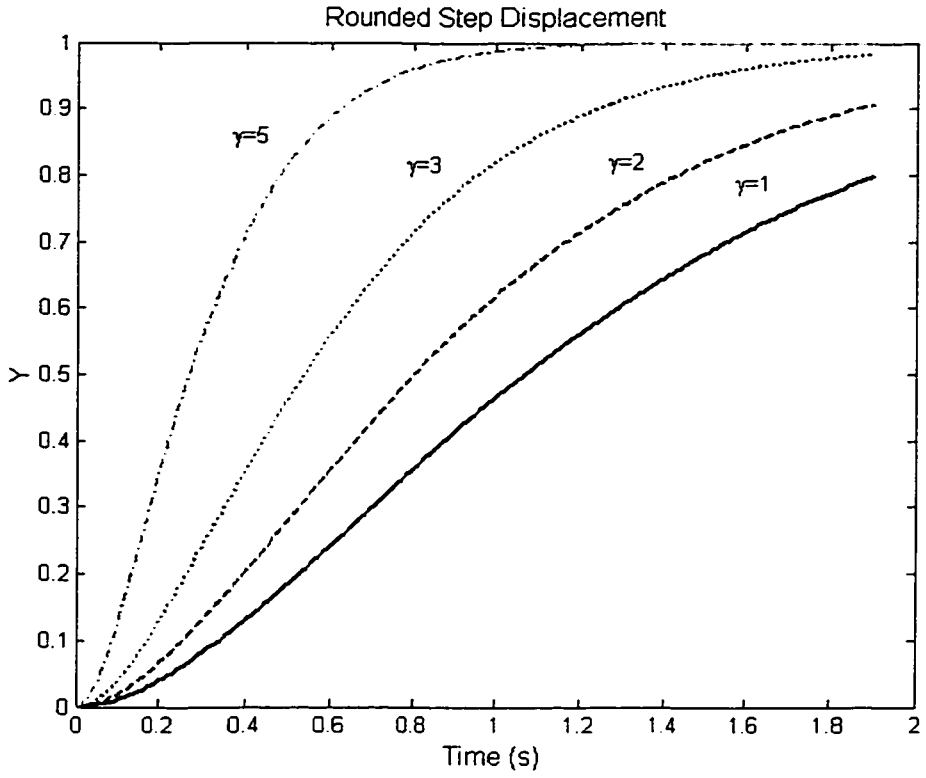

Figure 2.8 Rounded step displacement signal with different severity value γ

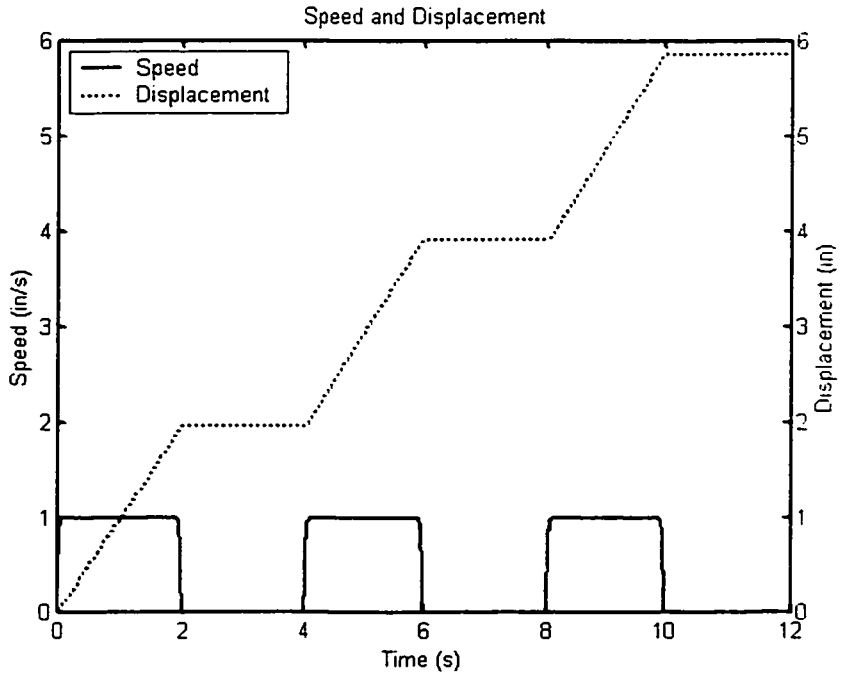

Figure 2.9 Simulated displacement with pseudo-speed signal

If repeated for n times, an n-cycle speed signal can be created; Figure.2.9 illustrates the speed signal and the integration of the speed, which is the displacement of the mass. These results represent a rise time for velocity equal to 0.05 second.

2.3 Experimental Studies and Results

Due to the lack of standardized test methods and highly nonlinear dependency of localized rubbing friction on various materials and environment factors, considerable variation could be observed among the values reported by different researches about friction coefficients on different sliding surface under static conditions. Moreover, while the friction coefficients between different surfaces have been reported extensively for vibration free environment, the influence of vertical vibration on the friction coefficients had not been reported. In view of the lack of this knowledge, and upon recognition of the significance of vehicle vibration in relation to the load securement, a series of experiments were carried out at CONCAVE Research Center to characterize the friction force under vertical vibration. The specific objectives of the study include characterizing the breakaway and sliding friction coefficients between selected loads and deck surfaces in a vibration free and with vertical vibration environment. The setup of the experiment and parts of the results will be introduced in this section for the validation of the model.

2.3.1 Experiment Set-up

The test fixture comprised a deck structure and a horizontal hydraulic actuator, as shown in Figure 2.7. The selected deck material was installed on the frame structure. The different skid materials were attached to a steel sled, which was placed on the flat deck surface. The skid materials representing steel pads and machine feet were directly attached to the sled, while the materials such as rubber, paper and plastic were attached to the smooth bottom surface of the sled. The study of concrete skid surface was performed by the concrete block directly on the deck surface. A hydraulic actuator was mounted horizontally on the frame to generate the necessary pull force. A compression-tension force transducer, mounted to the actuator piston rod, was coupled to the sled. The frame structure with the hydraulic actuator was installed on two electro-hydraulic vibration exciters. The software generated the position signal for the horizontal pulling actuator at a rate of 2.54 cm/s through the output board of a computer. The software was developed to generate the position command signal to create a series of 5 pulls (5cm each), where each pull occurred over a duration of 2s. The command signal also allowed a rest period of 2s between the successive pulls. The command signal was filtered through a low pass filter with cut-off frequency of 2 Hz and trigger signals were embedded to synchronize the motion of all the horizontal and vertical exciters. A multi-channel data acquisition board and associated software were configured to record the vertical acceleration, friction force, horizontal actuator displacement, and the displacement of two vertical vibration exciters.

Experimental results were obtained for different sets of surfaces under static platform and for platform under vertical vibrations. Selected results for static and dynamic cases are summarized under the following subheadings.

2.3.2 Experimental Result (Static Platform)

The measurements were initially performed in a vibration free environment in order to establish the breakaway and sliding friction coefficients between the selected skid and deck materials. These measurements provided the essential data to study the influence of vertical vibration on the coefficients of friction. Figure.2.10 illustrates the time history of friction forces and the horizontal displacement measured with one of the selected skid and deck materials combination, in which the deck is X-Groove Aluminum, and the skid is Concrete, while the normal load is 18011N.

The data acquired during pulls #2, 3, and 4 were adjusted to account for the residual forces. The breakaway friction forces measured during the pulls were extracted. The measured data revealed oscillations in the sliding friction force, which are most likely attributed to micro variations in the surface, transients following the breakaway, and signal noise. The mean sliding friction force corresponding to each trial was derived through the average values of sliding friction force data. The breakaway and average sliding friction forces derived corresponding to each trial are normalized with respect to the vertical load to determine the breakaway and sliding friction coefficients, μ_0 and μ_s, respectively. In this case, the two values are found as:

μ_0=0.565

μ_s=0.472

For relatively smooth contact surfaces, hardwood and plastic, the friction coefficients under a normal load of 1980N were obtained as:

μ_0=0.225

μ_s=0.150

2.3.3 Experiment Result (Vibrating Platform)

The measurement of the Dynamic Friction Coefficient (DFC) was carried out using the same apparatus used for static measurement. The sinusoidal vibration signals were generated using a multi-channel signal generator coupled to the servo controller to induces the vibration to the platform. The horizontal position of the load is monitored through a LVDT connected to the data acquisition system.

Although the study of friction forces under representative vehicular vibration are considered to be most relevant to the load security issue, a study under deterministic vibration is vital to gain an understanding of the important trends.

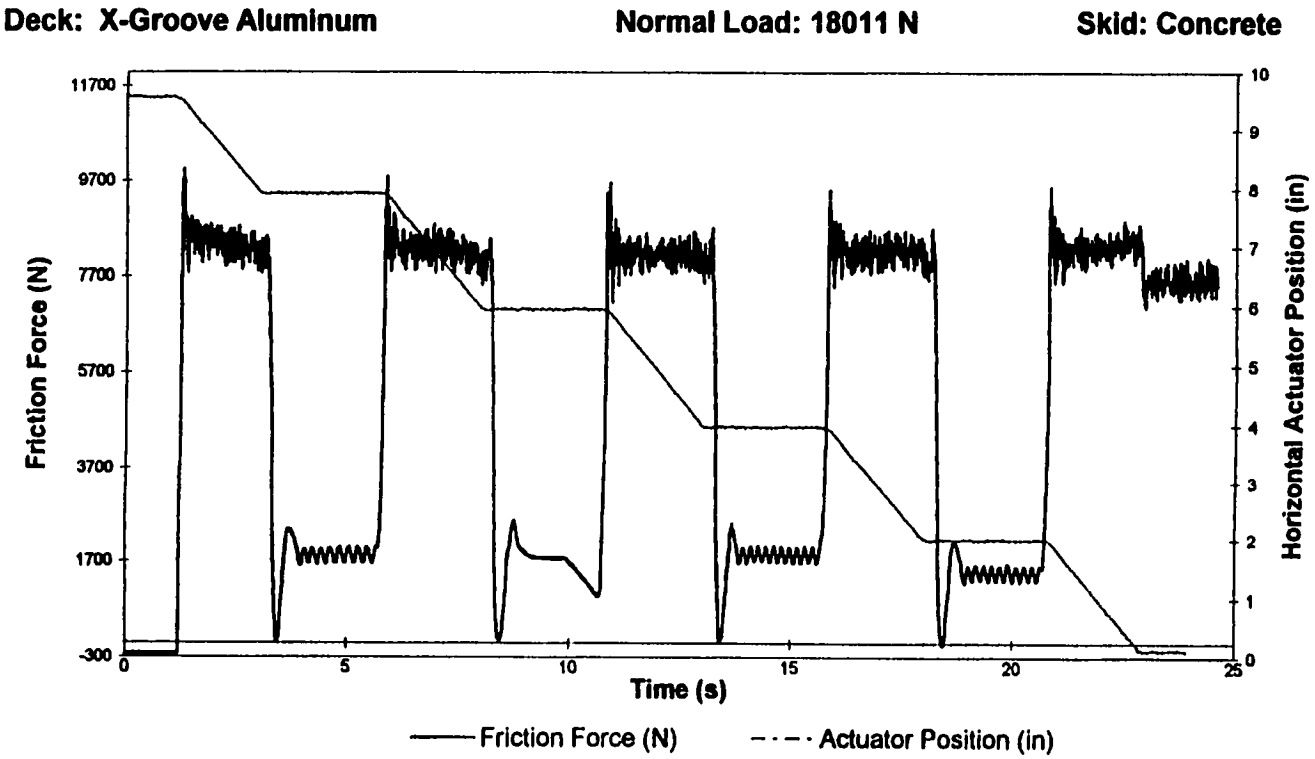

Figure 2.10: Time history of the friction force and load displacement under static condition from experiment result [4]

Figure 2.11 illustrates one of the measured friction forces time history under vertical acceleration excitation for plastic skid on smooth hardwood surface. This run represents vertical excitation of 0.25g at a frequency of 1.0Hz. The measurement reveals considerable oscillations of the friction force, which are mostly attributed to stick-slip phenomenon occurring during each cycle of vibration. While the breakaway friction forces were observed to be quite apparent in some of the measurements, other measurements did not reveal distinct breakaway. Most experiment, however, revealed breakaway corresponding to lowest instantaneous vertical acceleration. A series of experiments were carried out under sinusoidal excitation for a range of frequency and excitation amplitudes. The following subsection summarizes the results in the form of frequency analysis.

2.3.3.1 Frequency Analysis

In the experiment, the friction force and acceleration signals acquired under vertical vibration at different discrete frequencies were filtered to eliminate the high frequency components arising from the coupled dynamics of the sled and the deck, and the stick-slip motion. The filtered data was then analyzed to determine the mean, maximum and minimum values of DFC ($\mu_v=F/mg$), as a function of the mating surface, magnitude of vertical vibration and frequency of vibration. Some results are reproduced in Figures 2.12 and 2.13.

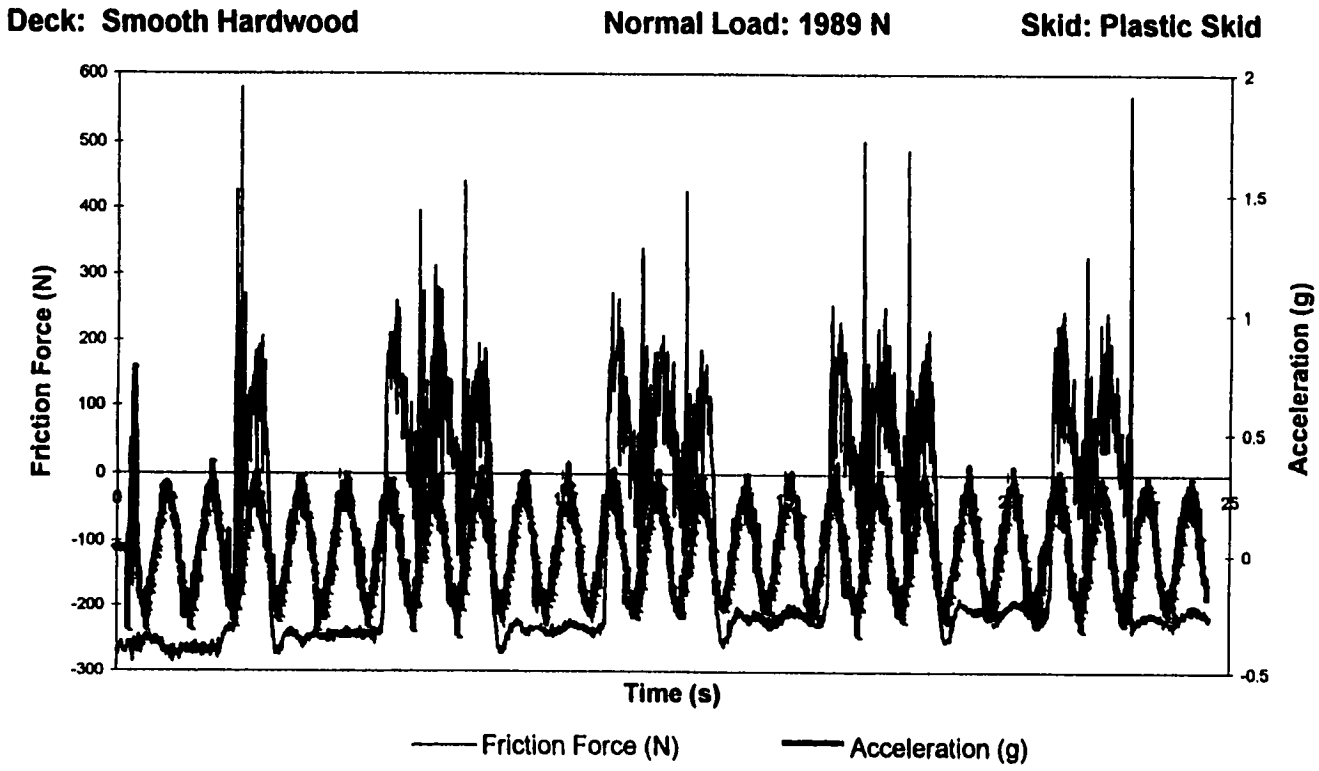

Figure 2.11: Time history of vertical acceleration and measured friction force [4] (Frequency: 1.0 Hz; Acceleration: 0.25g peak)

These results clearly illustrate the symmetry between the maximum and minimum value of μ_v, irrespective of the magnitude and frequency of excitation and the variations in the load. The mean value of coefficient of friction is observed to be quite close to the coefficient of friction measured under static conditions, irrespective of the excitation frequency and magnitude. Another important result observed from all of these different cases, is the occurrence of a peak or minimum value of μ_v around the frequency of 4Hz. Some cases even yielded almost loss of contact between the skid and deck surface at this frequency. This frequency must be connected with the natural frequency of the deck frame, the sled or other components involved in the experimental system. Nevertheless, the analytical model treats the deck structure as a rigid mass, which will transmit the vertical vibration directly to the sliding mass without any possible amplification due to system resonance. It is then expected that peak and minimum values will not be predicted by the analytical model considered in this investigation.

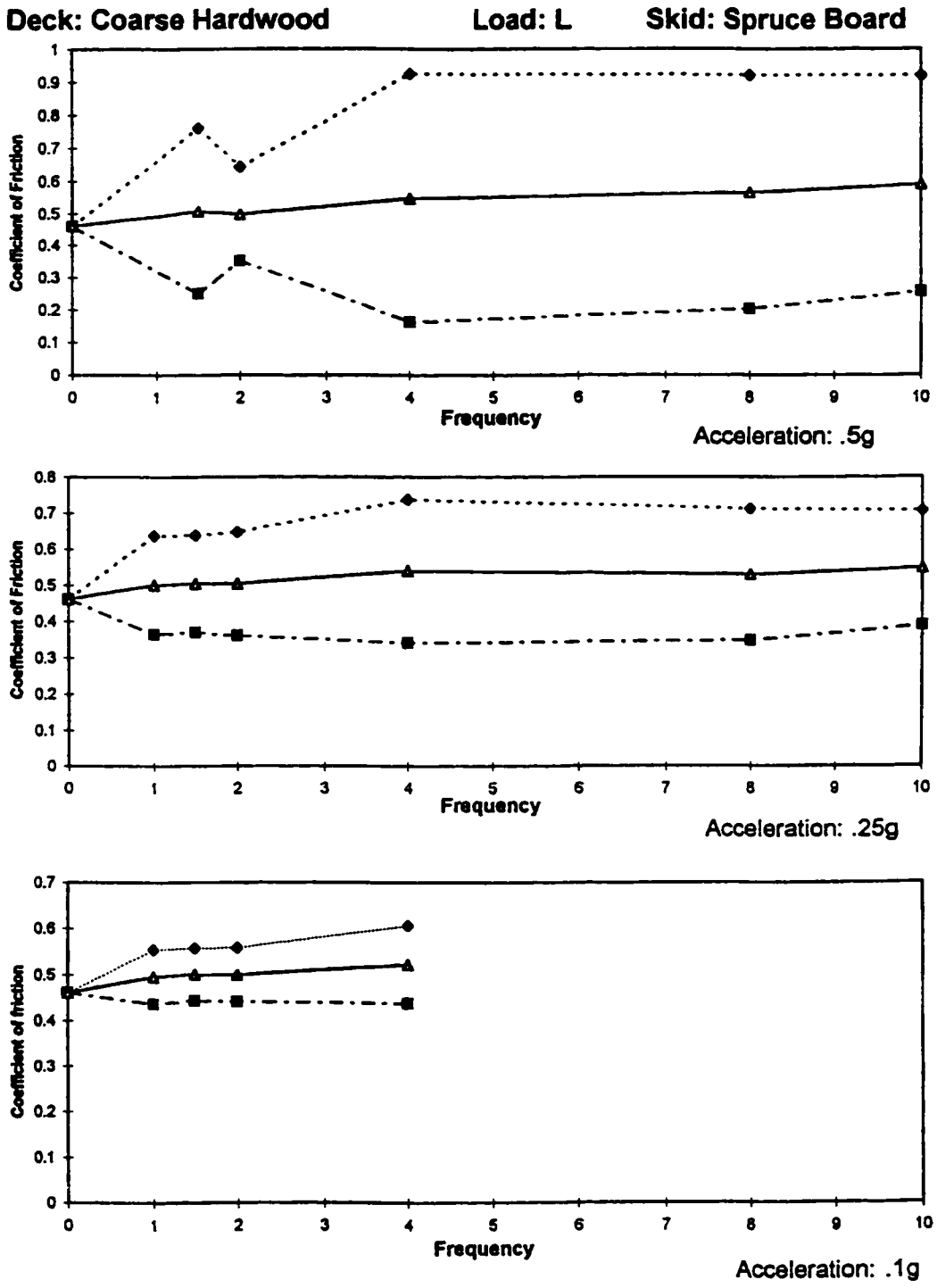

Figure 2.12 Influence of Vertical Vibration on the Coefficient of Friction from Experimental Data [4]

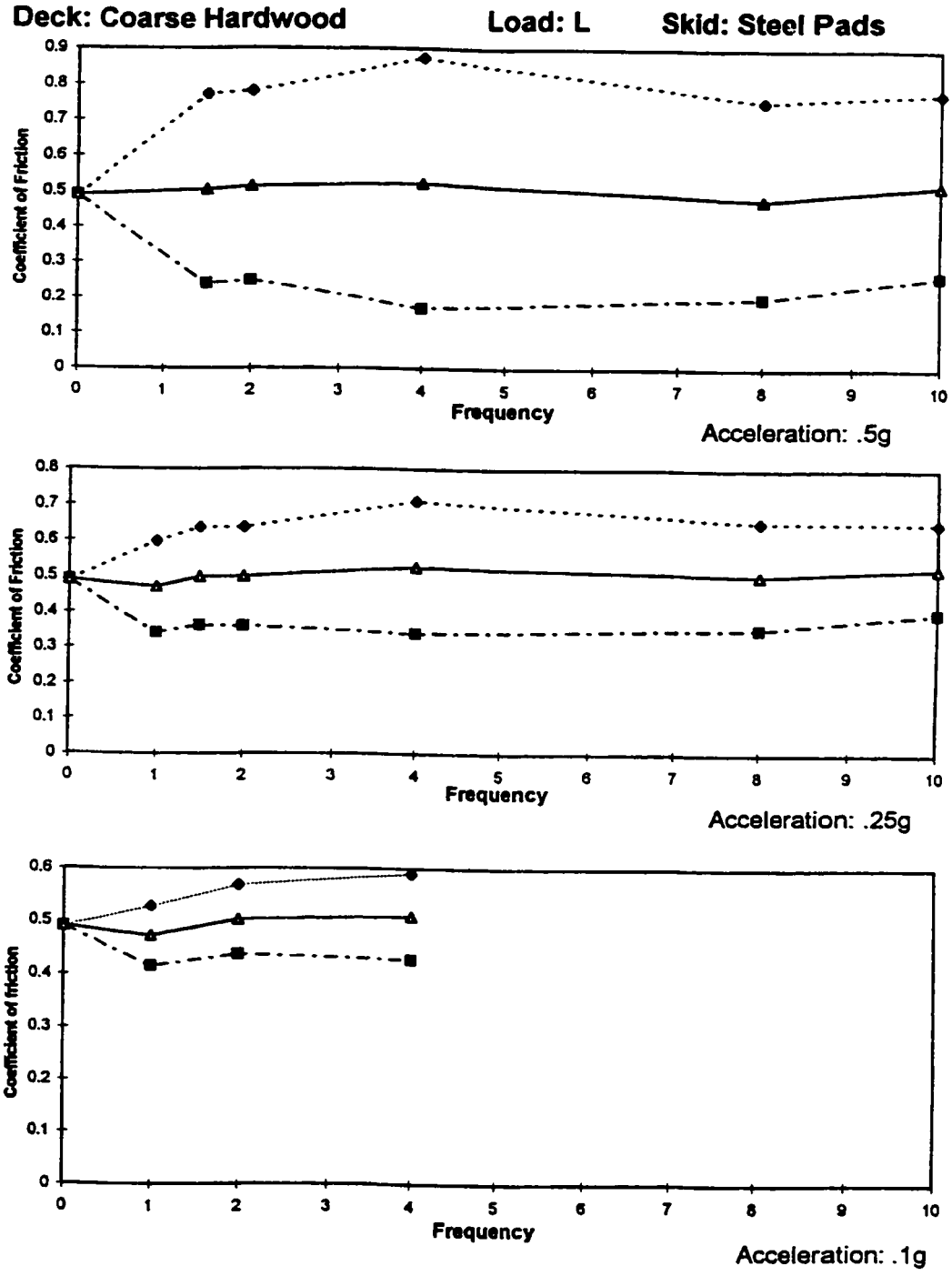

Figure 2.13 Influence of Vertical Vibration on the Coefficient of Friction from Experimental Data [4]

2.4 Validation of the Analytical Model

The simple load-platform model presented in figure 2.5 and expressed by equation (2.2) is simulated for motion defined by equation (2.8) to obtain force time history response. Such simulation results in the absence of platform vibration can be compared with static experimental results. Similarly, the model under vehicle vibration presented in Figure (2.6) and expressed by equation (2.6) can be utilized for the simulation under vehicle vibrations. The following subsections make an attempt to validate the simple model by comparing the simulation results with those of experimental presented in the previous section.

2.4.1 Validation of Static Case

The analytical friction model is validated by comparing the displacement of the sliding mass and the friction coefficients generated from simulation with the experiment result data. Figure 2.14 presents the simulation time history for three pulse velocity showing friction force and displacement. These results for data corresponding to concrete on X-groove aluminum can be compared with the experimental time history presented in Figure 2.10. Comparison of Figure 2.10 and 2.14 clearly reveal a good correlation between the analytical model and the experiment in terms of the displacement. This proves that the speed signal used in the simulation is close to the experimentally generated speed. Since the sliding friction coefficient used in simulation is taken from the experimental results, the simulated sliding friction coefficients certainly meet the measured data. The static friction coefficient from the simulation in figure 2.14 experiences some abatement that would not exceed 6%. However, as discussed in section

2.2.2, the breakaway friction is the sum of the sliding friction and the inertia. Thus the above error may come from the differences in the horizontal acceleration. Figure 2.15 presents simulation results for data corresponding to plastic on smooth hardwood surface showing similar trend as in figure 2.14

In the experiment, the hydraulic actuator is controlled through a software-generated position signal to apply the pulling force to the mass. The rise time was very short and could not be entirely monitored by the instrument. The rise time, 0.05 second used in the simulation, is a value resulted from trial. Further analysis revealed that the rise time of 0.033 second yields better fitting. Figure 2.16 illustrates the modified simulation result for both cases with the rising time of 0.033 seconds. The breakaway friction coefficients obtained from the model are 0.559 and 0.224 respectively. Such errors are all less than 1%. This result indicates that the modified rising time of 0.033 seconds is considerably closer to the real rising time in experiment. Therefore the rising time value of 0.033s will be further used in the simulation to evaluate the Dynamic Friction Coefficients (DFC) under the vibration environment.

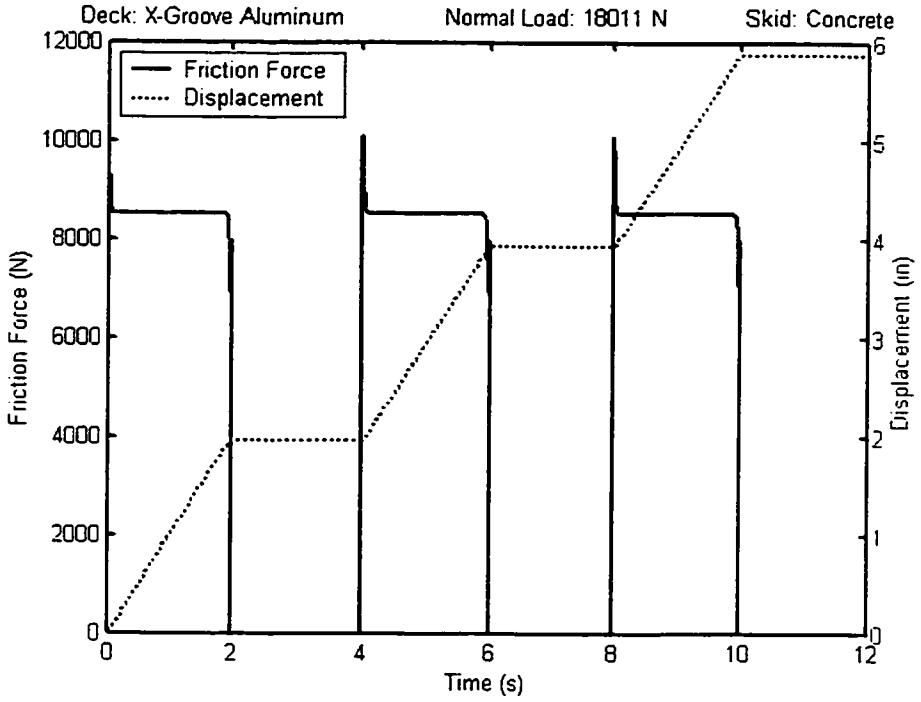

Figure 2.14 Time history of the simulated friction force and load displacement under static conditions

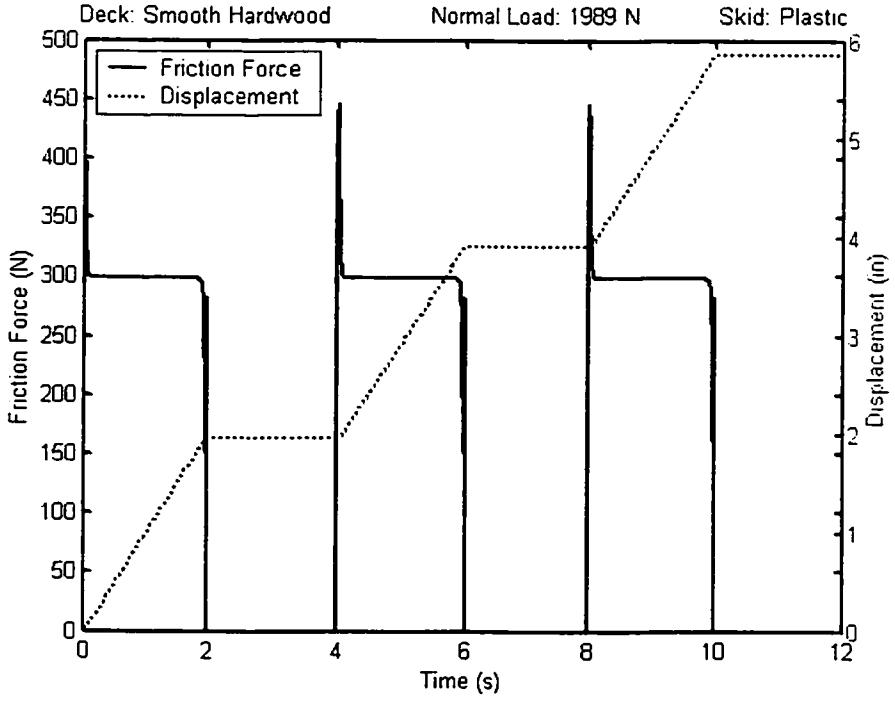

Figure 2.15 Time history of the simulated friction force and load displacement under static condition

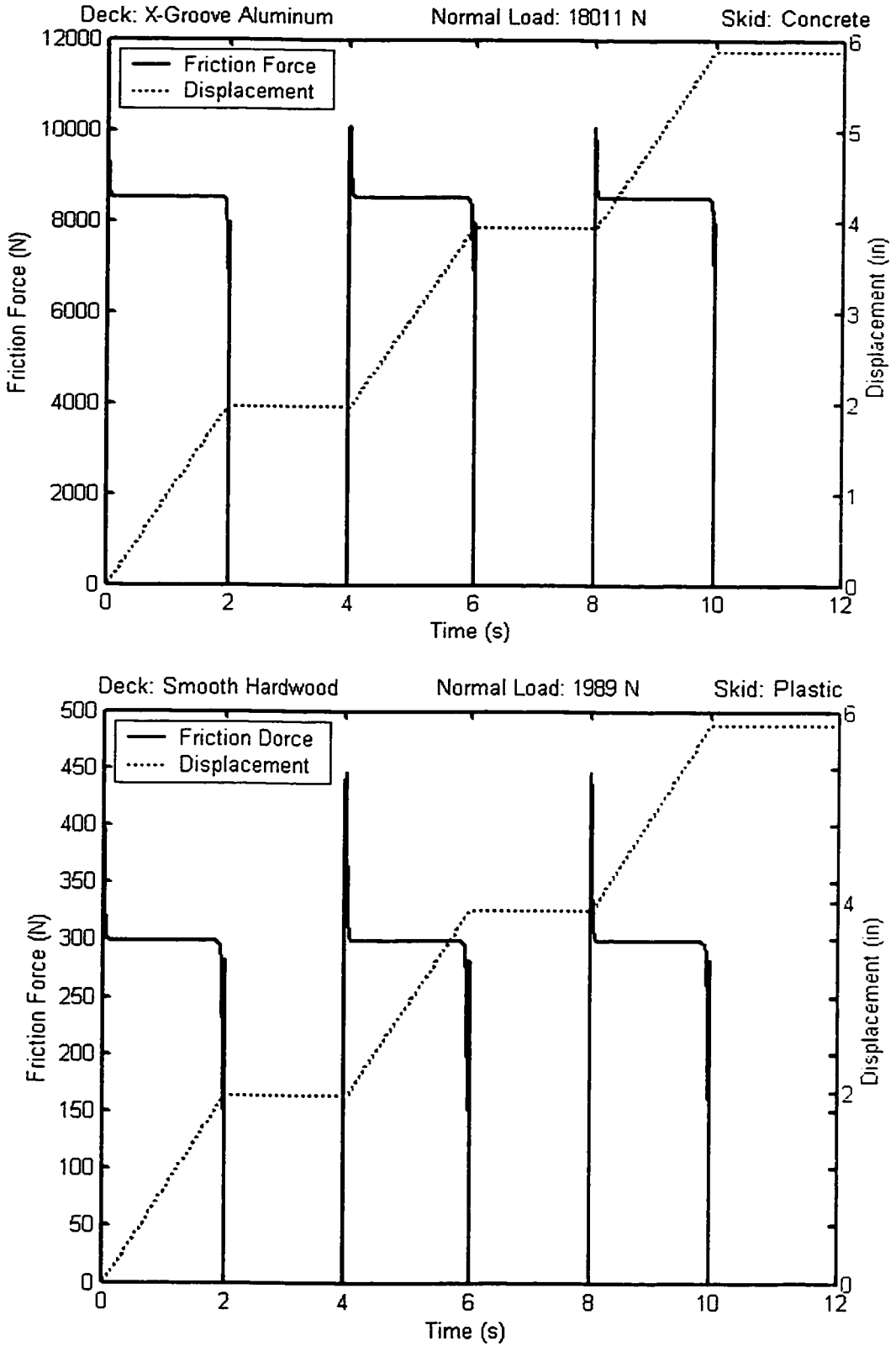

Figure 2.16 Modified simulation result for rising time changed to 0.033 sec

2.4.2 Validation of Dynamic Case

From the experiments presented in section 2.3.3, the friction forces between the selected skid and deck materials were measured under sinusoidal vibration of varying magnitudes at different discrete frequencies. The result showed that the maximum, minimum and mean values of friction forces between the selected material is a function of magnitude and frequency of vertical vibration, consequently, the mean, maximum and minimum values of DFC ($\mu_v=F/mg$), was determined as a function of the mating surfaces, magnitude of vertical vibration and frequency of vibration. Experimental results for selected mating surfaces were presented in section 2.3.3.

The analytical model for friction under vibration, relationship (2.6), reveals that the friction force is a function of both magnitude and frequency of the vertical vibration, thus, the equation of DFC as a function of the SFC and vertical vibration can be expressed as:

$$\mu_v = \frac{F}{mg} = (1 + \frac{1}{g}\ddot{z}_0)\mu_s + \frac{\ddot{x}}{g} \qquad (2.9)$$

The harmonic excitation selected for the validation is a 1Hz sinusoid signal with magnitude of the acceleration 0.25g, and the frequency is 1Hz. The mass and contact material are the same as in the static case.

Figure 2.17 illustrates the time history of the simulated friction force and the excited vibration acceleration for the X-groove aluminum on concrete case, and Figure 2.18 shows the comparison between the dynamic friction coefficients and static

coefficients simulated by the model. Figure 2.19 and Figure 2.20 show the same simulation result but for the case of the smooth hardwood –plastic skid.

Figure 2.19 illustrates the result of modeling under the hypothesis that the contact between load and deck is always maintained. The simulation is run for the conditions corresponding to experimental results presented in Figure 2.11. Comparison between the results in Figure 2.19 and 2.11 indicates that the simulation results experience almost the same trend and value with the experiment results, except those considerable oscillations probable due to stick-slip phenomenon. The above indicates that the DFC model as proposed can be effectively used for simulation of friction in vehicle load security application.

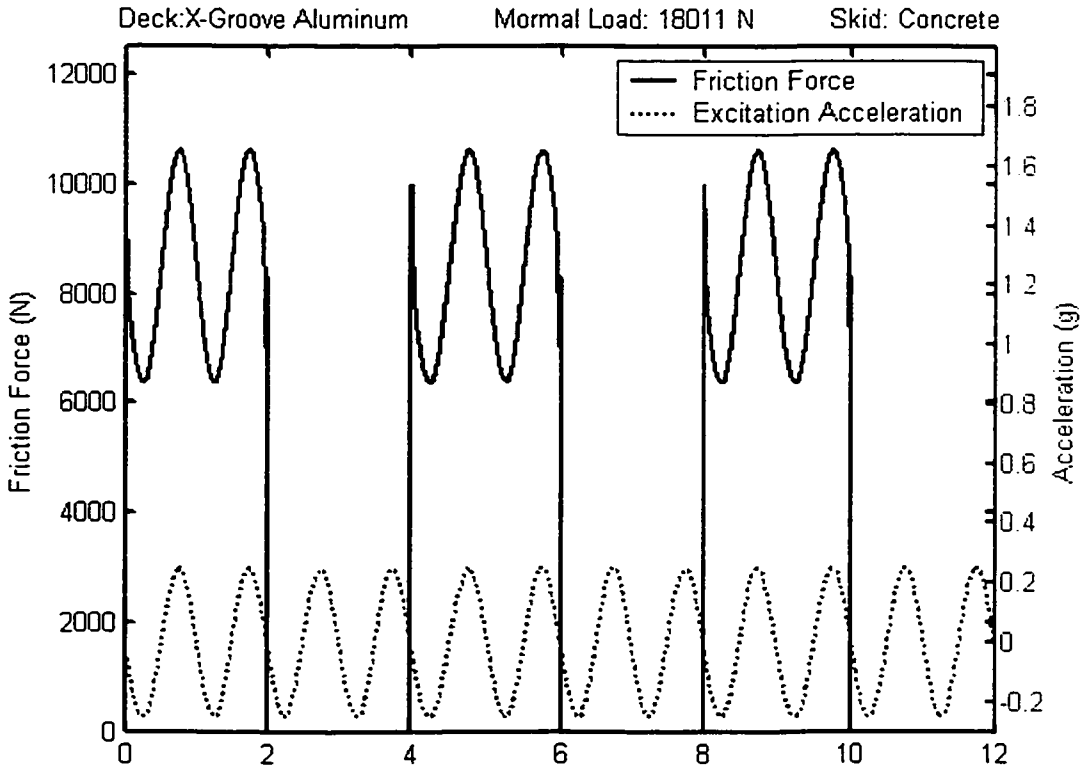

Figure 2.17: Time history of vertical vibration and dynamic friction force (Frequency: 1.0Hz; Acceleration: 0.25g peak)

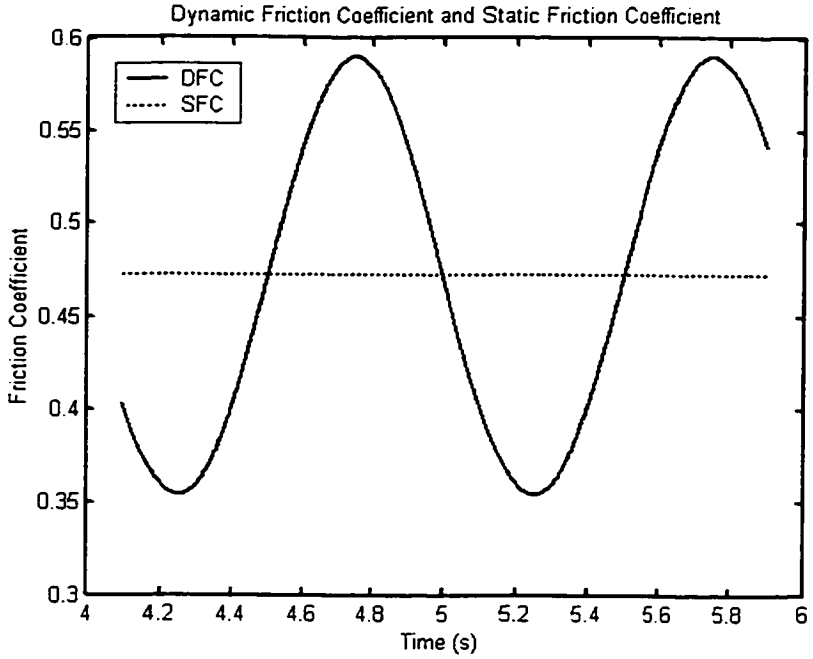

Figure 2.18: Dynamical friction coefficients and static friction coefficients in case of X-Groove aluminum-concrete contact-simulation (Frequency: 1.0Hz; Acceleration: 0.25g peak)

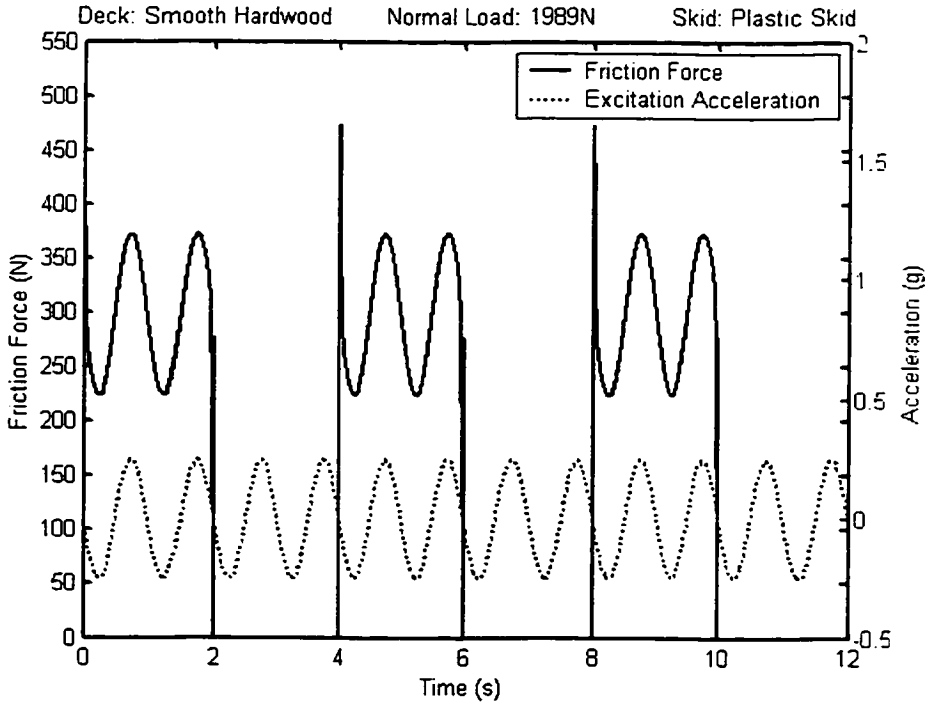

Figure 2.19: Time history of vertical vibration and simulated friction force (Frequency: 1.0Hz; Acceleration: 0.25g)

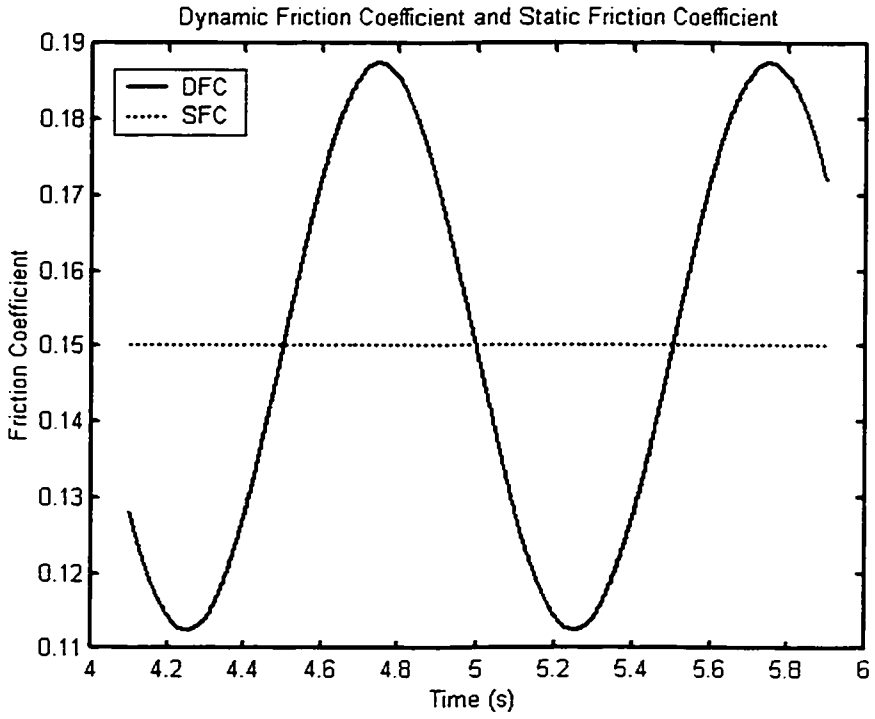

Figure 2.20: Dynamical friction coefficients and static friction coefficients in case of smooth hardwood-plastic skid contact-simulation (Frequency: 1.0Hz; Acceleration: 0.25g peak)

The simulation results in Figure 2.17 and Figure 2.19 revealed that the friction forces in most cases were in-phase with the vertical acceleration of the excitation signal. The peak force occurs when the acceleration approaches its peak value, while the friction force approaches its lowest value corresponding to minimum instantaneous acceleration. Moreover, it is noted that the breakaway friction were not caught up in all cases, as well in the experiment. The breakaway friction forces under vertical vibration, apart from the factors discussed under static conditions, are strongly dependent upon the frequency of vibration, dynamics of the mating surfaces, degree of contact or adhesion, and magnitude

of vibration. However, in the context of load security under vertical vibration, it is most appropriate to formulate the guidelines based upon sliding friction alone.

For vibrating platform, the oscillation of the DFC and SFC is depicted in Figure 2.18 and Figure 2.20. It is obvious that the dynamic friction coefficients (DFC) experience lower value than static coefficients for short duration of time, which are dependent on the frequency of vibration, the minimum value of the DFC fall to 75% of the static friction coefficients. Study for a higher-level vibration revealed that the magnitude of the vibration has significant influence on the minimum value of DFC. Figure 2.21 and Figure 2.22 illustrate the value of the DFC for the same load and contact material under different level of vibration, in which the magnitude of acceleration is 0.5g. The result showed that the minimum value of DFC fall to 50% of the Static Friction Coefficients (SFC). Hence if the load security standard were made based on the static friction coefficients, over the duration of low DFC, the load may slide on the deck due to the inertia force induced by directional maneuver.

Finally, a set of simulation results is obtained for concrete on X-groove aluminum at 0.25g vertical excitation over a range of frequency. The results in term of static as well as maximum and minimum friction coefficients over the frequency range are presented in Figure 2.23. These results may be compared with experimental frequency analysis results presented in Figure 2.12 and 2.13 for other material combinations. The comparison clearly reveals the similarity in trend. As expected, the analytical model does not show any fluctuation in the value at a specific frequency as the model neglects dynamics of the platform.

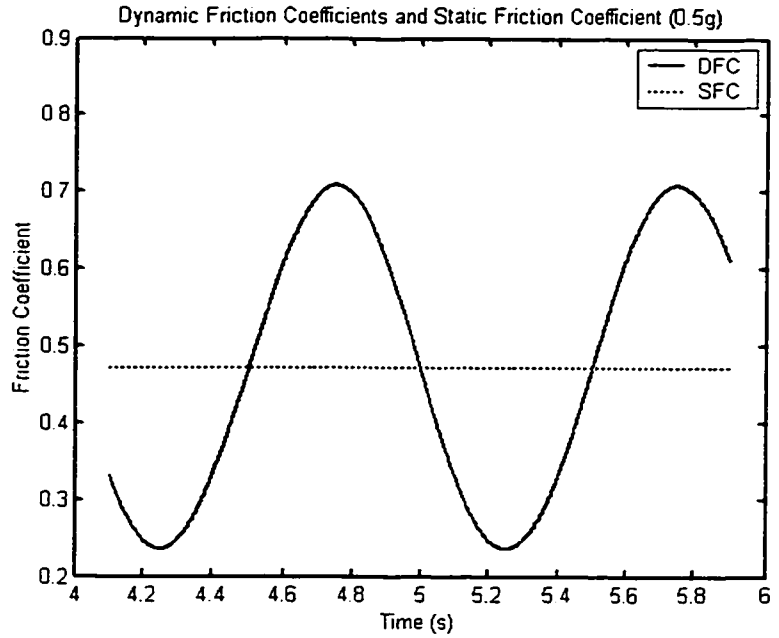

Figure 2.21: Dynamical friction coefficients and static friction coefficients in case of X-Groove aluminum-concrete contact-simulation (Frequency: 1.0Hz; Acceleration: 0.5g peak)

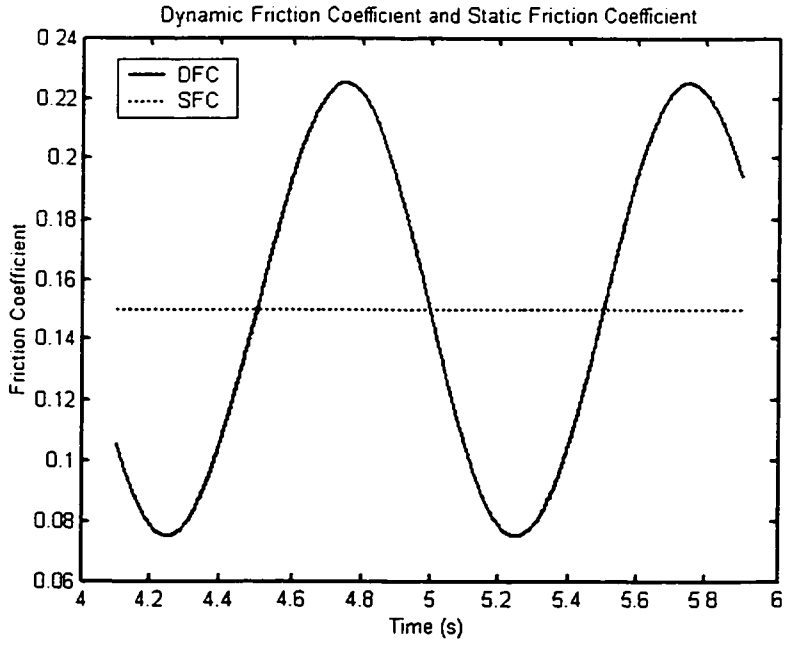

Figure 2.22: Dynamical Friction Coefficients and Static Friction Coefficients in Case of Smooth Hardwood-Plastic Skid Contact-Simulation (Frequency: 1.0Hz; Acceleration: 0.5g peak)

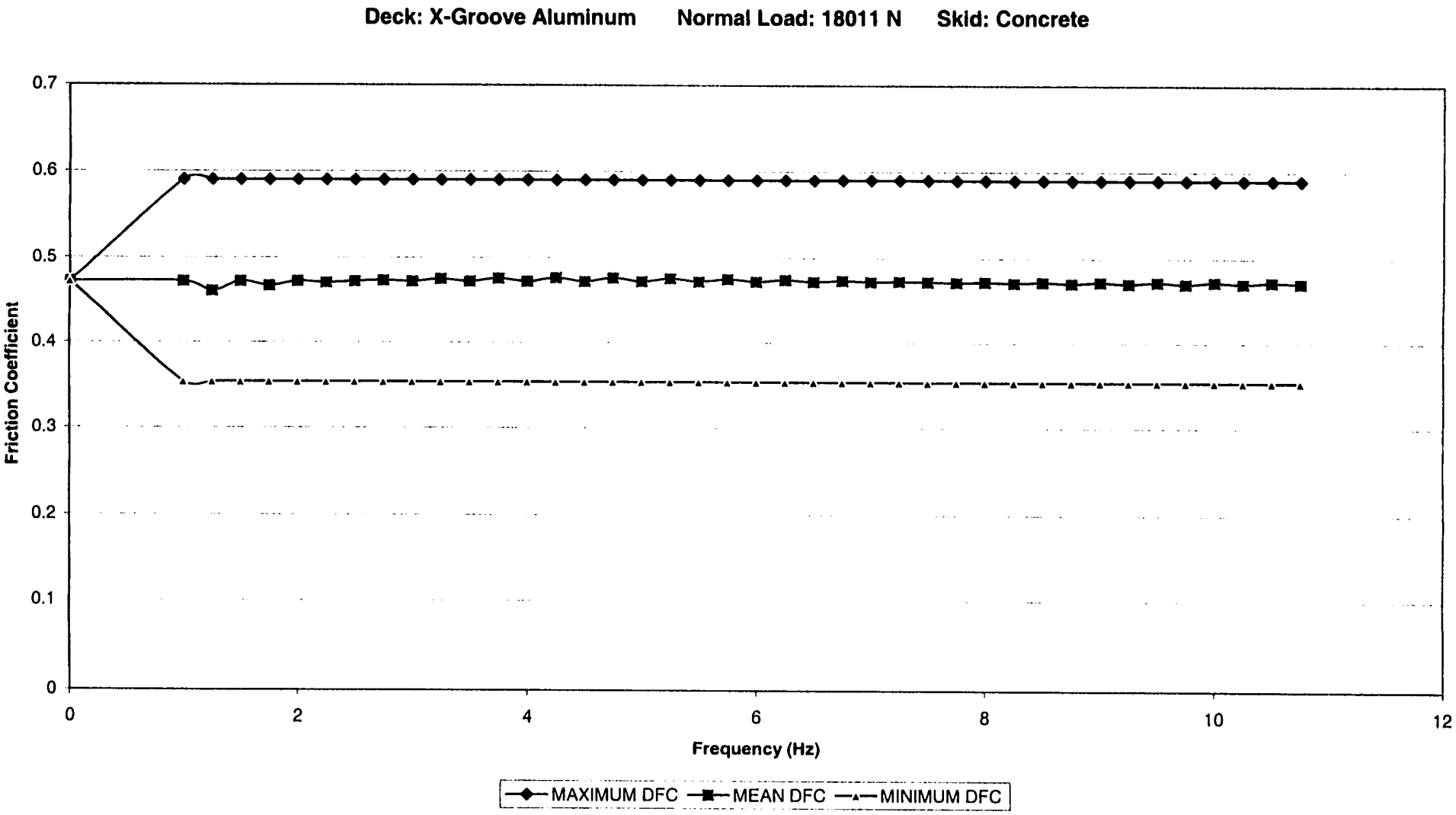

Figure 2.23: Influence of vertical vibration on the friction coefficient from the model simulation

Considering the complexity involved in friction phenomenon, the results obtained can be considered highly encouraging alone with effectiveness of simple models. It should be pointed out that several parameters neglected in this investigation do improve limitations for the model's capability and discussed in the following.

2.5 Limitation of the model

The simulation of the DFC model created above has close match with the experiment. Nevertheless, it has some limitation that cannot describe part of results from experiment. In the experiment, the results showed that the sliding friction coefficients further depend upon the normal load in a significant manner. This is a quite different conclusion, which cannot be included in the analytical model at this moment. Normal load is a parameter that cannot be considered alone without any attention of surface finish and area of contact. A variation in such parameter is indeed very wide and is highly difficult to incorporate with activity. Another limitation is the frequency analysis. The carried out experiment focused on the influence of the frequency on the DFC, which is very important for the study of the load security. However, complex conditions such as the stiffness of the Load-Platform cannot completely represent the dynamic structure of the experiment apparatus, when the deck experienced certain compliance.

2.5.1 Effect of Load

In the classical mechanics and general physics, friction coefficient μ is defined as F/N where F denote the friction force and N the load or the force normal to the surface.

The definition states that μ is independent of the apparent area of contact. This means that for the same load L the friction forces will be the same for a small block as for a large one. A corollary is that μ is independent of the load or, equivalently, the friction force is proportional to the load. The physical explanation is that the area of real atomic contact between two solids is usually proportional to the load.

That μ is approximately independent of the load N was demonstrated by many experiments. The most famous and simple one is described by G. Amontons [50] as shown in Figure 2.24. A plane was set up with a variable inclined angle θ, and a block of weight Mg was set on the plane. The plane is tilted to a steeper angle, until the block just begins to slide under its own weight. The component of the weight parallel to the plane is $Mgsin\theta$, and this must balance the friction force F. The component of the weight normal to the surface is $N=Mgcos\theta$. Under this condition $\mu=F/N=tan\theta$. If this law were exact, an object would start to slide at some definite inclination, independent of the weight Mg, as is indeed initially observed. The laws, however, are empirical and result from an extremely complex set of events.

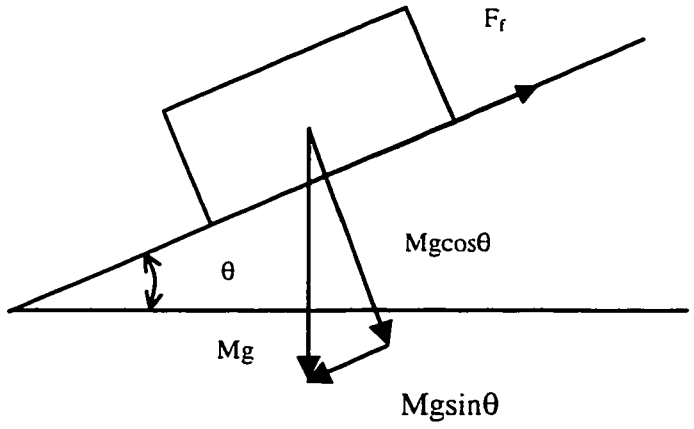

Figure 2.24 Diagram of Amontons's Tilt-Plane Friction Experiment

In CONCAVE's experiment, the variations in friction coefficients with changes in the normal load were observed to be strongly dependent upon the relative flexibility of the skid and deck materials. The relative flexibility of the mating surfaces affects the areas of contact and density of the distribution of the individual contact areas, which depend on many factors, such as roughness of contacting surface and their mechanical properties, surface waviness, intensity of normal load, elastic or elastoplastic deformations of the asperities leading to localized flat zones, and interpenetration of the surfaces. A general pattern of dependency on the normal load, however, cannot be established for different materials. The emphasizes of the model in this thesis is to study the affect of the vertical vibration on the friction force, and its role in load security. The proposed model is thus considered adequate for the study on hand.

2.6 Summary

A Load-Platform friction model was proposed, and the simulation result was compared with the experiment record for the validation. From the analysis of the simulation, it is apparent that the vertical vibration has significant influence on the magnitude of friction forces between the mating surfaces. The vertical vibration may lead to either higher or lower instantaneous friction forces, depending upon the direction of vertical acceleration. Sinusoidal vertical vibration result in extreme high and low values of friction coefficients during a vibration cycle. The degree of DFC reduction is depended on the level of vibration. In the context of load security, the low value of friction coefficient needs to be emphasized. Due to the insufficient dynamic structure modeling

of the platform, the load-platform model cannot reproduce experimental frequency response. However, the load security study incorporating vehicle model will include the dynamics of vehicle platform if not its flexibility.

CHAPTER 3

VEHICLE MODEL

3.1 Introduction

Vibrations of the vehicle body have been an important factor in the assessment of the ride quality. Since ride has been of more concern to the sensation or feel of the passenger/driver within the most of vehicles, much of the research have been directed towards the study of human response to assess the ride quality. These studies have clearly established that variations in the forces on the wheel transmitted to the pavement and ride vibration transmitted to the driver/passengers of a vehicle are strongly influenced by the various design and operating factors of the vehicle [51]. The operating factors such as road roughness, speed and gross vehicle weight, and design factors related to axle loads, axle configuration, and static and dynamic properties of suspension and tires, are known to contribute most significantly to both the dynamic wheel load and ride quality performance. The role of vehicle suspension and tires in the enhancement of road-friendliness of heavy vehicles has been emphasized in a large number of studies. Most of these studies are directly related to vibration modes of the vehicle. However, due to the fact that driver's perception on cargo is almost inexistent, minimal research have been carried out to study the response of the cargo and its other properties to the vibration. As a matter of fact, the surface irregularities, ranging from potholes to random variations of the surface elevation profile, act as a major source that induces vibration to the vehicle

body. The amplitude and frequency of the vibration will influence the magnitude of the dynamic friction force within the load layers, and between the load and the trailer bed surface. Thus the ride quality study is also very important for the load security assessment.

In the previous chapter, the vertical vibration and the horizontal force were emphasized in the creation of the DFC model. In the practical situation, the excitation is represented by the vibration arising from the surface irregularity and the horizontal force which is yielded by the vehicle maneuver, such as turning or braking. Thus the conventional vehicle model can be used to develop the DFC model.

In this chapter, three types of vehicle models will be analyzed and discussed. The parameters of a real heavy truck with cargo will be applied to the models for the study of the response of the DFC, and the results will be presented further in the chapter. The first model is created in bounce-roll plane with 4 degrees of freedom, having bounce, roll and lateral motion. The second model is a bounce model in the longitudinal plane, with only 2 degrees of freedom, having bounce and longitudinal motion. The third model is a bounce-pitch model in the longitudinal plane, with 4 degrees of freedom, having bounce, pitch and longitudinal motion.

3.2 Bounce-Roll Model

Figure 3.1 represents the model of a truck with cargo that is negotiating a constant radius turn while traveling on an uneven road. The cargo is assumed to be placed on the deck without any securing equipment. A 4 degrees of freedom model characterized the load-vehicle response to the maneuver and pavement input: two for the roll and vertical

responses of the sprung mass (Ψ, Z_s) and two for the roll and vertical responses of the unsprung mass (Φ, Z_u) respectively. If the cargo shift needs to be analyzed, another degree of freedom namely the lateral response of the cargo should be added. At this step, any movement of the cargo due to loss of friction means failure of the system, so the lateral response would not be necessary to be considered here.

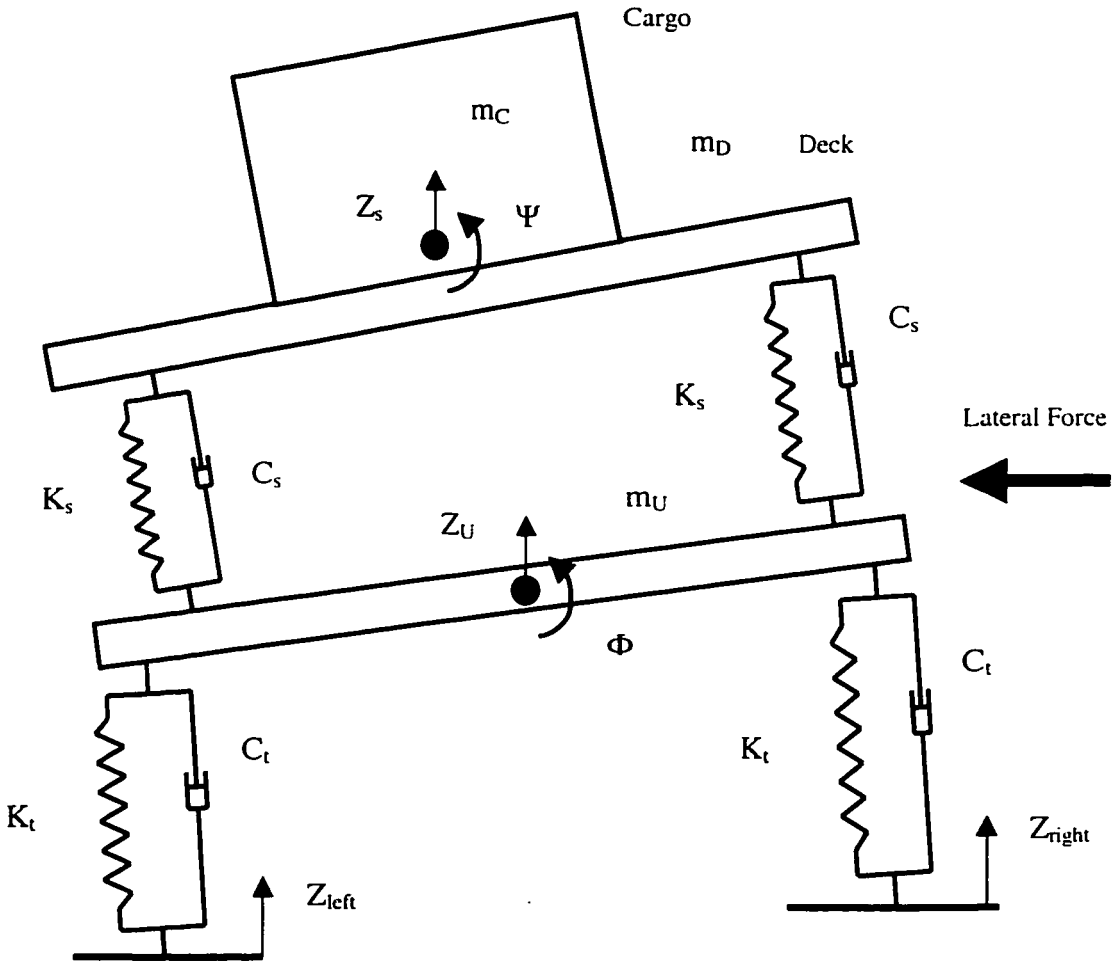

Figure 3.1 Cargo-vehicle systems in Roll Plane

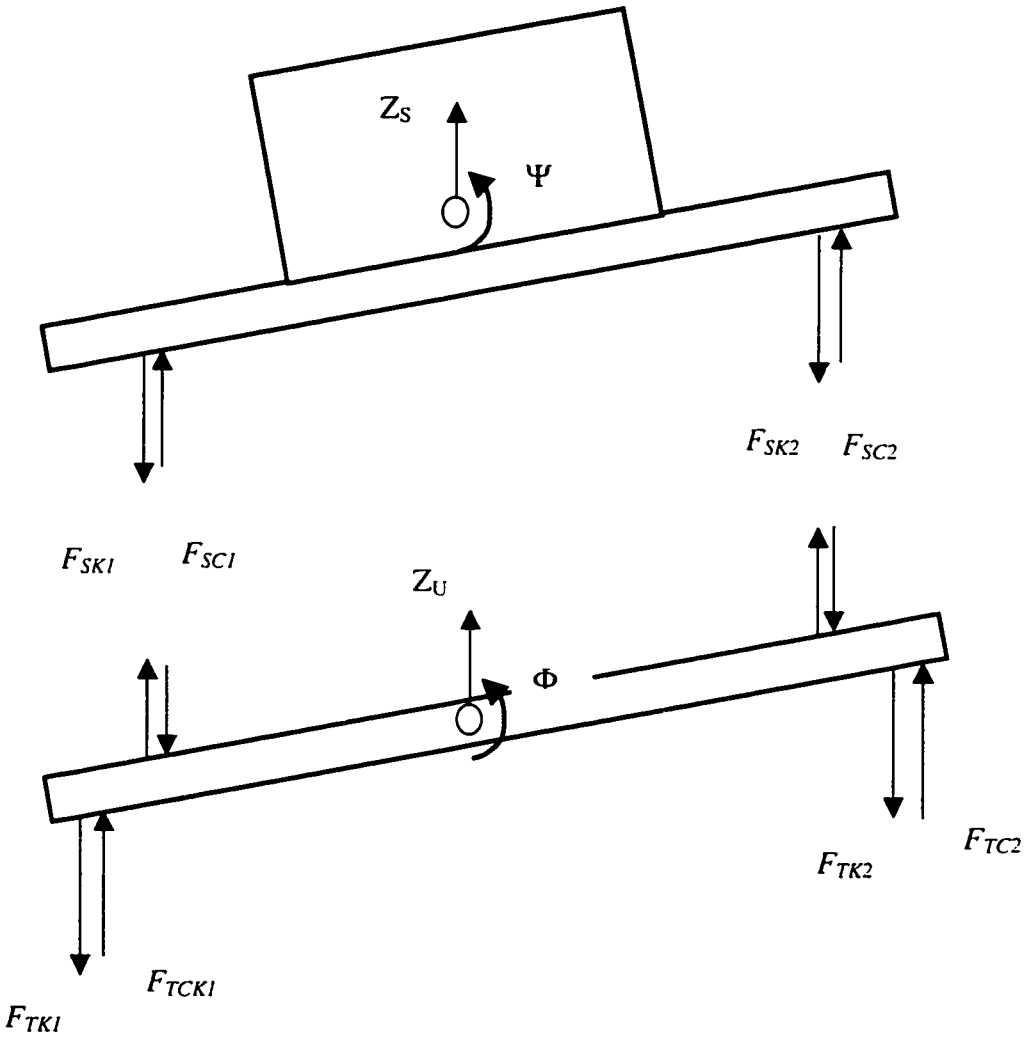

Figure 3.2 Suspension and tire forces

A constant radius (R) turning maneuver brings a constant lateral acceleration a_L to the vehicle-cargo system. As a result of suspension and tire compliance (K_t, C_t, K_s, C_s), the lateral acceleration causes a certain steady vehicle deck roll angle Ψ, which further affects the tangential and normal components of the external force applied to the cargo. Moreover, the vehicle dynamic response to pavement roughness has a direct effect on the friction between the cargo and the deck. Obviously, the occurrence of the load shift is associated with the load-deck tangential and normal forces and accelerations. The cargo will move whenever the sum of tangential resistance forces from the friction and road superelevation is lower than the sum of the tangential components of the applied accelerations coming from turning maneuver and vehicle deck roll, and bounce and in the case of lateral vibration. The normal components of such acceleration further affect the load-deck contact force [47].

The equation of motion for this model can be obtained from sum of forces and moment in a free body diagram as shown in Figure 3.2. The four equations of motion can be summarized as:

Sprung mass, vertical direction

$$(m_C + m_D)\ddot{Z}_S + F_{SC}(\dot{Z}_S, Z_U, \dot{\Psi}, \dot{\Phi}) + F_{SK}(Z_S, Z_U, \Psi, \Phi) = 0$$

Sprung mass, moments

$$I_S\ddot{\Psi} + M_{SC}(\dot{Z}_S, \dot{Z}_U, \dot{\Psi}, \dot{\Phi}) + M_{SK}(Z_S, Z_U, \Psi, \Phi) = 0$$

Unsprung mass, vertical direction

$$m_U\ddot{Z}_U + F_{TC}(\dot{Z}_S, \dot{Z}_U, \dot{\Psi}, \dot{\Phi}, \dot{Z}_{left}, \dot{Z}_{right}) + F_{TK}(Z_S, Z_U, \Psi, \Phi, Z_{left}, Z_{right}) = 0$$

Unsprung mass, moments

$$I_T\ddot{\Phi} + M_{TC}(\dot{Z}_S, \dot{Z}_U, \dot{\Psi}, \dot{\Phi}, \dot{Z}_{left}, \dot{Z}_{right}) + M_{TK}(Z_S, Z_U, \Psi, \Phi, Z_{left}, Z_{right}) = 0 \qquad (3.1)$$

Where F_{SC} and F_{SK} are suspension force developed by the spring and damper, M_{SC} and M_{SK} are moments acting on the deck by the suspension forces. F_{TC}, F_{TK}, M_{TC}, and M_{TK} are forces and moments applied on the unsprung mass from suspension and tire.

As mentioned previously, the vertical vibration transmitted to the deck will have significant effect to the DFC between the load and deck due to inertia force developed by the load vibration. In this model, $\ddot{Z}_S$ is the vibration that has direct connection with the DFC. Moreover, the lateral acceleration developed by the turning maneuver also has an influence on the normal load and on the tangential force to the cargo, and since the lateral acceleration is a function of the velocity and the turning radius, the DFC model in this case is also a function of velocity and turning radius. The normal and lateral acceleration applied to the load can be expressed as:

$$a_n = g\cos(\Psi) - a_L \sin(\Psi) \tag{3.2}$$

$$a_T = a_L \cos(\Psi) + g\sin(\Psi) + \ddot{\Psi}(H_P - H_D) \tag{3.3}$$

Where a_L is the lateral acceleration brought by the turning maneuver, H_P and H_D are the platform and loaded deck center of gravity heights respectively. Combined with the results discussed in (2.3) of Chapter 2, the final normal load should be written as:

$$N = m[g\cos(\Psi) - a_L \sin(\Psi) + \ddot{Z}_S)] \tag{3.4}$$

Consequently, the instantaneous friction force between the cargo and the deck is:

$$F_f = \mu N = \mu m[g\cos(\Psi) - a_L \sin(\Psi) + \ddot{Z}_S)] \tag{3.5}$$

Giving specific road profile input Z_{left}, Z_{right} and the forward velocity for a given turning radius, the response of the friction force can be obtained analytically. However,

the bounce-roll model is more emphasizing on the influence of the lateral acceleration. Thus vibration arising from the road irregularity is not the main influence on the friction in this model. Thus this model will not be used in the later chapters. As a matter of fact, further investigation of the friction using the lateral dynamics model could represent the subject for further investigations.

3.3 Two-Degree-of-Freedom Model

A vehicle is a complex dynamic system with many degrees of freedom. It is possible, however, to simplify the system by considering only some of the major motions of the vehicle. A linear model with two degrees of freedom, as shown in Figure 3.3, may be used. The model includes an unsprung mass representing the wheels and the associated components and a sprung mass representing the vehicle body and the cargo. Their motions in the vertical direction can be described by two coordinates, z_1 and z_2, one for each of the two lumped masses. This model can be used to represent a quarter of a vehicle. Here the mass of cargo and vehicle body are regarded as one mass, since we assume that the cargo never lose contact with the surface of the deck. Modeling of the horizontal sliding, on the other hand, requires another degree of freedom. Similar to the description provided in the previous section, any movement of the cargo might be evaluated as failure to the system under the specified conditions. So, the extra degree of freedom would not be added at this time. Further in this chapter, an analysis of horizontal motion will be carried out for response under braking.

Thus the equations of motion of the quarter-vehicle model shown in Figure 3.2, can be expressed as:

$$(m_c + m_s)\ddot{z}_2 + C_{sh}(\dot{z}_2 - \dot{z}_1) + k_s(z_2 - z_1) = 0$$

$$m_{us}\ddot{z}_1 + C_{sh}(\dot{z}_1 - \dot{z}_2) + k_s(z_1 - z_2) + C_t(\dot{z}_1 - \dot{z}_0) + k_t(z_1 - z_0) = 0 \qquad (3.6)$$

Considering the relationship between the DFC and the deck vibration, the DFC for this quarter-vehicle model can be written as:

$$\mu_v = (1 + \frac{1}{g}\ddot{z}_2)\mu_s + \frac{\ddot{x}}{g} \qquad (3.7)$$

and the instantaneous friction force is :

$$F_\mu = m_c g \mu_v \qquad (3.8)$$

In the above relationships, m_c is the cargo mass, m_s is the sprung mass, including the deck and vehicle body, in this model. μ_v is the dynamic friction coefficient, and μ_s is the static sliding friction coefficient of these specific contact surfaces. In simulation, the entire mass will be assumed as the corresponding mass of the vehicle body located at the position of the CG. C_{sh} is the damping coefficient of the suspension; C_t is the damping coefficient of the tire. K_s is the stiffness of the suspension spring, K_t is the equivalent spring stiffness of the tire. m_{us} is the unsprung mass, and z_0 is the elevation of the ground surface profile.

The weights and dimension parameters of the three-axle truck are identified from the data reported by the Road Transport Association of Canada [40]. The equivalent spring rates of the suspension and tires are also identified from the reported data. The simulation parameters for the vehicle model are summarized in Table 3.1.

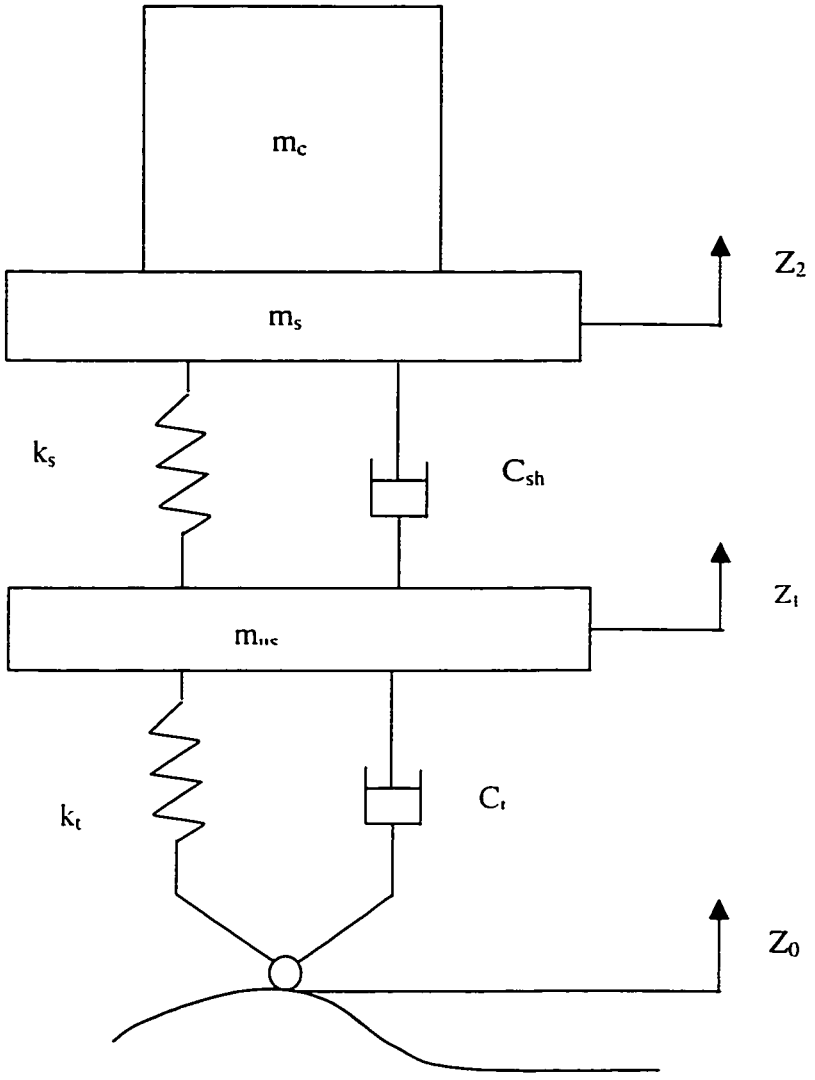

Figure 3.3 Two degree of freedom quarter vehicle model for the analysis of the cargo stability

The parameters in Table 3.1 are for both the front and rear. Either part can be used in quarter-model. Applying them to equation (3.5) and for linear system, can be easily

solved in frequency domain to obtain expressions for transmissibility. The characteristic equation obtained for zero input will yield the roots which are the natural frequencies of the two masses. The parameters lead to sprung and unsprung mass natural frequencies as:

$f_{n\_s} = 1.44\,Hz$

$f_{n\_t} = 10.00\,Hz$

Study of the transmissibility of the system shown in Figure 3.4 clearly shows the position of above natural frequencies. From Figure 3.4, it is obvious that the location of suspension's natural frequency has a more significant effect on the vibration transmitted to the vehicle's deck than the tire. In other words, when the vehicle travels over an undulating surface, which normally consists of a wide range of frequencies given by the asperities, the high-frequencies inputs can be effectively isolated through the suspension because of its lower natural frequency. Low-frequency excitations can, however, be transmitted to the vehicle body unimpeded, or even amplified, as the transmissibility ratio is high when the frequency of excitation is close to the natural frequency of the sprung mass [52]. Thus this specific regime should be emphasized in the study of DFC response.

Slightly different results are obtained if the parameters representing rear quarter vehicle is used. Figure 3.5 shows the transmissibility response of rear quarter vehicle model, where the sprung and unsprung mass natural frequencies are:

$f_{n\_s} = 1.84\,Hz$

$f_{n\_t} = 10.78\,Hz$

Table 3.1 List of simulation parameters for the three-axle truck model

Description of the Parameters	Parameter values
Mass of the truck (M_s)+Mass of the cargo(M_C)	7200 kg
*Mass of the truck and cargo corresponding to the front axle (m_s+m_c)	2835.62 kg =(1260.27+1575.35) kg
*Front tire and axle assembly mass (m_{uf})	353.0 kg
Rear tire and axle assembly mass (m_{ur})	653.0 kg
*Front axle suspension stiffness (K_{sf})	295.3 kN/m
Rear axle suspension stiffness (K_{sr})	797.3 kN/m
*Front axle suspension damping coefficient (C_{sf})	2.9 kNs/m
Rear axle suspension damping coefficient (C_{sr})	5.9 kNs/m
*Front tire suspension stiffness (K_{Tf})	1100.0 kN/m
Rear tire suspension stiffness (K_{Tr})	2200.0 kN/m
*Front tire suspension damping coefficient (C_{Tf})	0.4 kNs/m
Rear tire suspension damping coefficient (C_{Tr})	0.8 kNs/m
*Distance from front axle to CG (l_f)	3.757 m
*Distance from rear axle to CG (l_f)	2.441 m
*Static sliding friction coefficient (μ)	0.472
*Cargo mass corresponding to the front axle (m_c)	1575.35 kg

Items with * marks are parameters of front side of the truck.

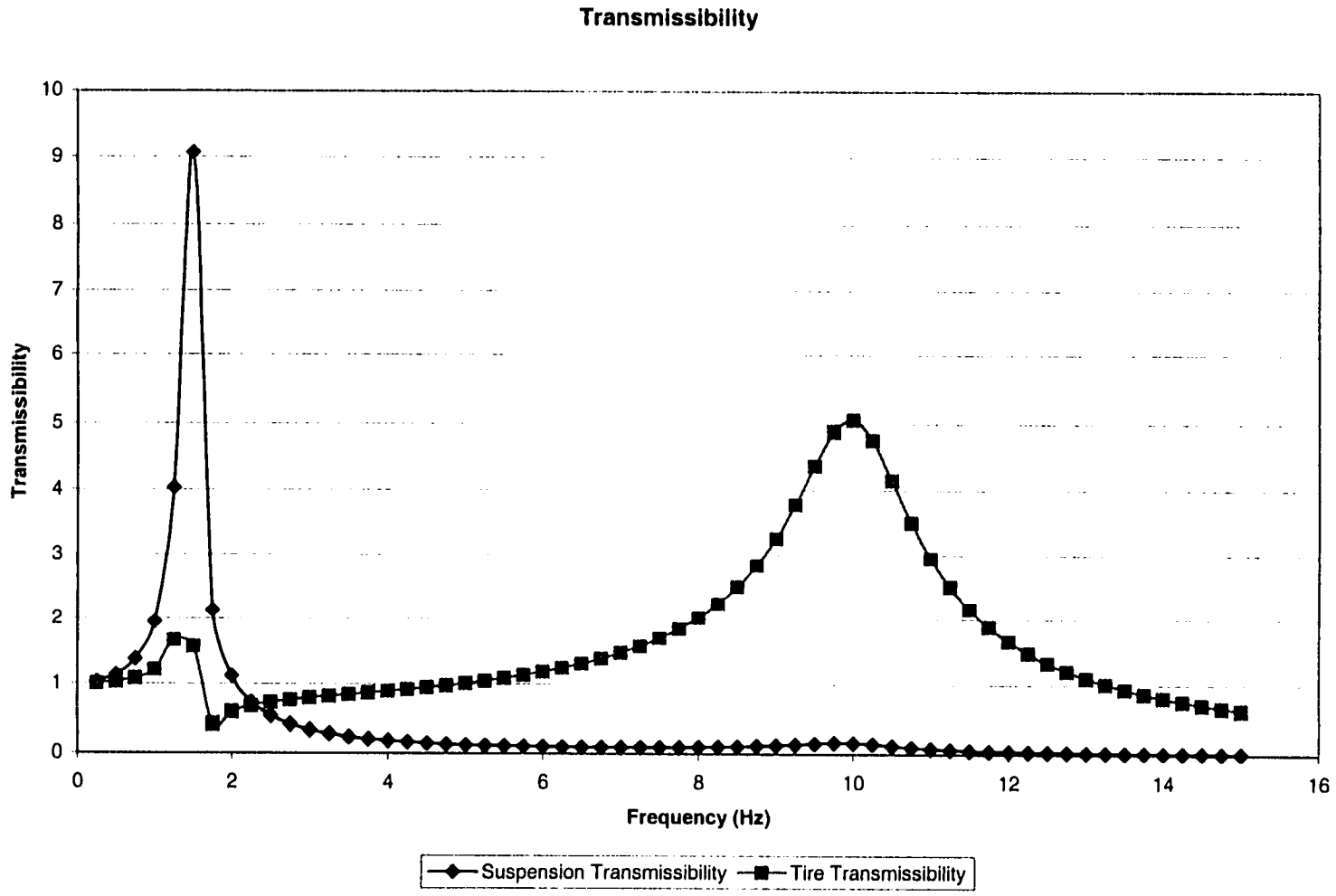

Figure 3.4 Transmissibility of quarter vehicle model (Front side)

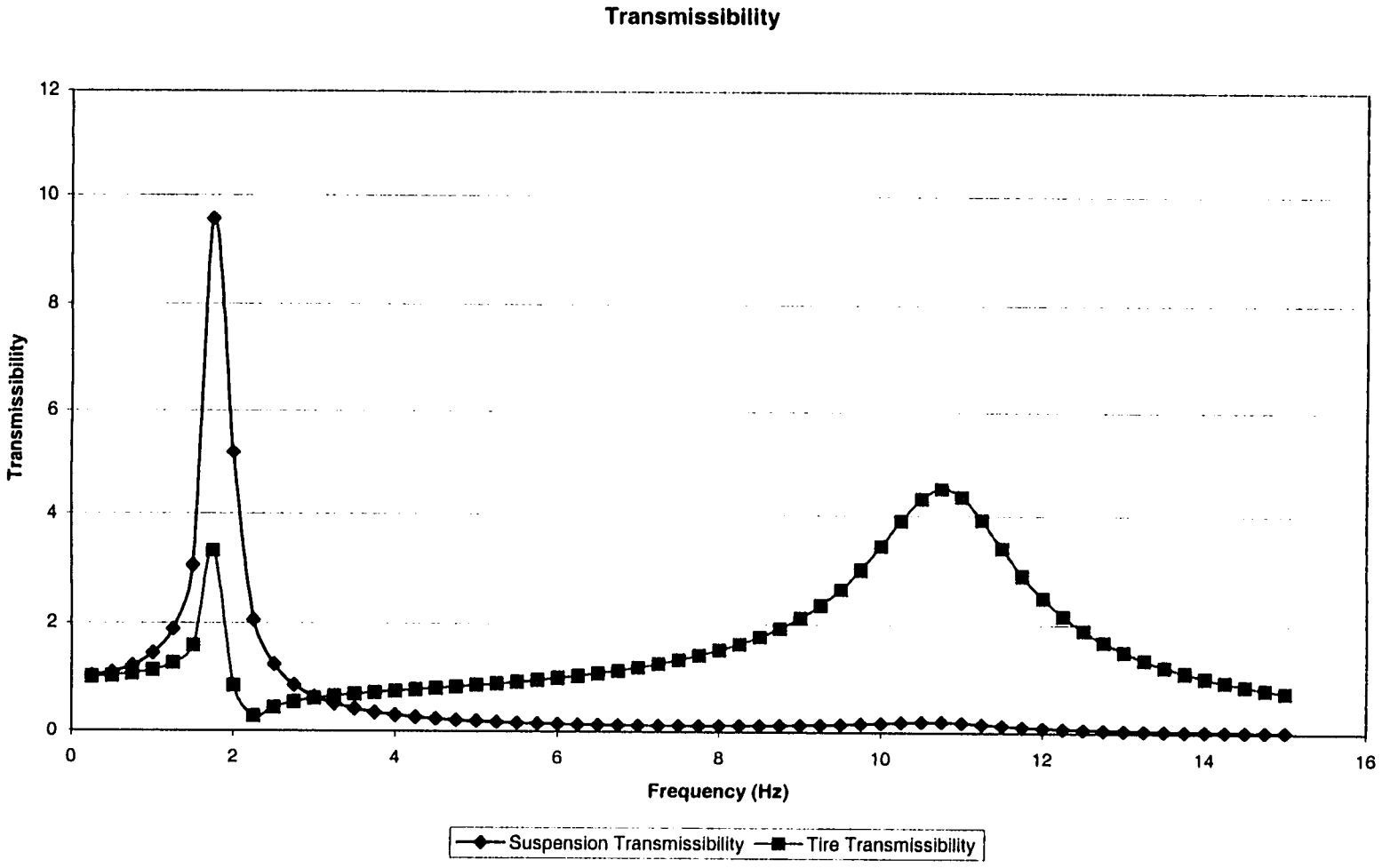

Figure 3.5 Transmissibility of quarter vehicle model (Rear side)

3.4 Four-Degree-of-Freedom Vehicle Model for Pitch and Bounce

The deck vibration transmitted from tire and suspension affects the friction force by changing the instantaneous normal load of the cargo, and can be studied from the 2-degree-of-freedom bounce model, which was formulated in the previous section. Other than vertical, the angular motion of the vehicle has also an effect on the normal load. In section 3.1, the effect of roll motion has been discussed. In this section, the pitch motion is introduced through the vehicle model.

Figure 3.6 is a real loaded truck to be formulated with a four-degree-of –freedom in-plan model. Figure 3.7 illustrates the lumped mass model. The cargo is placed on the deck surface without any securing means, assuming negligible contributions due to roll dynamics of the vehicle. The tandem of closely spaced rear axles are grouped together and represented by a single composite axle. The vehicle body, chassis and cargo will be characterized by a rigid sprung mass M_{S+C} with the assumption that there is no loss of contact between the cargo and the deck. The sprung mass is assigned two-degree-of-freedom (DOF), and is free to bounce and pitch. In the presence of horizontal force, the rigid mass may be separated into 2 masses, M_S and M_C. The front and composite rear wheel and axle assemblies are represented by independent rigid masses, referred to as unsprung masses, with only vertical DOF. Each unsprung mass is coupled to the sprung mass through the respective suspension components, modeled as parallel combinations of energy restoring and dissipative elements. The front and rear axle tires are modeled as damped elastic elements, assuming point contact with the road. The contribution of the

frame bending modes to the vibration behavior of the vehicle are considered to be insignificant due to relatively small deflections of the frame, and location of the suspensions near the nodes.

The equations of the four-degree-of freedom vehicle model shown in Figure.3.7, can be obtained through free-body-diagram presented in Figure 3.8 to yield:

$$M_{S+C}\ddot{z}_1 + F_{SF}(z_1, z_2, \theta) + F_{SR}(z_1, z_3, \theta) + M_{S+C}g = 0$$

$$I\ddot{\theta} + L_R F_{SR}(z_1, z_3, \theta) - L_F F_{SF}(z_1, z_2, \theta) = 0$$

$$M_{TF}\ddot{z}_2 - F_{SF}(z_1, z_2, \theta) + F_{TF}(z_2, z_{0F}) + M_{TF}g = 0$$

$$M_{TR}\ddot{z}_3 - F_{SR}(z_1, z_3, \theta) + F_{TR}(z_3, z_{0R}) + M_{TR}g = 0 \qquad (3.8)$$

Where F_{SF} and F_{SR} are suspension forces developed by the front and rear suspension respectively. I is the pitch mass moment of inertia of the sprung weight about the corresponding centroid.

The suspension forces depend upon the type of suspension employed in the vehicle. Heavy vehicles employ leaf spring or air suspension, which usually present non-linear stiffness and damping properties. Since they are not the important factors discussed in this thesis, for simplification purpose, the linear or equivalent linear spring rates will be applied in the model. The damping forces will vary linearly with the velocity as well. So the suspension forces due to linear springs may be expressed as:

$$F_{SF}(z_1, z_2, \theta) = K_{SF}(z_1 - L_F\theta - z_2 - \delta_{SF}) + C_{SF}(\dot{z}_1 - L_F\dot{\theta} - \dot{z}_2)$$

$$F_{SR}(z_1, z_3, \theta) = K_{SR}(z_1 + L_R\theta - z_3 - \delta_{SR}) + C_{SR}(\dot{z}_1 + L_R\dot{\theta} - \dot{z}_3) \qquad (3.9)$$

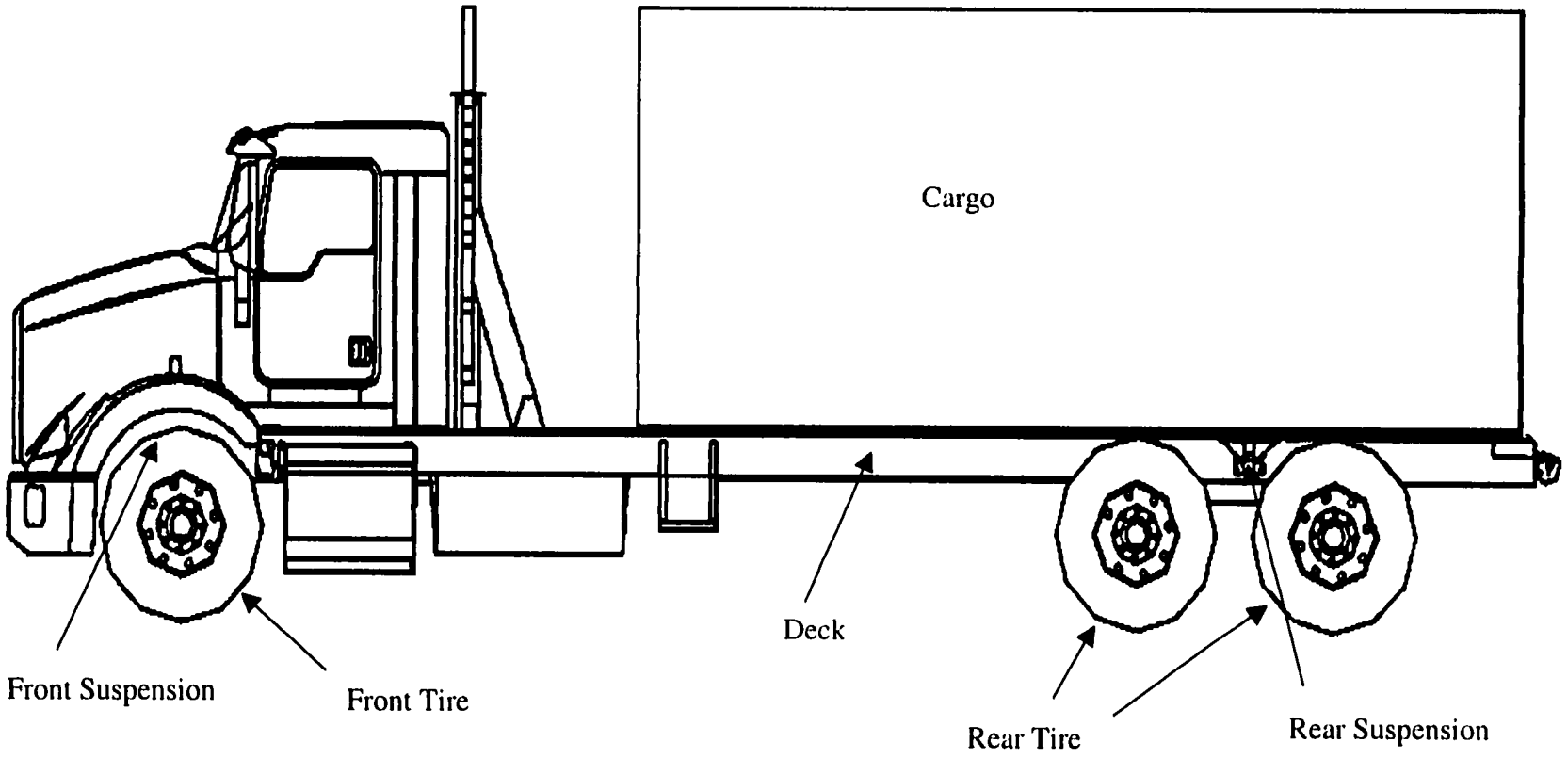

Figure 3.6 A real loaded truck to be modeled

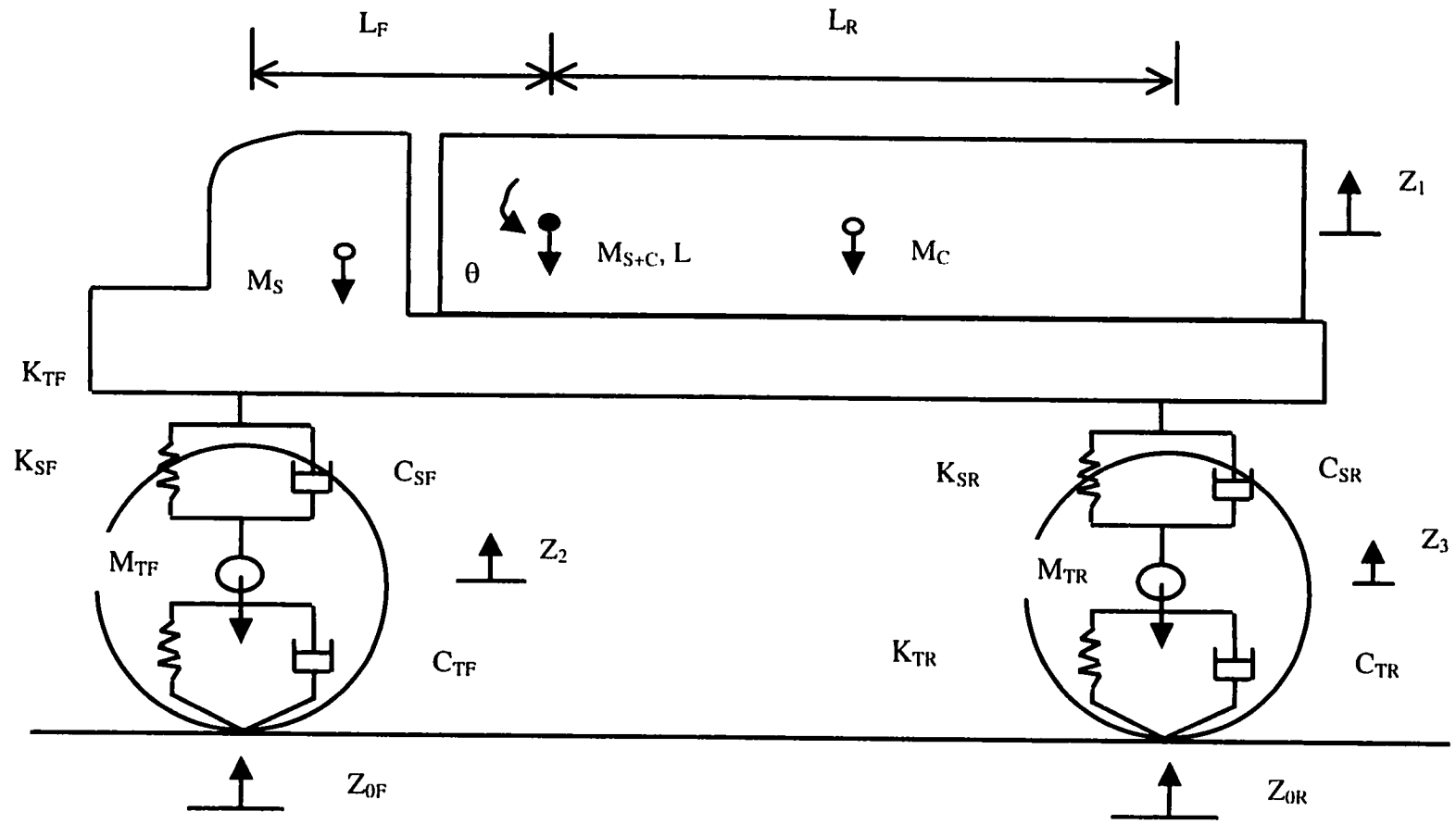

Figure 3.7 In plane model representation of a strait truck

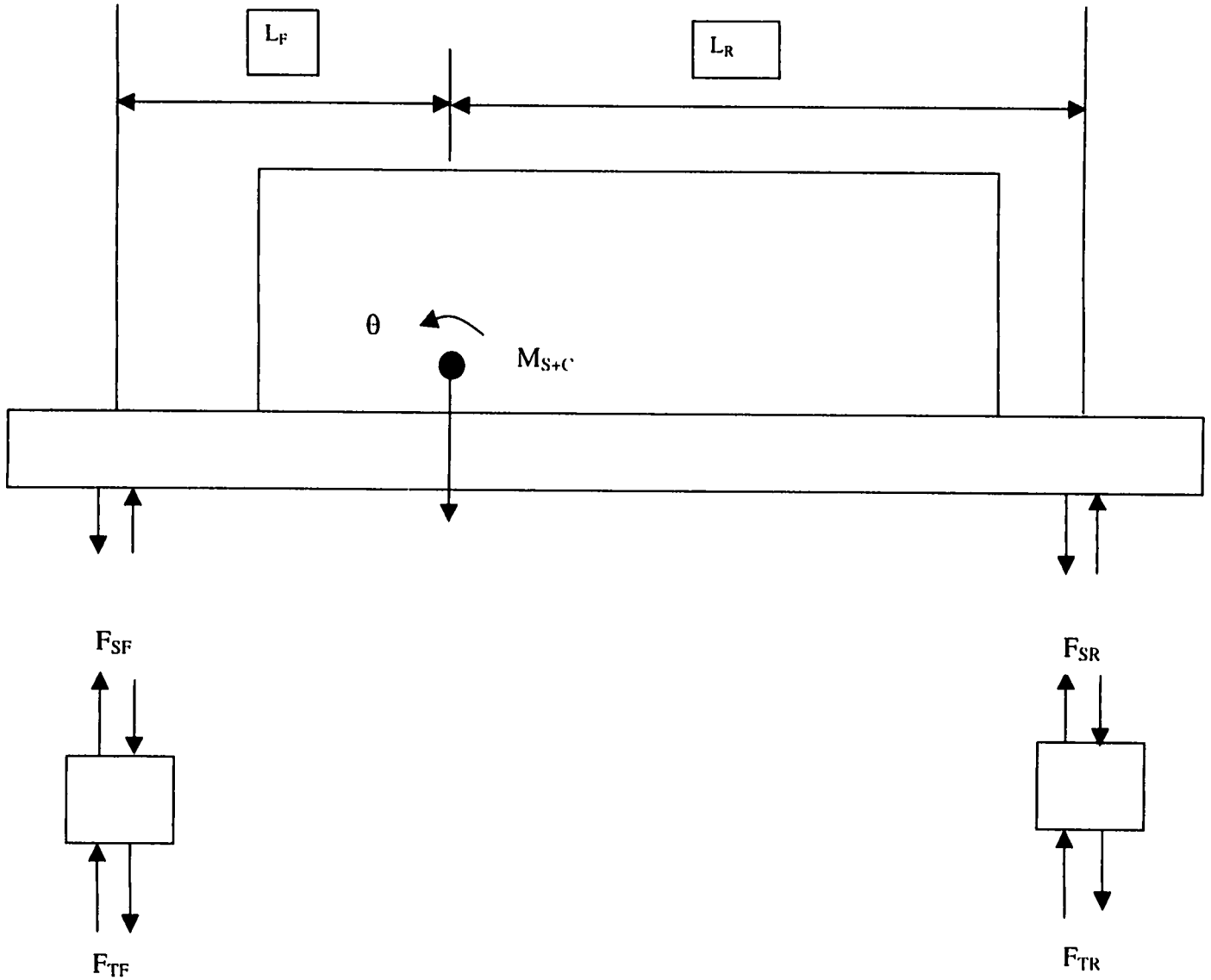

Figure 3.8 Suspension and tire forces

Where K_{SF} and K_{SR} are the linear or equivalent linear spring rates of the front and rear suspension, and C_{SF} and C_{SR} are the respective damping coefficients. while δ_{Si} is the static deflection of the suspension i $(i=F, R)$. The tire is modeled as a parallel combination of a nonlinear asymmetric spring and a linear damper, assuming point contact with the road. F_{TF} and F_{TR} are the forces developed by the front and composite rear axle tire.

$$F_{TF}(z_2, z_{0F}) = K_{TF}(z_2 - z_{0F} - \delta_{TF}) + C_{TF}(\dot{z}_2 - \dot{z}_{0F}); \qquad for\,(z_2 - z_{0F} - \delta_{TF}) \le 0;$$

$$F_{TR}(z_3, z_{0R}) = K_{TR}(z_3 - z_{0R} - \delta_{TR}) + C_{TR}(\dot{z}_3 - \dot{z}_{0R}); \qquad for\,(z_3 - z_{0R} - \delta_{TR}) \le 0;$$

$$F_{TF}(z_2, z_{0F}) = 0; \qquad for\,(z_2 - z_{0F} - \delta_{TF}) \ge 0;$$

$$F_{TR}(z_3, z_{0R}) = 0; \qquad for\,(z_3 - z_{0R} - \delta_{TR}) \ge 0. \qquad (3.10)$$

where K_{Ti} and C_{Ti} ($i=F,R$) are the vertical spring rate and viscous damping coefficient of the tire i respectively, and δ_{Ti} is its static deflection. Z_{0F} and Z_{0R} are the displacement excitations encountered at the front and rear tire load interface, respectively. M_{TF} and M_{TR} are the masses of the front and rear axles. Equation (3.8) to (3.10) describe the vertical and pitch dynamics of the three-axle truck.

The same vehicle parametres from Table 3.1 have been applied to the equations above to study the transmissibility of the system, as shown in Figure 3.9. Similar to the quarter model, the natural frequency of the suspension produces a more significant effect to the vibration arising on the deck surface, whereas the natural frequency of the tire has little influence on the deck vibration. In general, the pitch and bounce motions are coupled, and an impulse at the front or rear wheel excites both motions. In considering the natural frequencies for the front and rear ends, it should be noted that excitation from

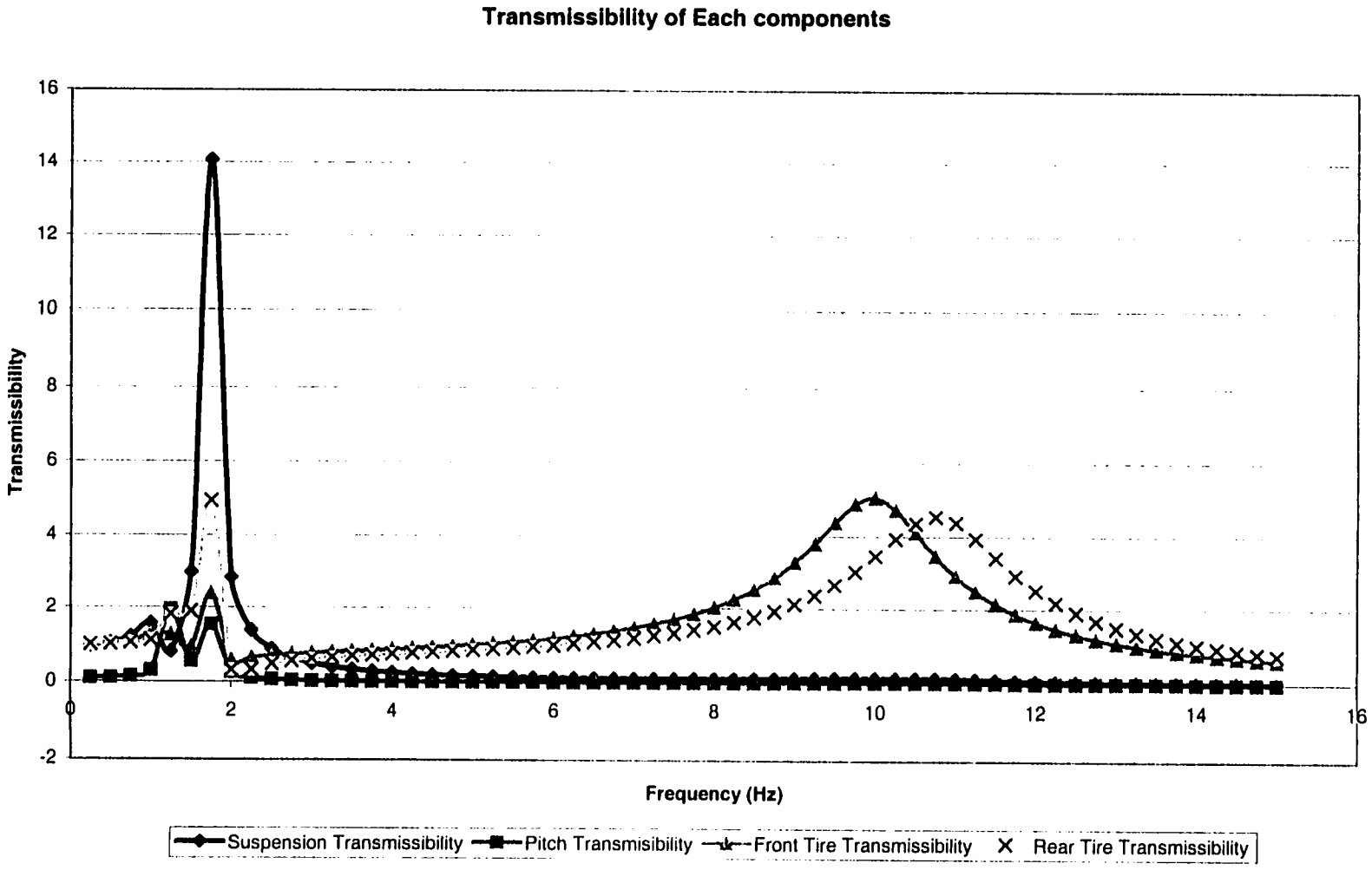

Figure 3.9 Transmissibility of the in-plane vehicle model

the road to a moving vehicle will affect the front wheels first and the rear wheels later. Consequently, there is a time lag between the excitation at the front and that at the rear wheels. This results in a pitching motion of the vehicle body. Usually, the natural frequency for pitch is slightly higher than that for bounce, but for vehicles with coupled front-rear suspension systems, the natural frequency for pitch may be lower than that for bounce. However, they are all approximately around the lower frequency area, and make this area the most dangerous condition for the avalability of friction force for load security.

To develop the DFC model with this four-degree-of-freedom vehicle model, the masses of the cargo and vehicle body should be assumed to be able to seperate when the horizontal force analysis is needed. Figure 3.10 illustrates the free body diagram of the interaction between the cargo and deck surface under the vibration environment. It is obvious that the normal force N and friction force F are influenced by the vertical vibration acceleration and the pitch motion.

By applying Newton's second law, the normal load and friction force can be written as:

$$N = (M_C g + M_C \ddot{z}_1)\cos\theta$$

$$f_{real} = f - (M_C g + M_C \ddot{z}_1)\sin\theta \qquad (3.11)$$

Substituting the expression for dynamic friction force presented in Charpter 2, the force in the presence of pitch is:

$$F = \mu_s (M_C g + M_C \ddot{z}_1)\cos\theta - (M_C g + M_C \ddot{z}_1)\sin\theta + M_C \frac{d\dot{x}}{dt} \qquad (3.12)$$

and the Equation (2.13), which describ the dynamical friction coefficient becomes:

$$\mu_v = \frac{F}{M_C g} = (1 + \frac{1}{g}\ddot{z}_1)\mu_s \cos\theta - (1 + \frac{\ddot{z}_1}{g})\sin\theta + \frac{\ddot{x}}{g} \tag{3.13}$$

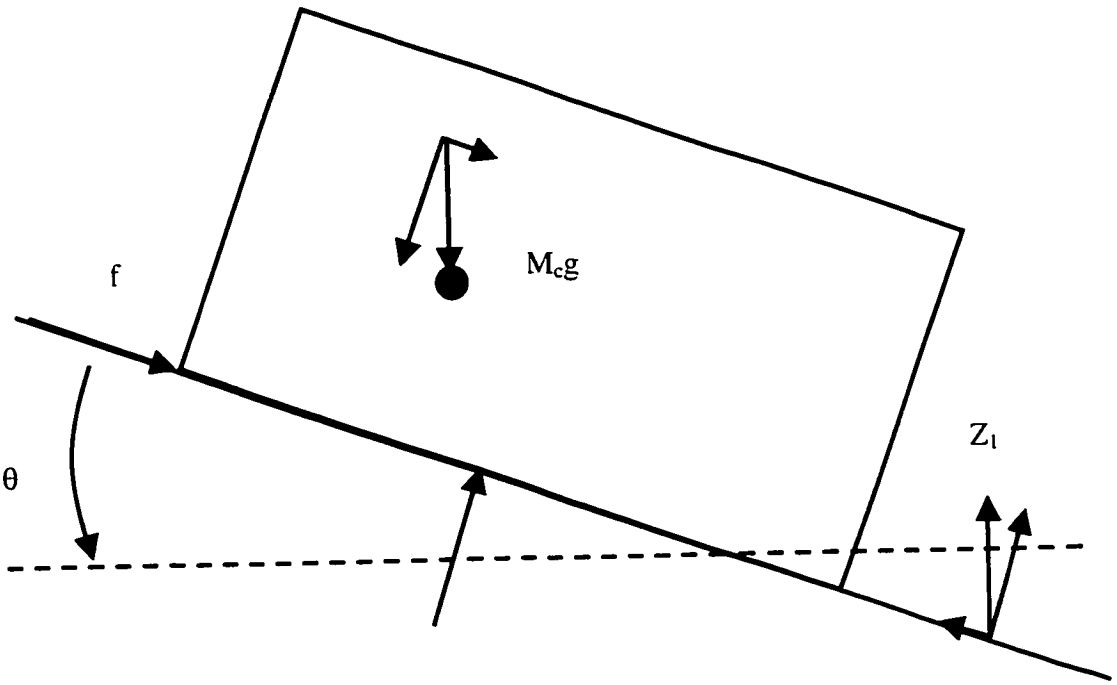

Figure 3.10 FBD of the cargo and deck under dynamic environment

One should note that similar to the bounce motion effect on the normal load, pitch motion can also cause the friction force to weaken and strengthen in turn. Therefore there is a possibility that two weaken instants coincide, which would yield the minimum friction force and consequent potential for movement of the load.

3.5 Summary

The study of this thesis is focused on the influence of the vertical motion on the vertical and the horizontal motions of the cargo, and their correlation related to the variation of the normal load of the cargo on the deck. The most conventional vehicle analytical models are emphasized to evaluate the dynamic response of the vehicle to the road irregularities. In the mean time, many types of vehicle maneuvers induce a horizontal force to the vehicle itself and to the cargo, such as turning and braking. The creation of vehicle model in this chapter is based on these circumstances. Three kinds of vehicle model were created. The first is a bounce-roll model, which studies the combined effect of the bounce and roll motion on the vehicle deck surface. The corresponding horizontal force is mainly the lateral force coming from the turning maneuver. The second and third models are created in the vehicle pitch plane. The second model is a simple 2-degree-of –freedom model, while the third model is a 4-degree-of-freedom model with the pitch motion. The corresponding horizontal force for these two models are all braking maneuver. The study of the transmissibility of the system for the later two models revealed that the most dangerous area for the friction force between the cargo and deck surface that would yield to the cargo motion would occur in the vivcinity of the natural frequency of the suspension, which is in the lower frequency range.

CHAPTER 4

LOAD SECURITY FROM FRICTION UNDER SINUSOIDAL ROAD EXCITATION

4.1 Introduction

When the vehicle travels over an undulated surfaces, the excitation will normally consist of a wide range of frequencies. Since the road surface is irregular, it is more accurately described as a random process. However, steady state frequency response analysis for deterministic input is a highly useful tool that provides important insight in the dynamic performance of the system over a frequency range. In this chapter, two vehicle models developed in chapter 3 will be used for simulation to study the response of dynamic friction coefficients to the sinusoidal road input, and the potential failure analysis of the load security supported by friction will be evaluated in the frequency domain.

If the vehicle travels forward without performing any other maneuver, the cargo would not slide, rather the friction force has the possibility of reducing to zero. In practice, the vehicles are always subjected to other maneuvers, which apply forces to the vehicle body and to the cargo. Brake is such a typical maneuver. In the later section of this chapter, a braking simulation will be carried out to study the braking performance of the DFC model under vertical vibration environment.

4.2 Two-Degree-of-Freedom Vehicle Model under Sinosoidal Excitation

The ride performances and dynamic wheel load of a vehicle system are strongly related to the input vibration frequencies and the modes of vibration of the system. The DFC model associated with two-degree-of-freedom bounce vehicle model formulated in the previous chapter is further analyzed for its response to the sinusoidal road input. A simple model simulation of the load support had been presented in chapter 2 to understand the relationship between the reaction force and the vertical vibration. In this section, the system of DFC model with 2-degree-of-freedom vehicle will be studied with sinusoidal input, to evaluate the effect of the magnitude and frequency on the dynamic friction coefficients.

4.2.1 Sinusoidal Excitation

As discussed above, this part of the analysis deals with deterministic frequency response. A range of sinusoidal excitation can be selected based on a fixed magnitude of acceleration or displacement. First, sinusoidal signal with constant value of acceleration magnitude, is set in the form:

$$\ddot{z}_0 = Z \sin \omega t \qquad (4.1)$$

therefore, the displacement of the excitation from the road is

$$z_0 = -\frac{Z}{\omega^2} \sin \omega t \qquad (4.2)$$

The simulation is performed under different magnitudes and frequencies of the sinusoidal excitation. Three different acceleration levels selected are 0.1g, 0.25g and 0.5g peak, while different discrete frequencies in the 0.25-15 Hz range are used. Such a range of input can provide the relationship between the DFC and vibration magnitude, and the frequency response.

The second way of selecting the sinusoidal excitation is the constant magnitude of displacement which can be written in the form:

$$Z_0 = \bar{Z} \sin \omega t \qquad (4.3)$$

$\bar{Z}$ is 0.5cm for a low level excitation and 1cm for a medium level excitation. The frequency of excitation may be treated as a function of vehicle forward speed V for a fixed wavelength λ such that:

$$\omega = 2\pi \frac{V}{\lambda} \qquad (4.4)$$

In this manner, vibration is used to describe the motion and velocity of the tires in the equations of motion. Further, the constant magnitude will help to better describe the time delay between the front and rear tire when the 4-degree-of-freedom model will be used.

4.2.2 Response to Sinusoidal Excitations

Two differential equations of motion plus two equations for the friction force and coefficients presented in Equation (3.5) to (3.7) along with the inputs for the tires described above are solved simultaneously in time domain. Simulations are carried out long enough to ensure that the response has reached its steady-state level. The steady-

state peak responses are used to compute the transmissibility for each response. A numbers of frequencies have been carried out at different constant acceleration to obtain the frequency response in the range of 0.25 to 15 Hz.

The simulated transmissibility response of the suspension and tire as bounce acceleration ratio corresponding to the truck parameters are presented in Table 3.1 and are illustrated in Figure 3.3 for the front quarter side, and Figure 3.4 for the rear quarter side.

Figure 4.1 to Figure 4.4 show the simulated response of the DFC to the sinusoidal input to different acceleration levels. In Consideration of load security, the curves of minimum friction coefficients in all figures should be emphasized. Since the relationship between the DFC and friction force is a simple proportional relation, thus the trend of the minimum friction force is the same as the minimum DFC. As predicted in a previous chapter, the lower frequency area is critical for the security of the load. There are many locations at which the coefficients dropped to very low values, sometimes to zero, while the values hardly change in the high frequency area. This means that around the lower frequency area, the friction force may decline to very small values till zero, which is very dangerous from the point of view of the load security dependent on friction. Furthermore, comparison of the Figure 4.1 to 4.3 indicates that the acceleration level also has significant effect on the DFC in the lower frequency zone. An Increase in the acceleration magnitude result in the DFC having the zero value over a wider frequency around the sprung mass resonance. Figure 4.4 illustrates the influence of acceleration level to the minimum value of DFC.

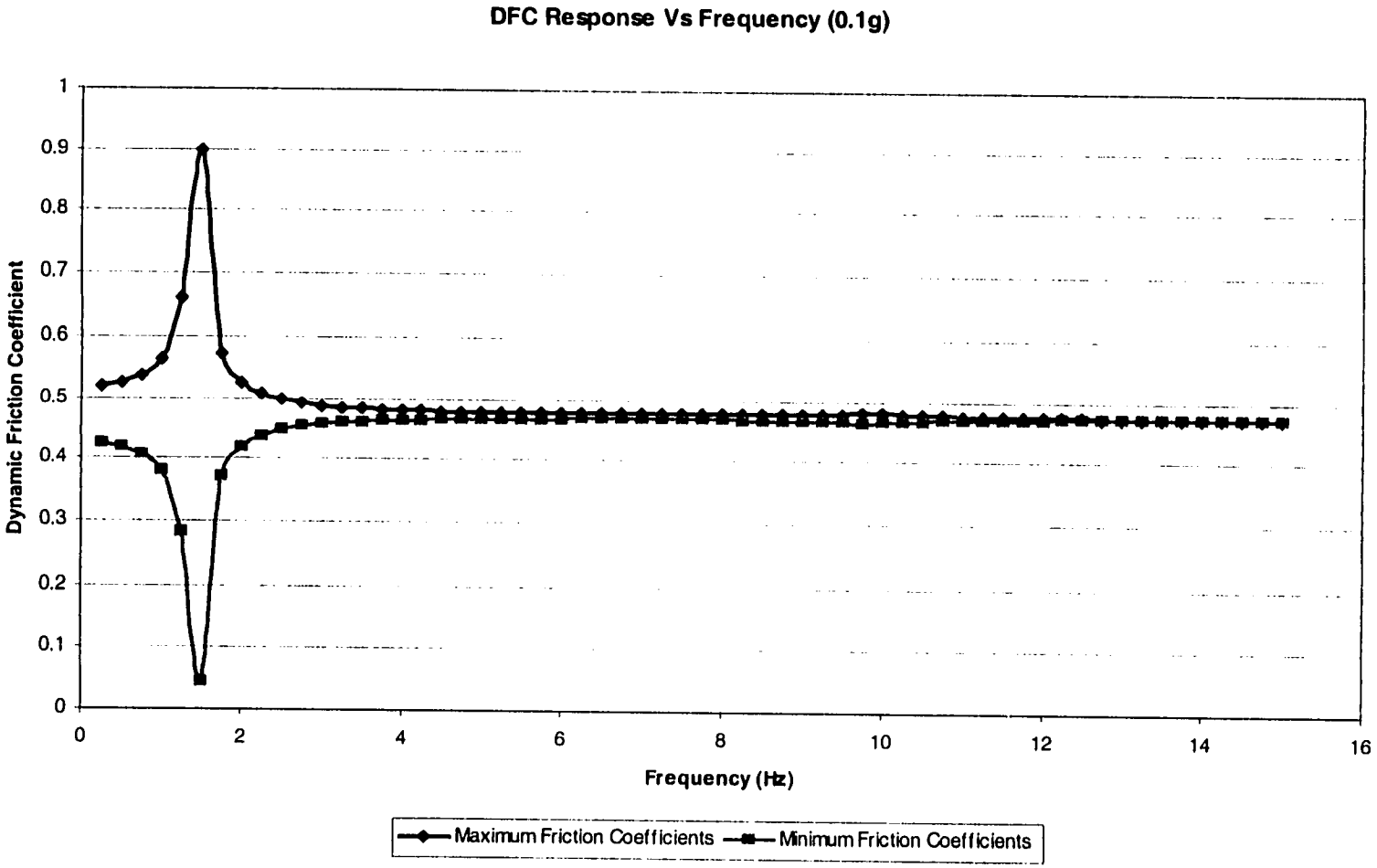

Figure 4.1 Simulated DFC Response to the Sinusoidal Excitation for input excitation amplitude 0.1g

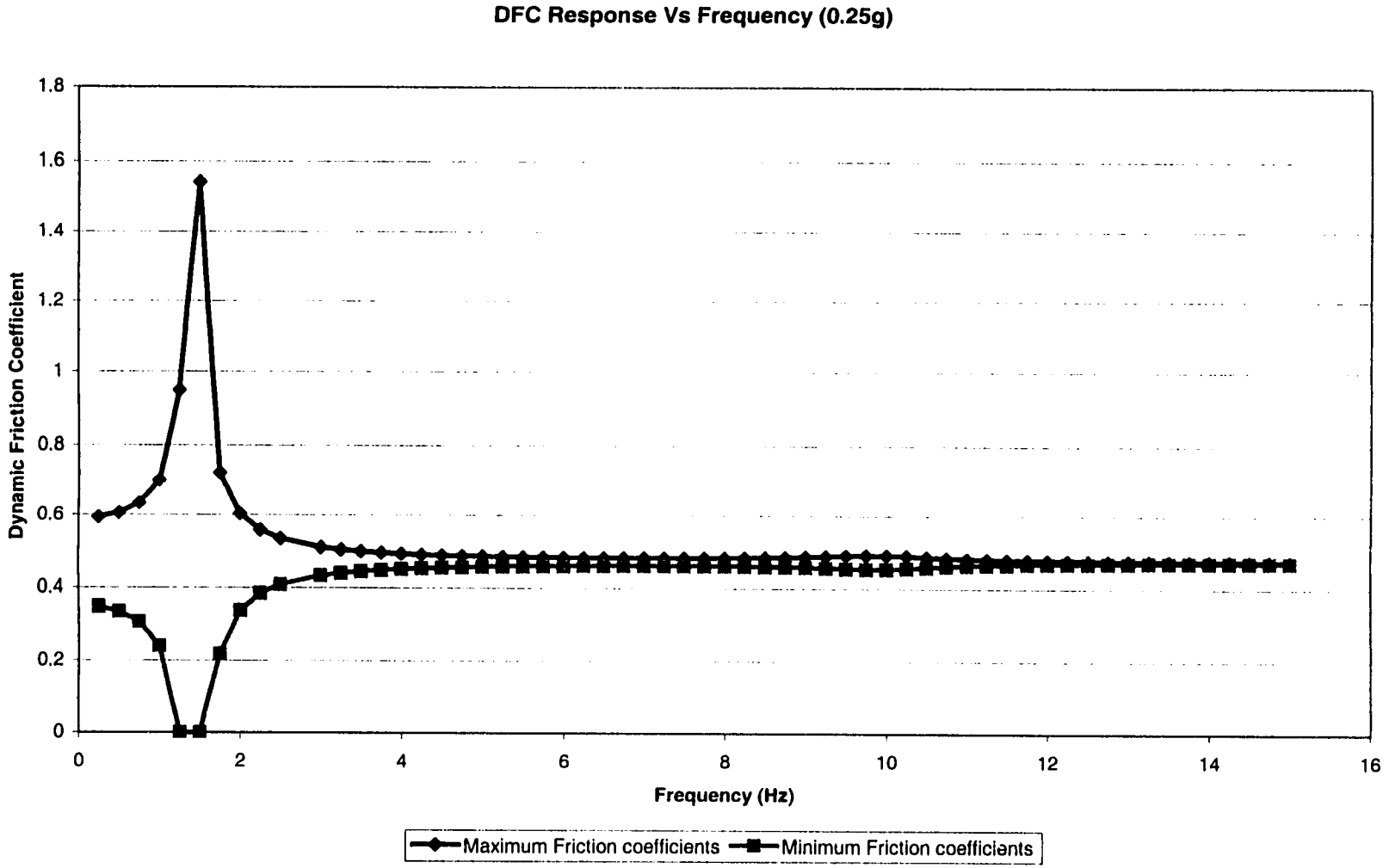

Figure 4.2 Simulated DFC Response to the Sinusoidal Excitation for input excitation amplitude 0.25g

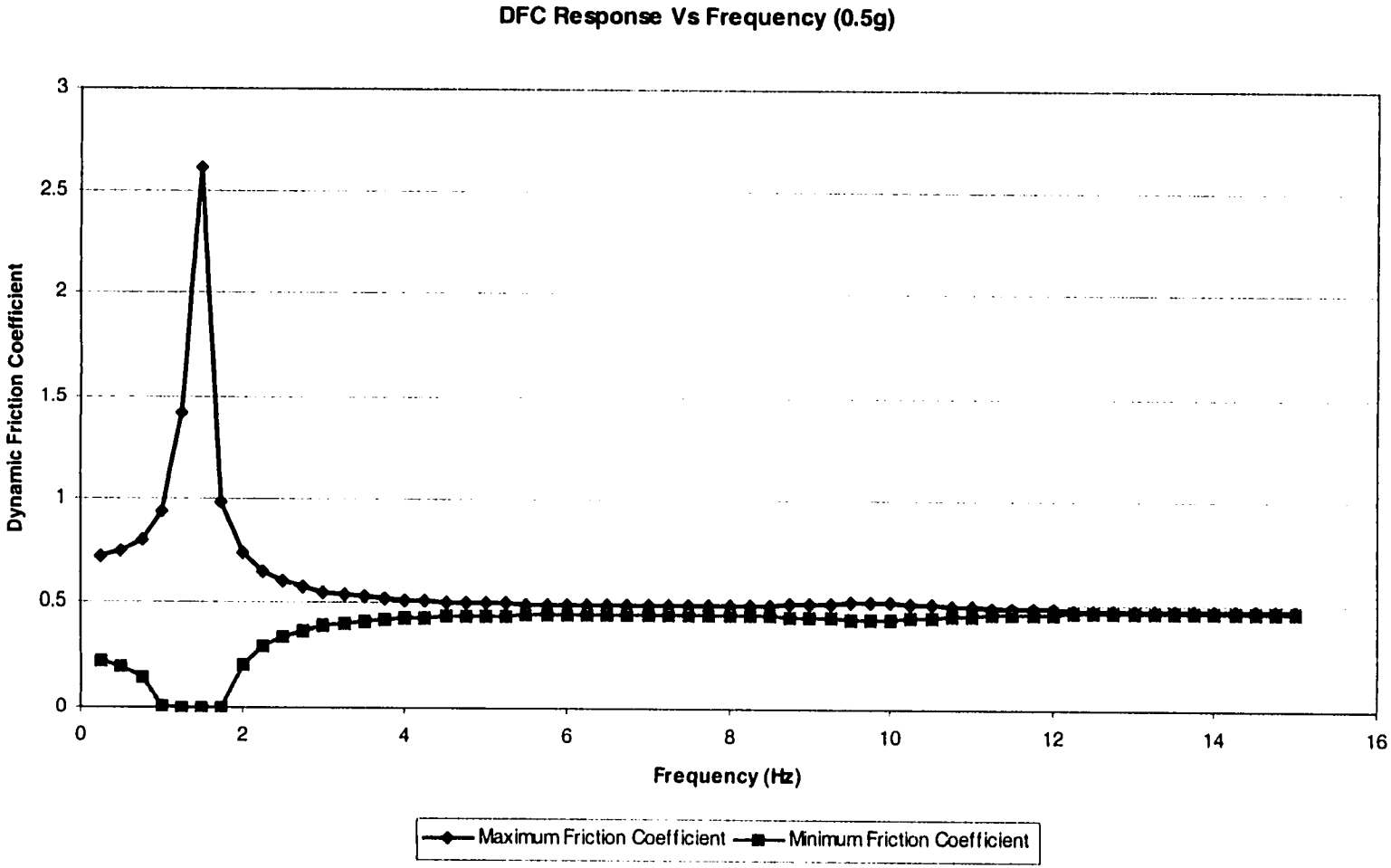

Figure 4.3 Simulated DFC Response to the Sinusoidal Excitation for input excitation amplitude 0.5g

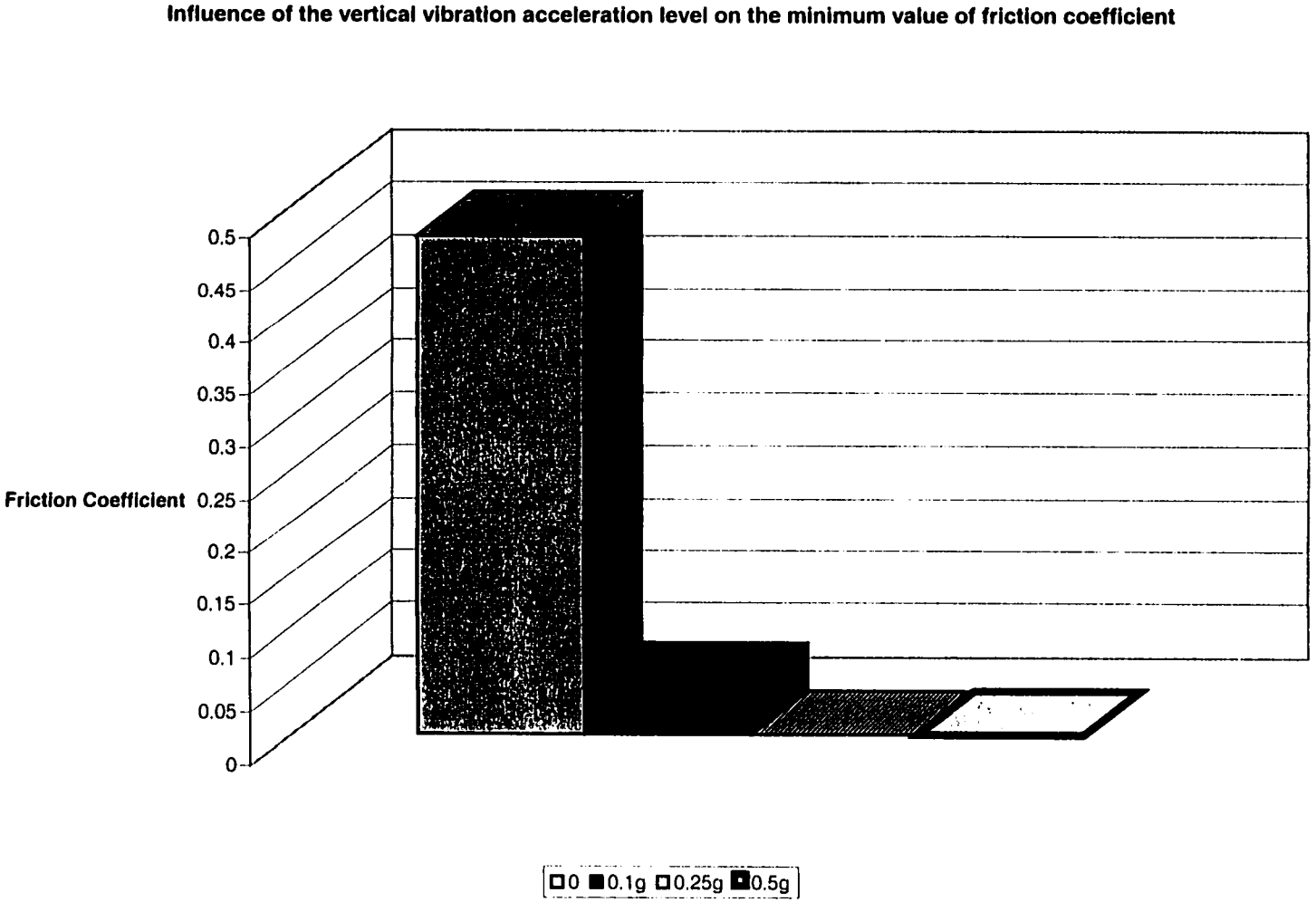

Figure 4.4 Influence of Vibration Level to the Minimum DFC

4.3 Four-Degree-of-Freedom Vehicle Model under Sinusoidal Excitation

In the four-degree-of-freedom vehicle model, a pitch motion was introduced. As discussed in the previous chapter, pitch motion will weaken or strengthen the friction force and will be induced by the oscillation of the angular motion. Though its effect due to the small pitch angle is not as significant as the bounce acceleration, the combination of two motions may produce significant instability of the cargo.

4.3.1 Sinusoidal Excitation

Basically, the core issue of the load security of the heavy vehicle is related to the characterization of the load on the deck in correlation with the vehicle and the road. In the vehicle-road system, bounce and pitch motions of the vehicle are determined by the vehicle related parameter, while the speed of the vehicle is related to the spectrum of the frequency input.

A sinusoidal excitation under constant amplitude will be used in simulation such that the frequency of excitation will be related to the forward speed V of the vehicle. For a given velocity, the input to rear-axle can be defined with a constant time delay such that

$$z_{0R(t)} = \bar{Z} \sin \omega(t + \tau) \qquad (4.5)$$

where the time delay τ is defined as a function of the wheelbase L, and the velocity V of the vehicle:

$$\tau = \frac{L}{V} \tag{4.6}$$

Assuming that the sinusoidal road has a fixed wavelength of 2 meter, the relationship between the frequency input and forward speed is:

$$\omega = \frac{V}{\lambda} = \frac{V}{2} \tag{4.7}$$

thus, to get the frequency ranged from 0.25 to 15 Hz, the input speed will vary from 0.5 m/s to 30 m/s. As a matter of fact, a loaded heavy truck, traveling at a speed of 108 km/h (30m/s), on a wavy road with wavelength of 2 meter and height of 3 cm will experience an extremely unstable state due to the wheel hop. In such case, the response of the system will be in a different non-linear state, which is beyond the scope of this thesis. A result of such situation will be presented but not be completely discussed.

4.3.2 Sinusoidal Response

Similar to the previous section, the equations of motion for the pitch plane vehicle models that include the friction model presented in Equation (3.9) to (3.12), and the input for the front and rear tires described above are solved simultaneously in time domain. The steady-state peak response values were collected to show the response of each of the components of the system. Discrete velocity ranged from 0.5 m/s to 30 m/s are utilized to obtain the frequency response in the range of 0.5 to 15 Hz.

The transmissibility response for the steady state peak displacement ratio of each mode was illustrated in Figure 3.9. As discussed above, the sprung mass bounce response has a dominant frequency somewhere between 1 and 2 Hz corresponding to its bounce natural frequency and pitch. Similarly, the unsprung masses exhibit the dominant natural frequency around 10 Hz. Figure 4.4 and Figure 4.5 show the DFC response to the sinusoidal excitation under different level of displacement magnitude.

Since the magnitude of the acceleration is proportional to the magnitude of the displacement with a ratio of the square of frequency, an increase in amplitude of displacement will yield increase in acceleration at the same frequency. This is reflected in the DFC frequency responses presented in Figure 4.4 and 4.5. High-level excitation makes the minimum DFC drops to lower values as shown in Figure 4.5.

While the DFC response has a similar trend in the low frequency area with the quarter vehicle model, the in-plane model showed a different response in the high frequency area, which occurs around 10 Hz, corresponding to the natural frequency of the tire. As discussed in a previous section, the excitation used in the quarter model is a sinusoidal signal of uniform acceleration. Thus, the deck acceleration transmitted from the suspension has the same trend as the transmissibility of the sprung mass. In the simulation of the in-plane model, the sinusoidal excitation is set to a uniform displacement peak signal. Thus, under these conditions, the acceleration is not constant any more. Since the acceleration is proportional to the square of the frequency, the absolute value of acceleration transmitted from the road in the high frequency range will become extremely large. Consequently, the acceleration level of the deck is also very

large, especially in the frequency range located around the natural frequency of the tire, though the transmissibility is the same as the one in the quarter vehicle model.

For example, in the case illustrated in Figure 4.5, the acceleration peak value of excitation at the frequency of 10 Hz is:

$$\left|\ddot{Z}_0\right| = \omega^2 Z_0 = (2\pi f)^2 Z_0 = (2*\pi*10)^2 *0.01 = 39.4 m/s^2 = 4g$$

Though this is an acceleration that would not occur in the practical situation, it revealed that the forward speed could affect the friction coefficient through changing the acceleration of vertical vibration. In other words, high speed may bring failure to the load security system that depends on the friction force only.

Figure 4.6 illustrates the response of the minimum dynamic friction force to the same road excitation of 0.01m level sinusoidal inputs, corresponding to the DFC response as shown in Figure 4.5. The results indicates that the minimum friction force is smaller than the static sliding friction force most of the time, and experiences two domains of very low value, as predicted from the response of DFC. The first low friction value occurs around the natural frequency of the sprung mass; the other is around the natural frequency of the unsprung mass. It is obvious that the excitation in the natural frequency range of sprung mass has more significant influence than the other. As a matter of fact, the wheel hop frequently occurs when the truck travels at high speed in an uneven road, especially for those trucks without full load, since the design of the truck parameters are based on fully loaded situation. When wheel hop takes place, the response of the system shifts in a non-linear state that would be described by alternate equation. It should be noted that in the simulation model of the cases corresponding to figure 4.4 to Figure 4.6, no wheel hop condition was assumed in the simulation. Figure 4.8 illustrates the

simulated DFC response of the in-plane model while encountering hop condition. The comparison of Figure 4.8 and 4.4 indicates that wheel hop occurs in the high frequency domain, around the natural frequency of the tire. The DFC response in that area displayed an unstable state, nevertheless, the basic trend of the minimum DFC value is to drop to a lower level that can cause failure of the friction load security system, through the motion of the cargo.

It is worth mentioning that there is no friction force if the load would not slide left/right, or forward/backward. However, the model is used to evaluate the reaction force and from there, to calculate the friction coefficient based on the friction model.

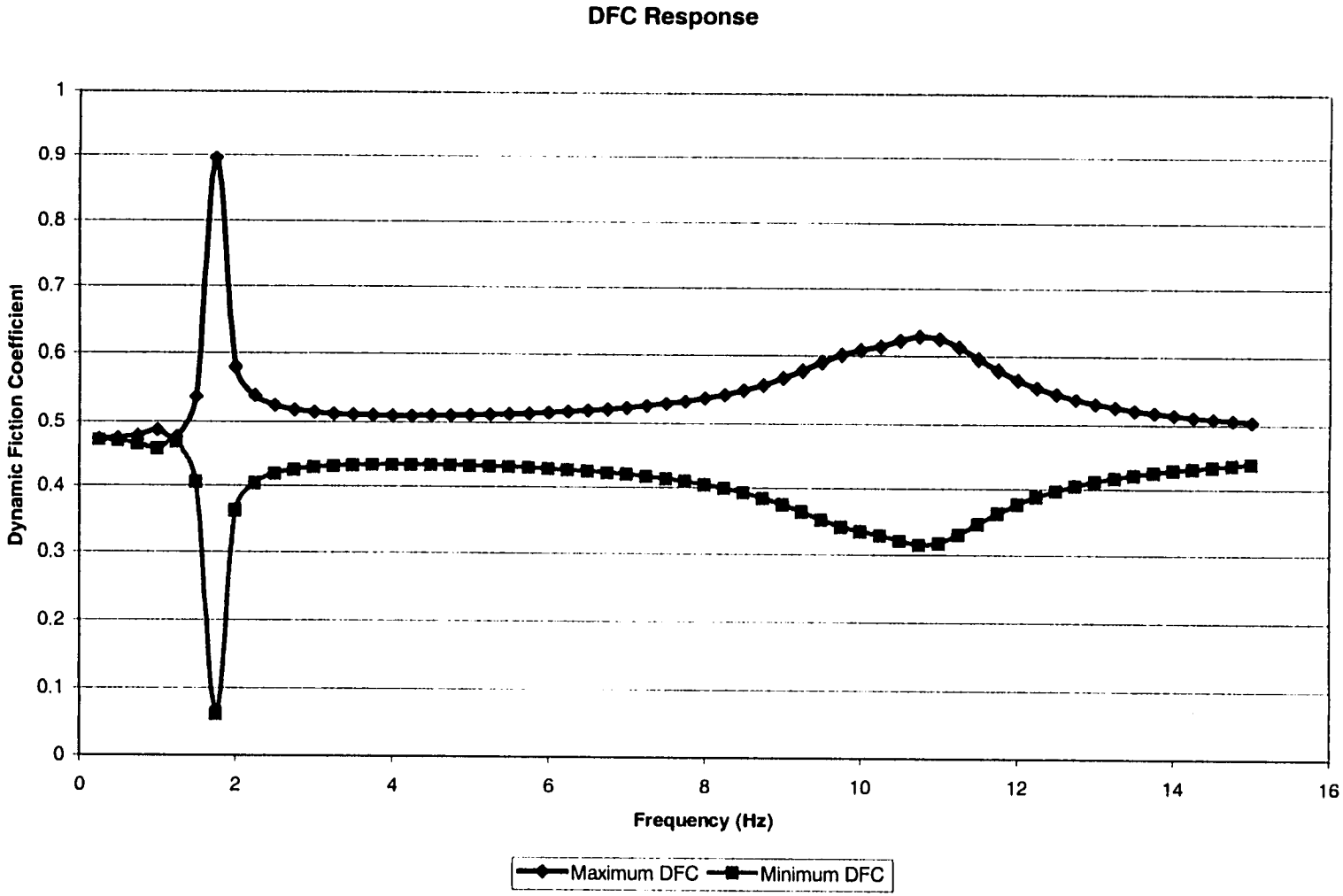

Figure 4.5 Simulated DFC Response to the Sinusoidal Excitation (Constant amplitude of 0.005m)

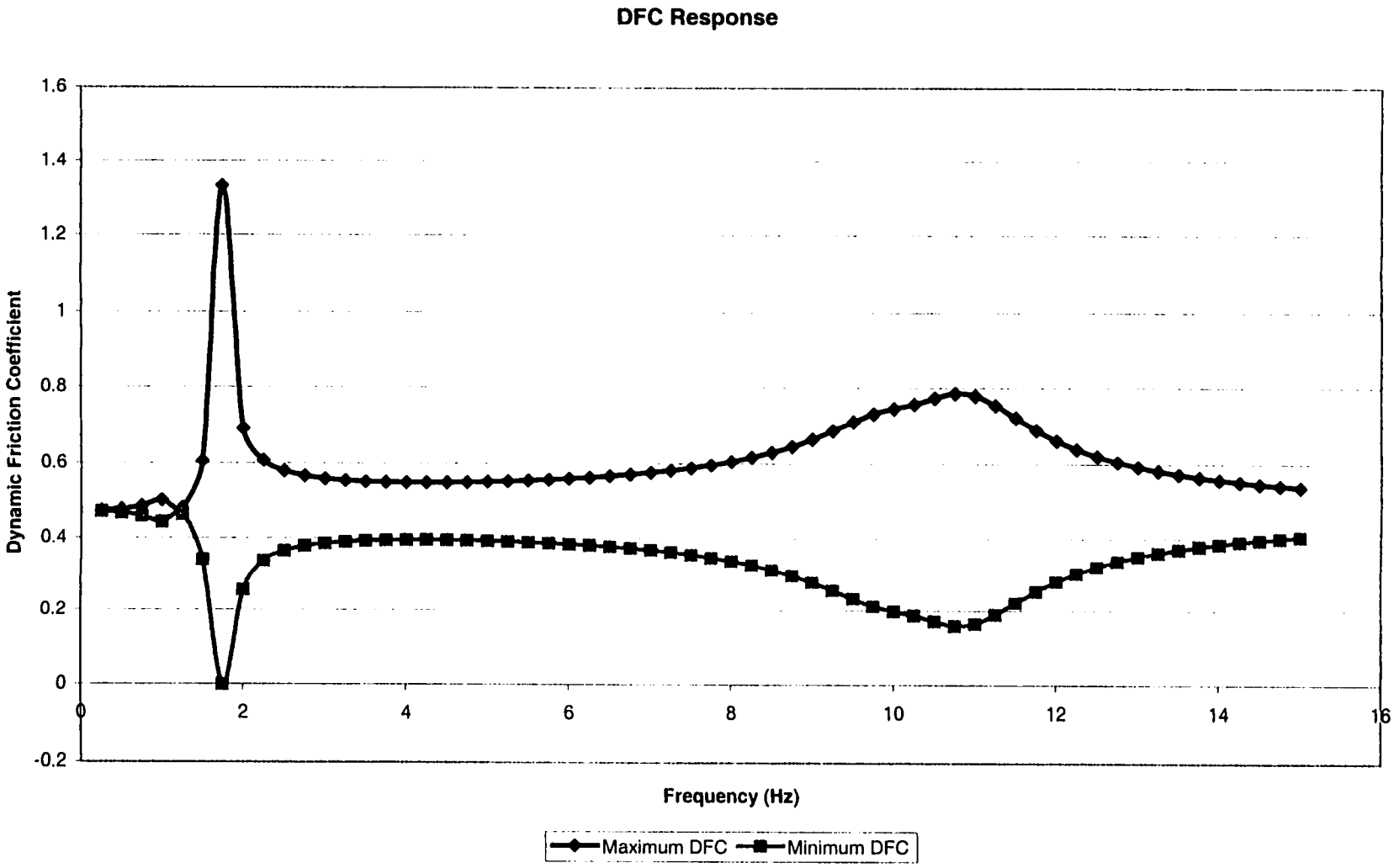

Figure 4.6 Simulated DFC Response to the Sinusoidal Excitation (Constant Amplitude of 0.01m)

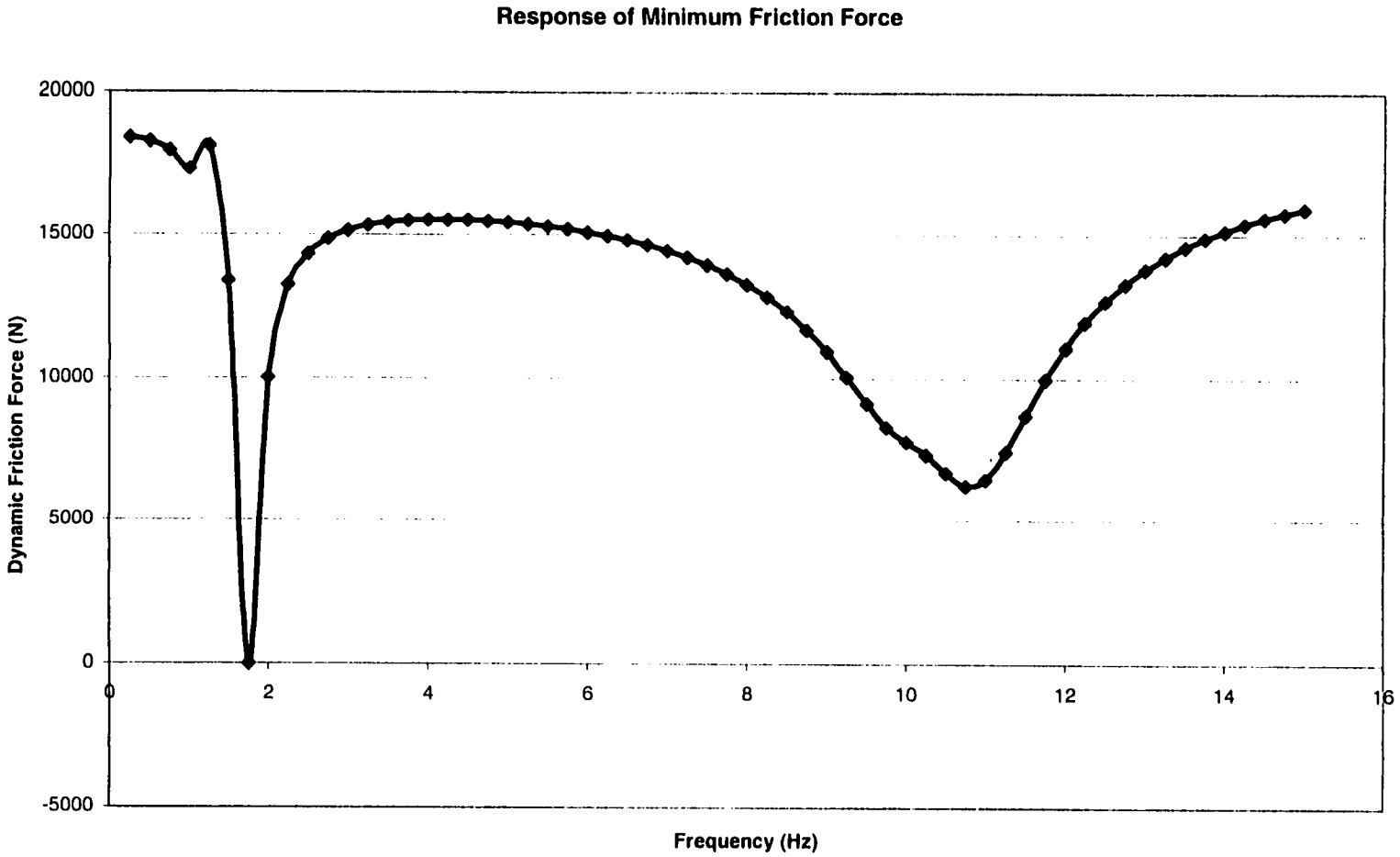

Figure 4.7 Simulated Response of Minimum Dynamic Friction Force

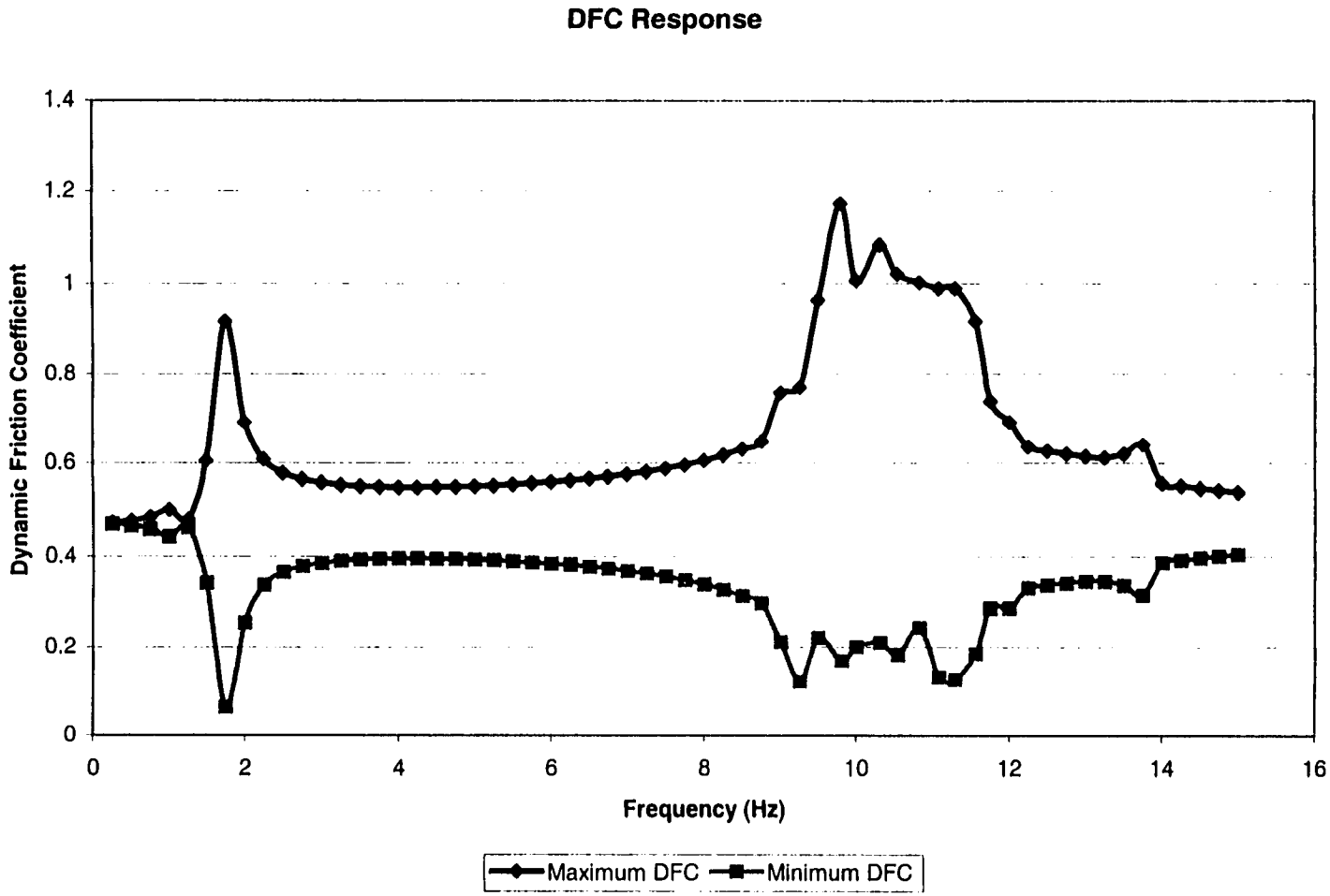

Figure 4.8 Simulated DFC Response to the Sinusoidal Excitation (0.005m of displacement magnitude with hop included)

4.4 Braking Performance of the DFC Model

As discussed in previous sections, if external forces are not applied in any direction to the cargo, the cargo would not slide even if the friction coefficient reduces to zero. The study of the response of the friction coefficient is directly linked to the potential trend of the friction force. Friction force is the tangential reaction force between two surfaces in contact and depends not only on the friction coefficient, but also on the trend of motion and relative velocity of the bodies. The normal reaction force between the cargo and deck is thus dependent on the of the horizontal acceleration resulting from a maneuver such as braking.

It can be easily shown that for a truck with load traveling at constant velocity on rough road, may induce a hop motion of the cargo. However, in the absence of any lateral or longitudinal acceleration, the cargo will keep the same relative position with respect to the deck as illustrated in Figure 4.9(a). On the other hand, as illustrated in Figure 4.9(b), if the vehicle motion is accompanied by a longitudinal acceleration such as in braking, the cargo will not drop back to the original position on the deck because of their relative different velocity that will shift the load by an amount δD on the deck. In other words, the horizontal acceleration is the basic force that would force the cargo to have horizontal motion.

In the analysis of the load security provided by friction force between the cargo and the deck, it is obvious that the cargo will move whenever the sum of the tangential resistance forces from the friction is lower than the external horizontal force applied to

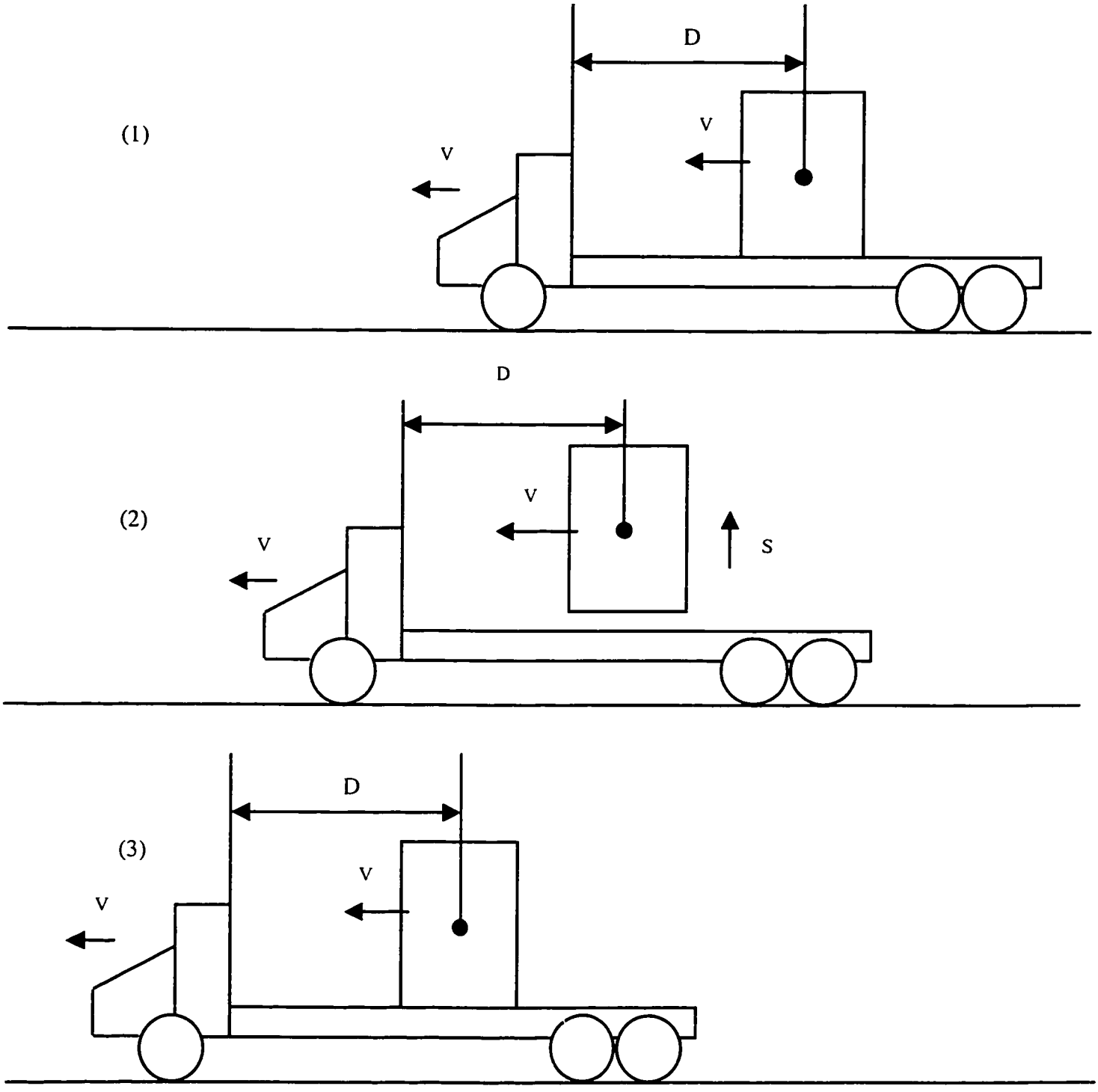

(a)

(1). The position of the cargo on a traveling truck; (2). The cargo is hopping from the truck deck ; (3).The cargo drop back to the original position on the deck

Figure 4.9 (a) A Diagram of cargo's moving on a traveling truck at constant speed

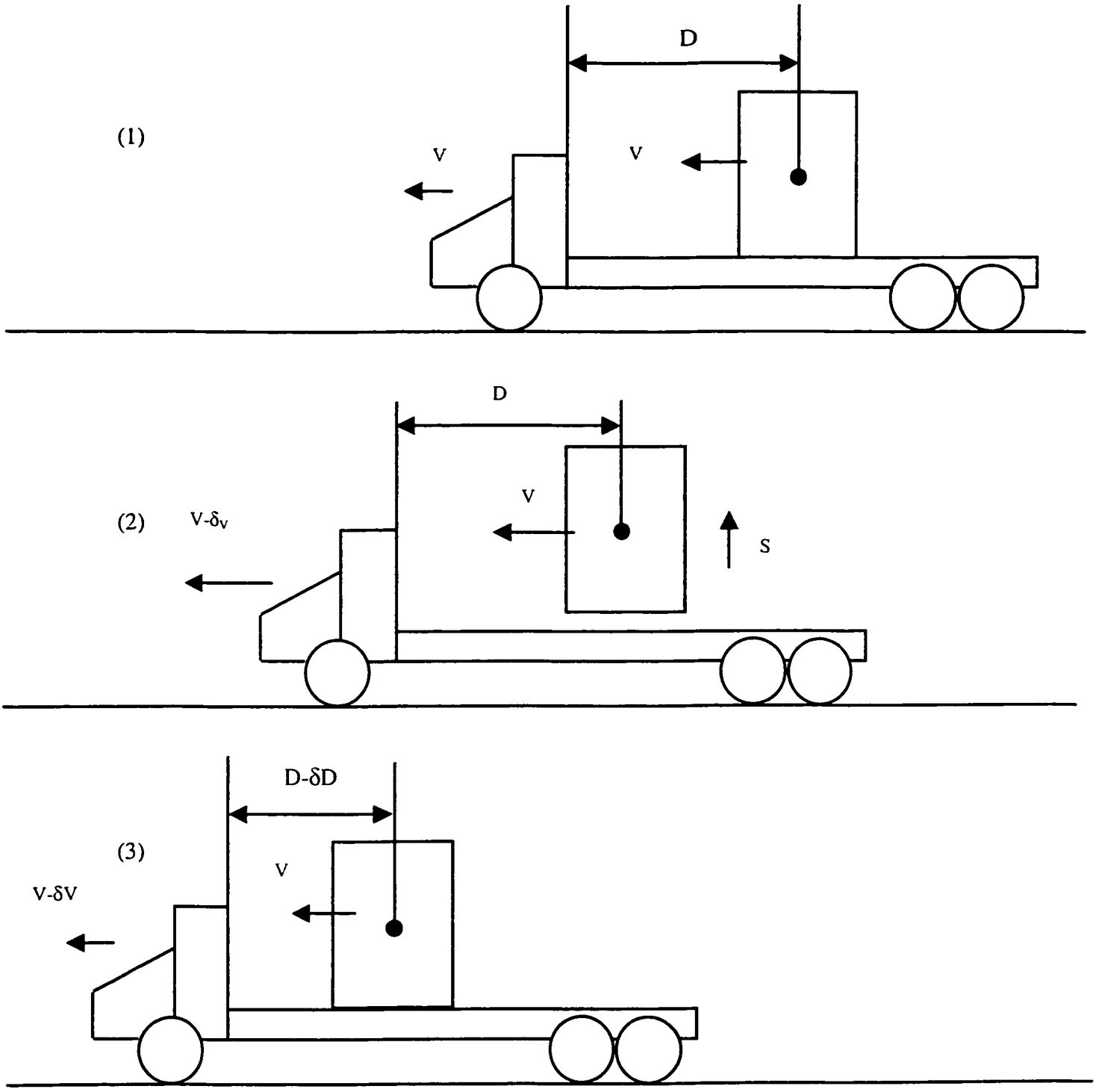

(b)

(1).The position of the cargo on a traveling truck; (2)The cargo is hopping from the truck deck while the truck brake; (3).The cargo drops back to a different position on the deck

Figure 4.9 (b) A Diagram of cargo moving on a traveling truck during braking

the cargo. When the vehicle is negotiating a maneuver involving braking or acceleration, the external force on the cargo will be the inertia. On the other hand, as discussed in Chapter 2, the horizontal acceleration has also influence on the breakaway friction coefficients as described in Equation (2.14). Basically, this influence occurs only at the very moment when the cargo starts to move. In the context of load security under vertical vibration, it is most appropriate to formulate the guidelines based upon sliding friction alone.

The braking performance of the DFC model and the trend of cargo movement in the brake maneuver is investigated. The simulation of the quarter-vehicle model described in Chapter 3 in conjunction with braking maneuver will be carried out in this section. It is assumed that the road profile is sinusoidal with a fixed wavelength of 2 meter with magnitude of 0.01-meter, and the truck travels with a uniform velocity before braking. An acceleration of 0.6g has been selected to represent the maximum longitudinal acceleration achievable by a heavy truck under "normal emergency" braking. Many aspects of the current load security requirements and system are based on this value [31]. Thus the different braking acceleration ranging from 0.2g to 0.5g will be utilized in the simulation to obtain the critical safe deceleration value for the specified model.

Simulation is first carried out for 20 seconds to ensure that the vehicle-cargo motion has reached its steady state for a uniform forward speed of 10 m/s (36km/h). Thus the excitation frequency is 5 Hz during the uniform speed period. When brake is applied, the speed and frequency will drop to zero introducing a frequency sweep for the vehicle motion.

Figure 4.10 to Figure 4.12 illustrate the simulation results of DFC vehicle model's braking performance with the deceleration rate of 0.2g.

Figure 4.10 presenting the time history of DFC indicate that there exists a variation in the DFC value during constant velocity due to the vehicle excitation. During this period the DFC varied between 0.38 and 0.57. When braking acceleration is applied at 20 second, the variation in DFC gradually increases as the frequency of vertical acceleration is reduced. The variation reaches its peak at around 24 second where the vehicle motion is around the sprung mass natural frequency. At this point, the DFC variation is found to be between 0,17 and 0.78. This minimum value represents a 38% reduction of static friction coefficient for a short period of time. Depending on the mass of the load, such reduction in DFC even for short period will promote a shift of the load. From these results, it further appears that the critical issue is the vertical vibration at sprung mass natural frequency. While braking from any speed on any road profile, before coming to full stop, the vehicle will experience vertical motion around the sprung mass natural frequency, and will be the likely critical moment for load security. It is easy to see that same scenario is possible during the process of acceleration from 0 speed to a high speed, as the vertical frequency of excitation sweeps from 0 through the natural frequencies

Figure 4.11 illustrates the comparison between the braking force and friction force. It is clear that there is a short moment when the friction force is smaller than the braking force. As noted before, the friction force curve in this figure is not the real friction force, but the potential trend of the friction force. Actually, when the value of the friction force appeared larger than the braking force in Figure 4.11, the real value was

equal to the braking force. Thus the final resultant of the external force applied to the cargo is shown in Figure 4.12. Integrating the acceleration that results from the overall external force will enable the calculation of sliding distance of the cargo, which is under the specific condition is found to be 1.73cm.

Figure 4.13 to Figure 4.15 illustrate the same simulation results under the deceleration rate of 0.3g. Similar trend of the DFC could be noticed in this case, and even more instants when the friction force is smaller than the braking force could be seen in Figure 4.14. The sliding distance in this case is larger and found to be 7.10cm. Such shift in cargo under 0.3g braking is significant.

Figure 4.16 to Figure 4.21 illustrate the simulation results under 0.4g and 0.5g respectively. The sliding distance increases to 29.8cm under 0.4g, while the sliding distance under 0.5g is 100.5cm. Both distances present a highly shift of the load which may directly influence the handling and stability of the vehicle as well as spillage of the load imposing direct danger to the safety of the cargo and other road users.

When comparing the 4 cases of deceleration rate, a simple conclusion could be drawn: the high braking deceleration may induce failure to the load security system that depends only on the friction force. Furthermore, the most critical point is when the vehicle speed reaches a speed that corresponding to excitation at the bounce natural frequency. Figure 4.22 shows the influence of the deceleration rate to the sliding distance for this vehicle model. From the results obtained in this section, it is evident that it is dangerous to rely on friction alone to provide security of load in vehicles. Even additional load security device used should consider this contribution of load security from friction.

The results obtained here from simple model of DFC braking performance can provide data for an effective design for constraining the cargo on the deck of the truck.

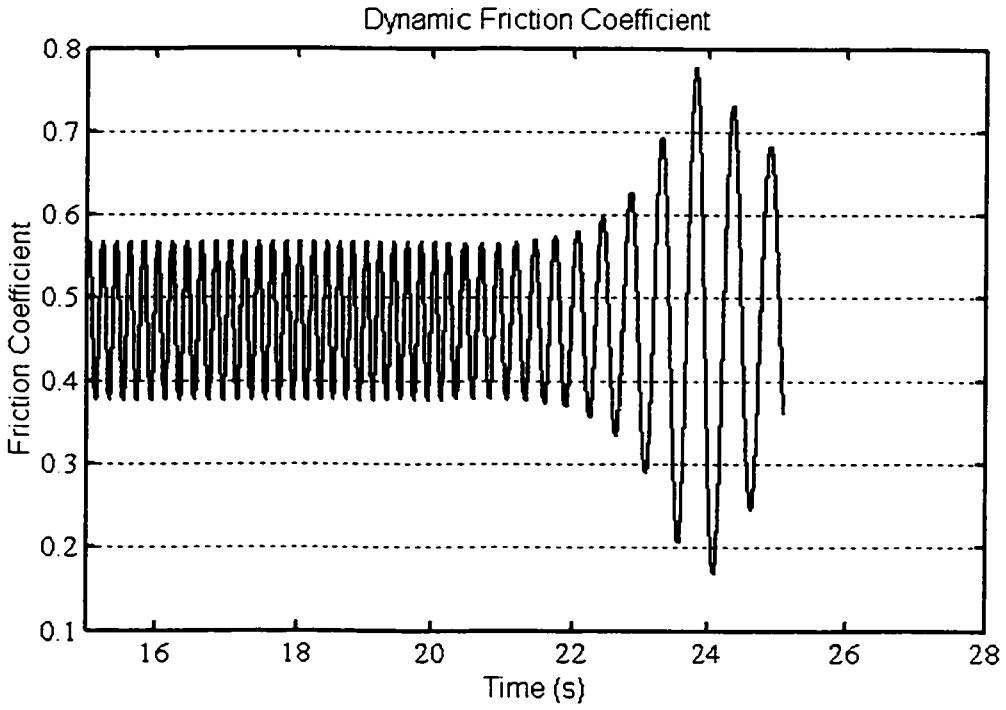

Figure 4.10 Time History of the DFC in Braking Maneuver (Deceleration 0.2g)

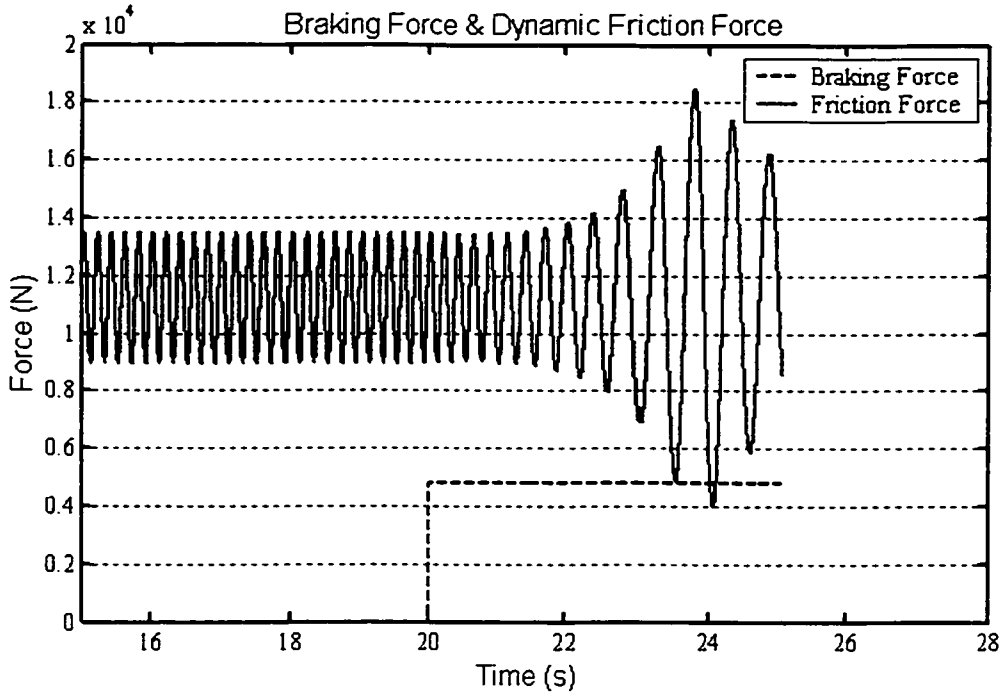

Figure 4.11 Time History of Dynamic Friction Force & Braking Force (0.2g)

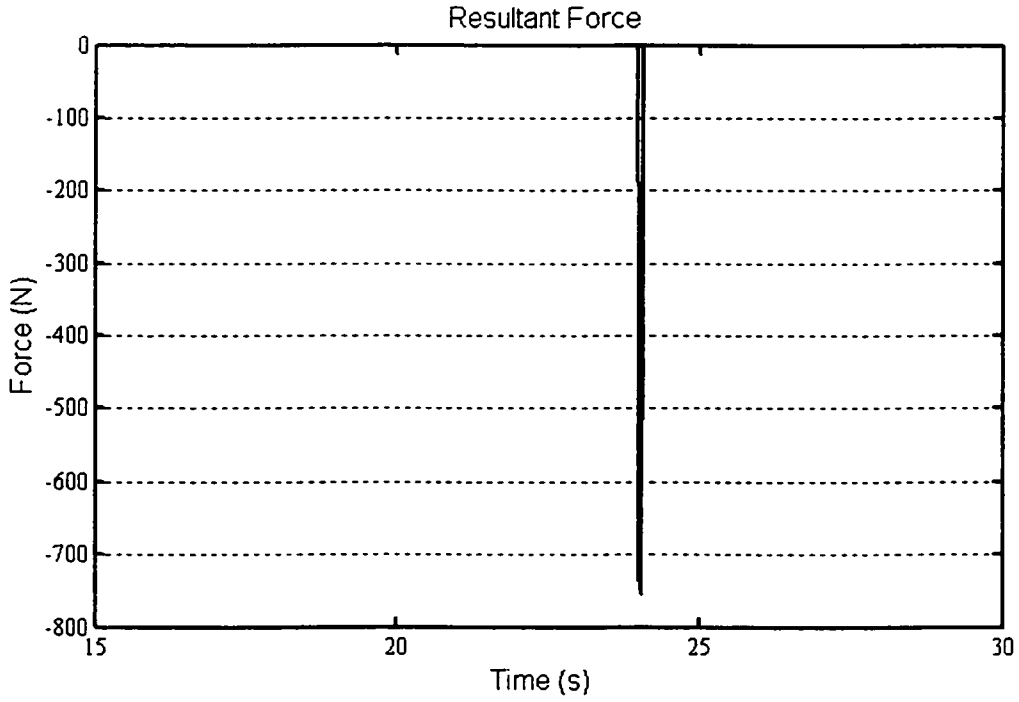

Figure 4.12 The Resultant Force Applied to the Cargo (0.2g)

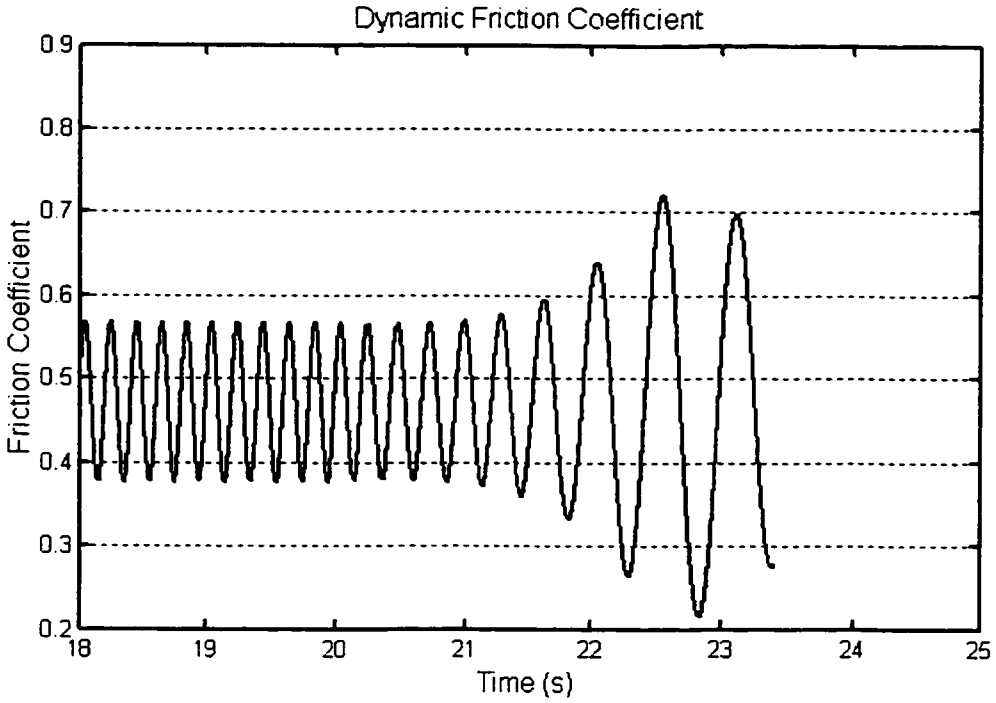

Figure 4.13 Time History of the DFC in Braking Maneuver (Deceleration 0.3g)

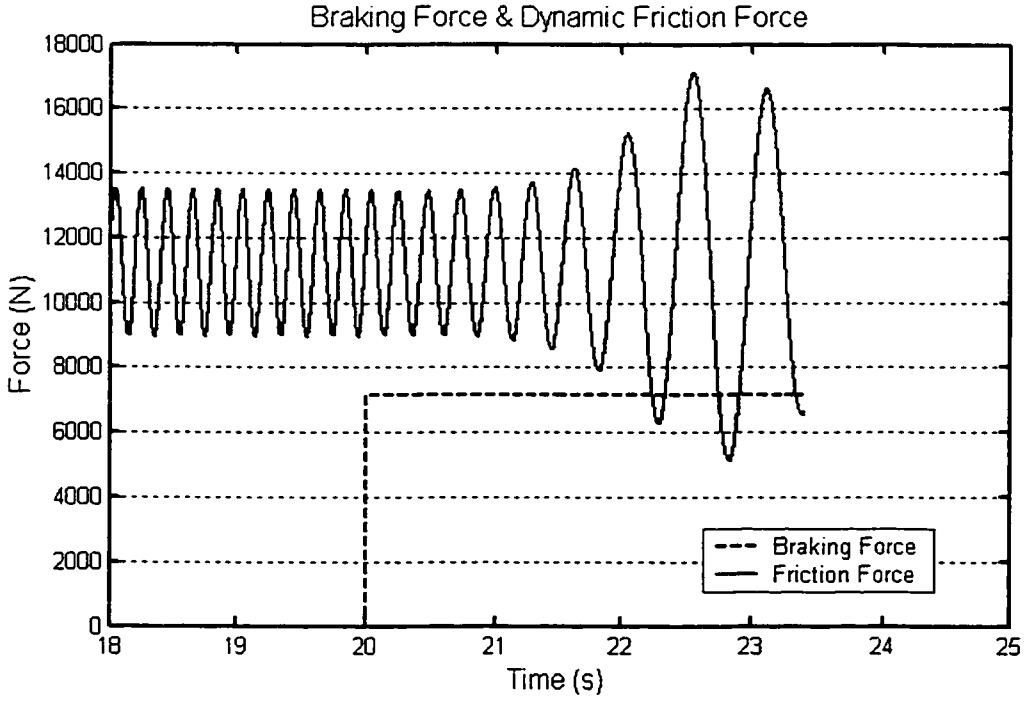

Figure 4.14 Time History of Dynamic Friction Force & Braking Force (0.3g)

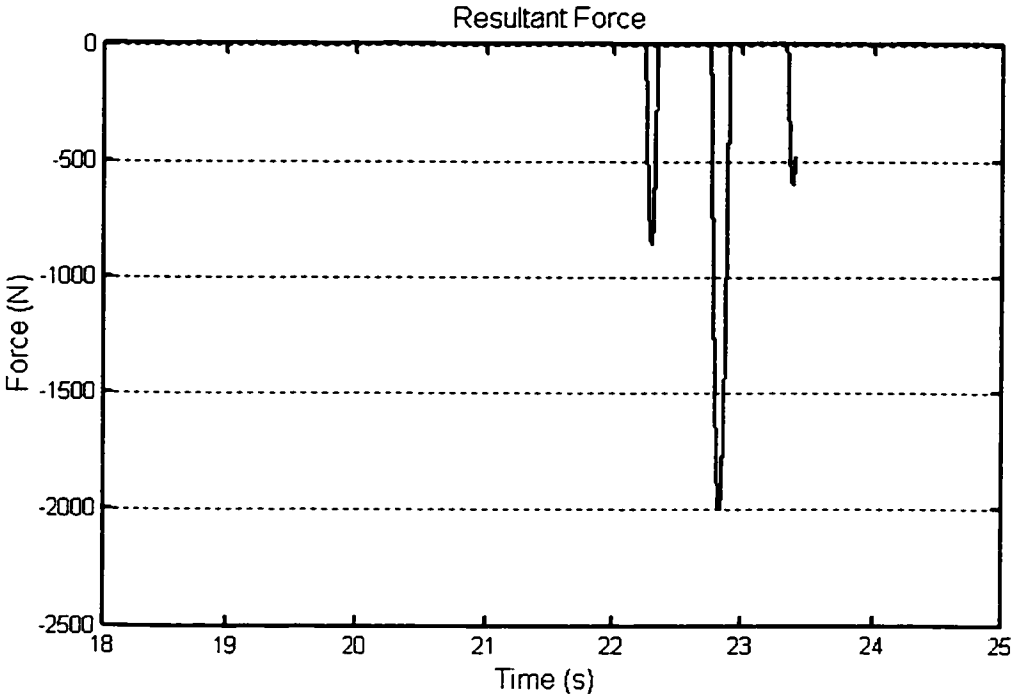

Figure 4.15 The Resultant Force Applied to the Cargo (0.3g)

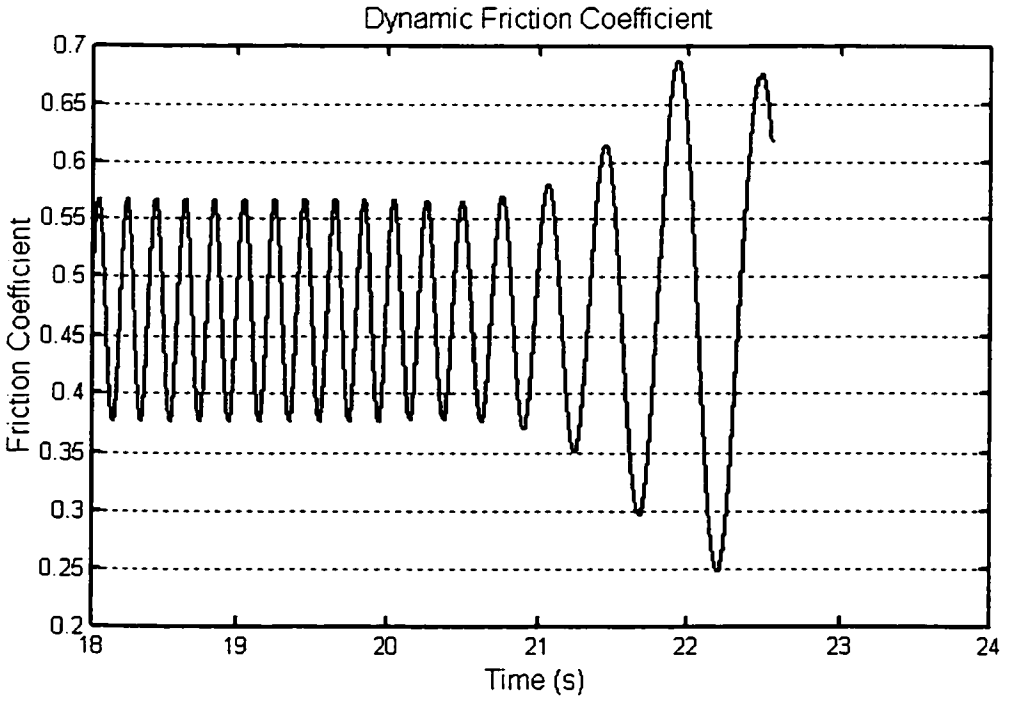

Figure 4.16 Time History of the DFC in Braking Maneuver (Deceleration 0.4g)

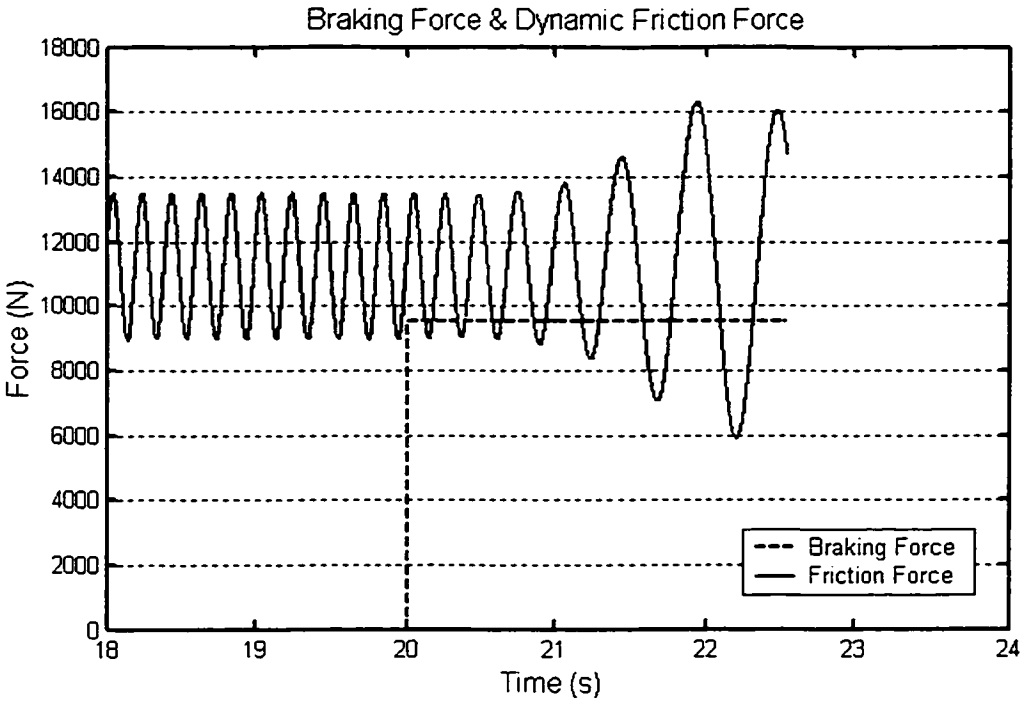

Figure 4.17 Time History of Dynamic Friction Force & Braking Force (0.4g)

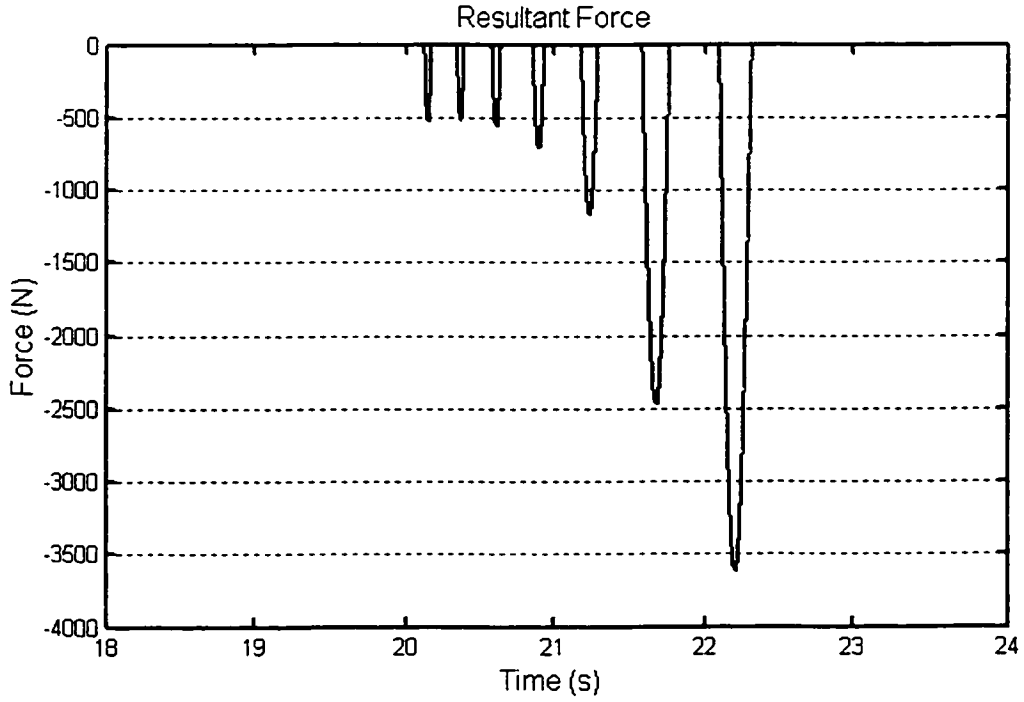

Figure 4.18 The Resultant Force Applied to the Cargo (0.4g)

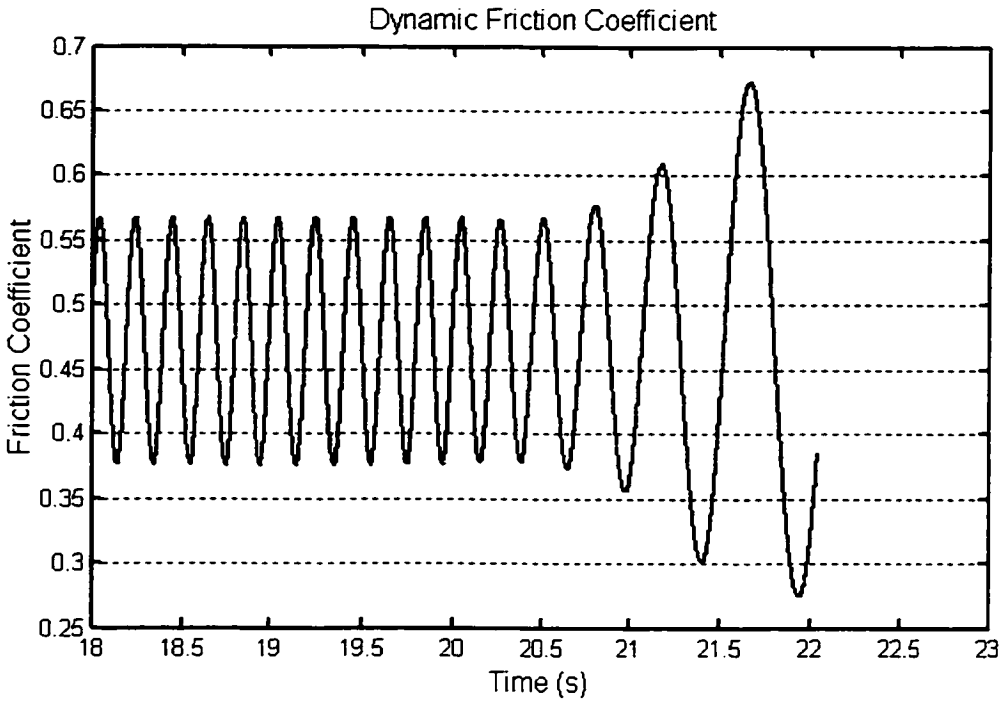

Figure 4.19 Time History of the DFC in Braking Maneuver (Deceleration 0.5g)

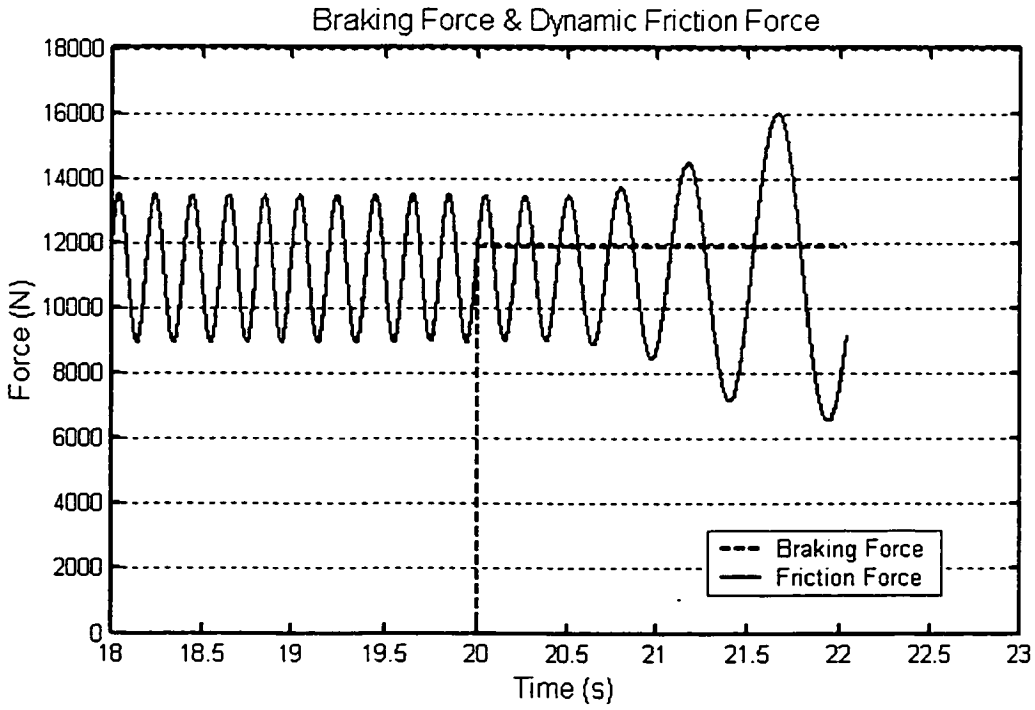

Figure 4.20 Time History of Dynamic Friction Force & Braking Force (0.5g)

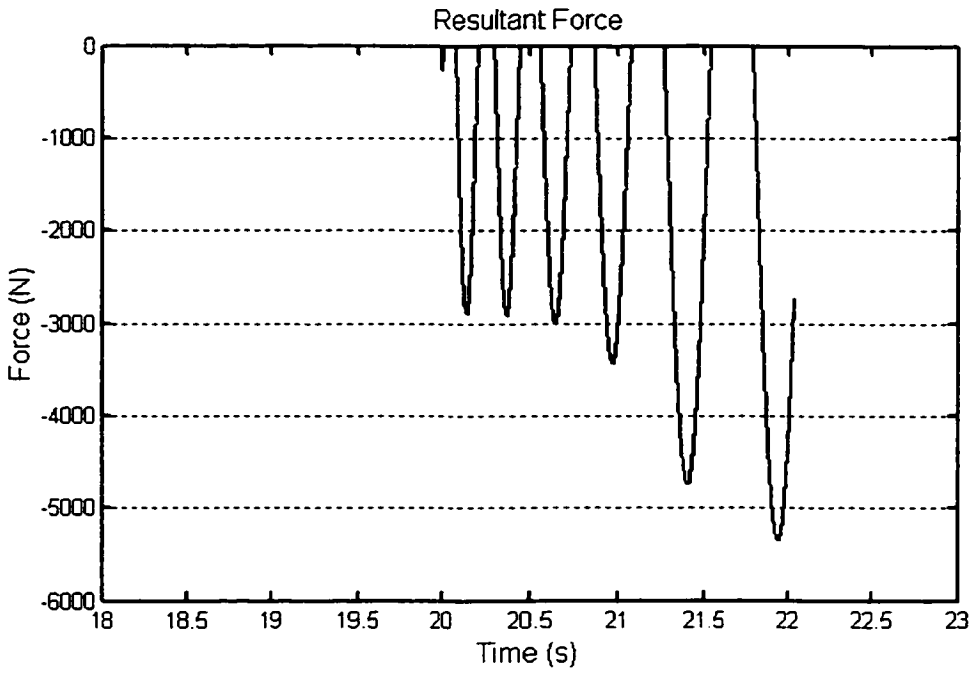

Figure 4.21 The Resultant Force Applied to the Cargo (0.5g)

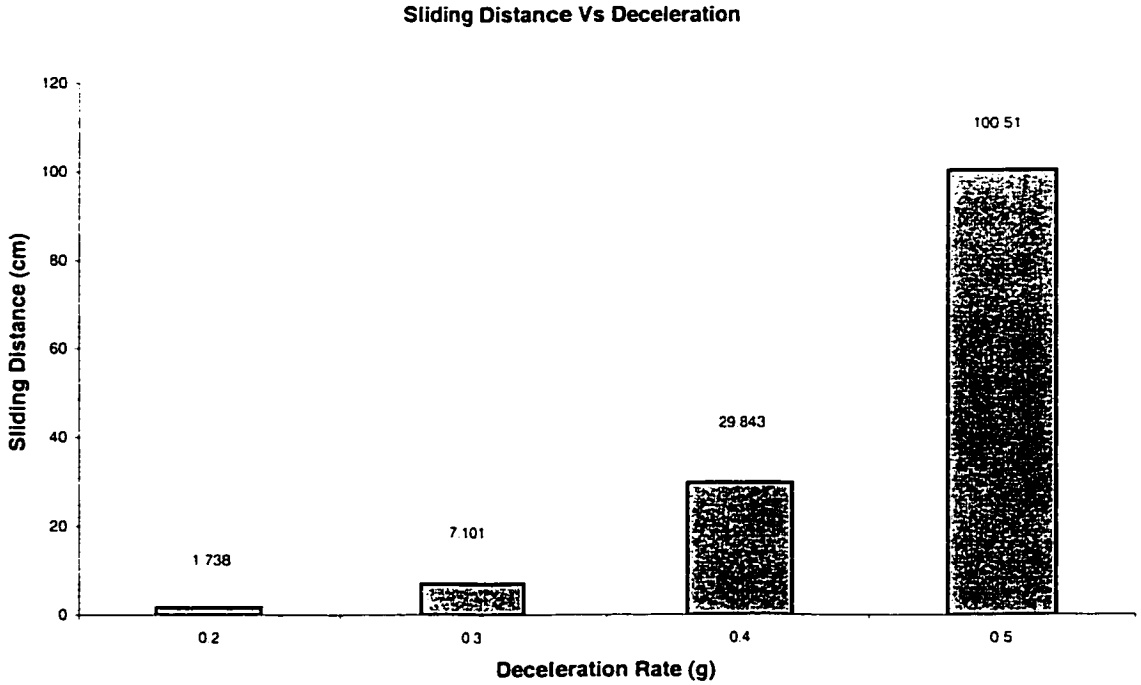

Figure 4.22 Influence of Deceleration Rate to the Cargo Sliding Distance

4.5 Influence of Vehicle Parameters on the Braking Performance

The same model can be used to investigate the relationship between the braking performances and vehicle parameters. The most important parameters in the vehicle vibration system are the rate of stiffness and damping coefficients of the suspension and tire. Thus varied suspension and tire parameters will be applied to study the dynamic behavior of the load.

The simulation uses the same quarter vehicle model and road profile used in the previous section. The braking deceleration rate is assumed to be 0.5g. It is recalled that in previous section, the sliding distance under 0.5g-deceleration rate was found to be 1.005m.

4.5.1 Varied Parameters of Suspension

The first simulation is to investigate the dynamic behavior of the load under different stiffness and damping coefficients of the suspension. Both parameters are varied st the same time from 25% to 300% of the baseline value. Table 4.1 shows the simulation results under this situation, and Figure 4.23 illustrate the relationship between the load sliding distance and varied parameters. It's obviously that the sliding distance is linear to the changing rate of the combination of stiffness and damping. To investigate that which parameter influences the sliding distance mainly, further simulation is carried on with only one parameter varied at a time. Table 4.2 shows the simulation results under varied stiffness and damping. Figure 4.24 illustrates the comparison of two results.

Table 4.1 Simulation Results (Based on the Parameter in Previous Section)

Stiffness	Damping Coefficient	Sliding Distance (m)
25%	25%	0.554
50%	50%	0.662
75%	75%	0.826
100%	100%	1.005
125%	125%	1.183
150%	150%	1.351
175%	175%	1.51
200%	200%	1.657
250%	250%	1.922
300%	300%	2.156

Table 4.2 Simulation Results (for one parameter varied)

Stiffness (With fixed damping)	Sliding Distance (m)	Damping (With fixed Stiffness)	Sliding Distance (m)
25%	0.563	25%	1.014
50%	0.671	50%	1.008
100%	1.005	100%	1.005
150%	1.361	150%	1.007
200%	1.686	200%	1.013
250%	1.97	250%	1.022
300%	2.226	300%	1.035

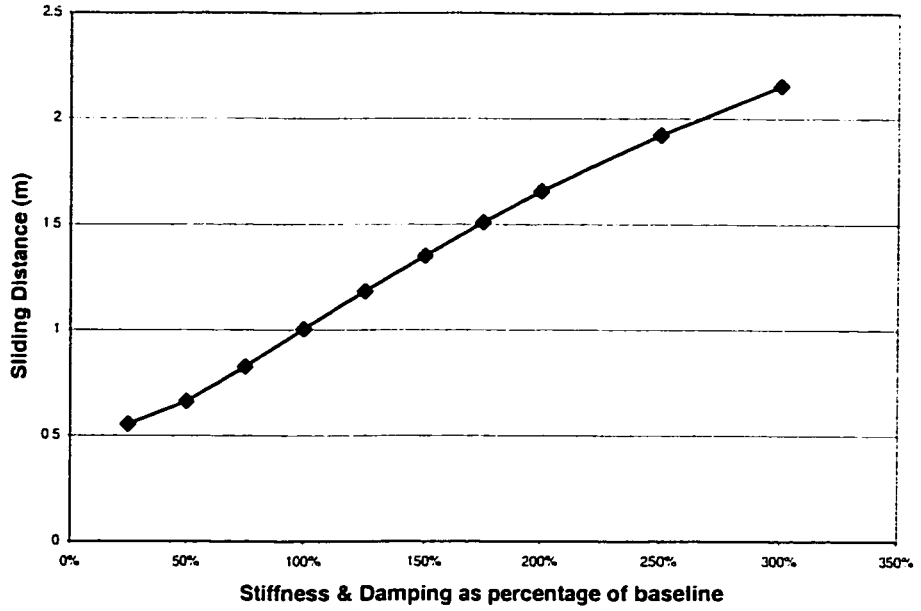

Figure 4.23 Sliding distance of the load for varied suspension parameters

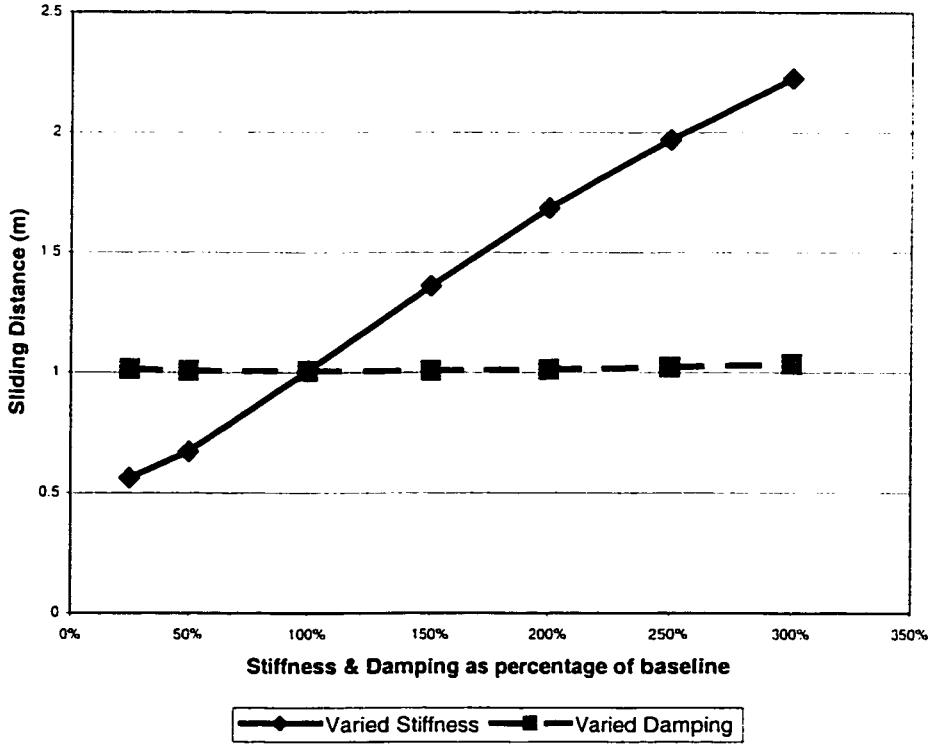

Figure 4.24 Comparison of the influences of suspension stiffness and damping

Comparing the curve of varied stiffness in Figure 4.24 with the curve in Figure 4.23 reveals that only suspension stiffness effect the sliding distance performance of load under braking while damping influence is negligible. As the suspension stiffness is increased, the natural frequency of sprung mass increases, which in turn lead to reduced damping ratio given by: $C/2\sqrt{km}$. For the vehicle parameters used, increase in k, increases more significant effect on the vertical response than those of reduced C.

4.5.2 Varied Parameters of Tire

The same simulation is finally repeated for variation of tire parameters. Both tire stiffness and damping value are first varied as percentage of nominal value from 25% to 300%. Table 4.3 summarizes the results in terms of sliding distance for the load when breaked from 10 m/s with deceleration of 0.5g. These results also presented in Figure 4.25 show similar trend as that of variation in suspension properties. In this case, however, the influence is significantly less that of suspension properties. Furthermore, in this case, the effect of increase in parameter is less than the effect of decrease. This is due to the fact that softer tire stiffness has more influence on the ride vibration leads.

The results for variation of one tire parameter at a time are presented in Table 4.4 and Figure 4.26. Once again these results demonstrate that the contribution of tire damping for load shift performance is insignificant while the tire stiffness has certain influence.

Table 4.3 Simulation Results (Based on the Parameter in Previous Section)

Stiffness	Damping Coefficient	Sliding Distance (m)
25%	25%	0.667
50%	50%	0.829
75%	75%	0.935
100%	100%	1.005
125%	125%	1.054
150%	150%	1.09
175%	175%	1.117
200%	200%	1.138
250%	250%	1.169
300%	300%	1.19

Table 4.4 Simulation Results for one parameter varied

Stiffness (with fixed Damping)	Sliding Distance (m)	Damping (With fixed Stiffness)	Sliding Distance (m)
25%	0.667	25%	1.005
50%	0.828	50%	1.005
100%	1.005	100%	1.005
150%	1.09	150%	1.005
200%	1.138	200%	1.004
250%	1.17	250%	1.004
300%	1.19	300%	1.004

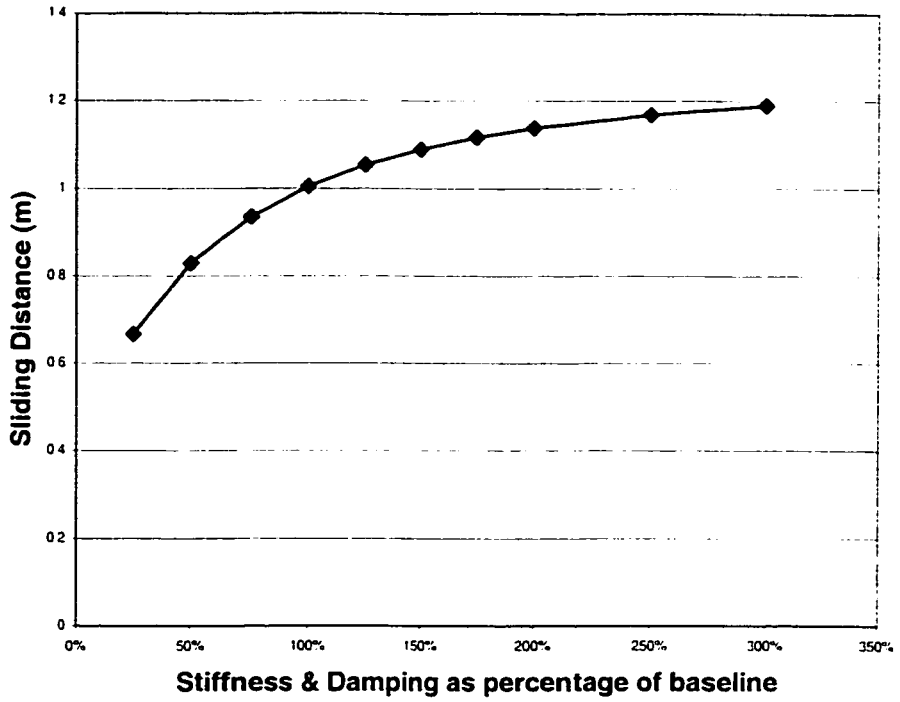

Figure 4.25 Sliding distance of the load for varied tire parameters

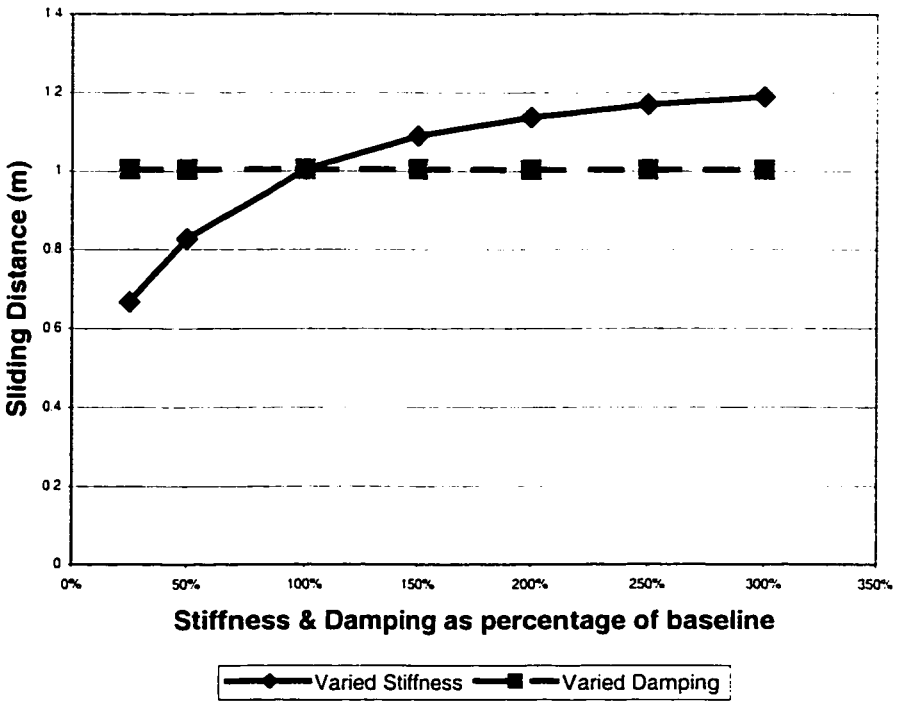

Figure 4.26 Comparison of the influences of tire stiffness and damping

4.6 Summary

The vehicle models in conjunction with the DFC model created in Chapter 3 were evaluated assuming sinusoidal excitation as input to the point contact wheel. Frequency responses were evaluated for both quarter vehicle model and in-plane model. The results indicated that natural frequency of the sprung mass has a more significant effect on the DFC peak value than that of the frequency of tire. In the view of load secured only through friction, the low frequency excitation will significantly induce the slide tendency of the cargo due to the huge reduction of the friction force, which may come down to zero under certain condition and instants. The results of the simulation of in-plane model also revealed that the natural frequency of the unsprung mass has some influence on the DFC peak value, which would correspond to the high-speed range only. The level of influence is much less than that of the sprung mass.

A simulation of braking maneuver was carried out with a quarter vehicle-DFC model. Different deceleration rate were utilized to study DFC performance and the trend of cargo sliding. The results indicate that the occurrence of the friction force loss can always happen during the process of braking, mainly in the low frequency area response. Moreover, under this specific model and specific sinusoidal excitation, the deceleration rate of more than 0.3g will produce an unacceptable sliding distance of the cargo on the deck. The modeling also indicates that a higher deceleration rate in braking would induce a higher insecurity of the cargo on the deck, result that corresponds with the real situation under emergency braking.

Further simulation investigated the relationship between the braking performance and vehicle parameters. Results indicated that the rate of stiffness, either in suspension or in tire, plays the main role in the influences to the load sliding distance from the vibration components of the vehicle. The influence of suspension stiffness is significant more than of the tires.

CHAPTER 5

LOAD SECURITY FROM FRICTION UNDER RANDOM ROAD EXCITATION

5.1 Introduction

Road surface description plays an important role in ride quality evaluation of the heavy vehicles. While the excitation from ground in the form of sinusoid waves were used in the modeling to provide a basis for comparative evaluation of DFC, the approach could not serve as a valid basis for studying the actual ride behavior of the vehicle since surface profile are rarely of simple forms. It has been recognized that ground profile should be more realistically described as a random function. The main characteristic of a random function is that its instantaneous value cannot be predicted in a deterministic manner.

A multi-axle vehicle traveling on a roadway is subjected to displacement inputs at all of its road-wheel contact points. Consequently, a complete description of the road surface is sought to adequately describe the displacement imposed at each wheel and all correlations between the displacements. The concept of power spectral density is used to describe the randomly irregular road surface roughness. Various analytical techniques of increasing complexity have been developed to describe stochastically the road surface undulations [53, 54, 55]. In the previous investigation at CONCAVE Research Center, measurements were taken on several different roads in and around Montreal. One of the

measurement will be used as a sample in the simulation of the vehicle DFC model as the road file input to study the friction force response to the random vertical vibration. The braking performance simulation in conjunction with the cargo motion will also be presented.

5.2 Characterization of Road Profile

The dynamic characteristics of the road vehicle, and thus the dynamic wheel loads and ride quality are strongly related to the road profile. As motioned before, the roads basically exhibit randomly distributed roughness. A number of studies have established that road roughness closely follows a Gaussian distribution, and proposed spatial spectral density functions to characterize the mean roughness profiles of various roads. Damien reported the roughness profiles of various Ontario roads, ranging from extremely smooth to rough roads [56][57]. Measurement of the Montreal roads carried out at CONCAVE Research Center included different rough level roads. Since the comparison of the response to the different roads does not represent an objective of this work, only one road profile is used in the simulation. For illustration one average roughness city road was considered. Figure 5.1 illustrates the power spectral density (PSD) of the roughness of Road Cote-des-Neiges in Montreal. In the figure, measurements taken from four wheels are shown together, and the left one is used in the quarter vehicle model.

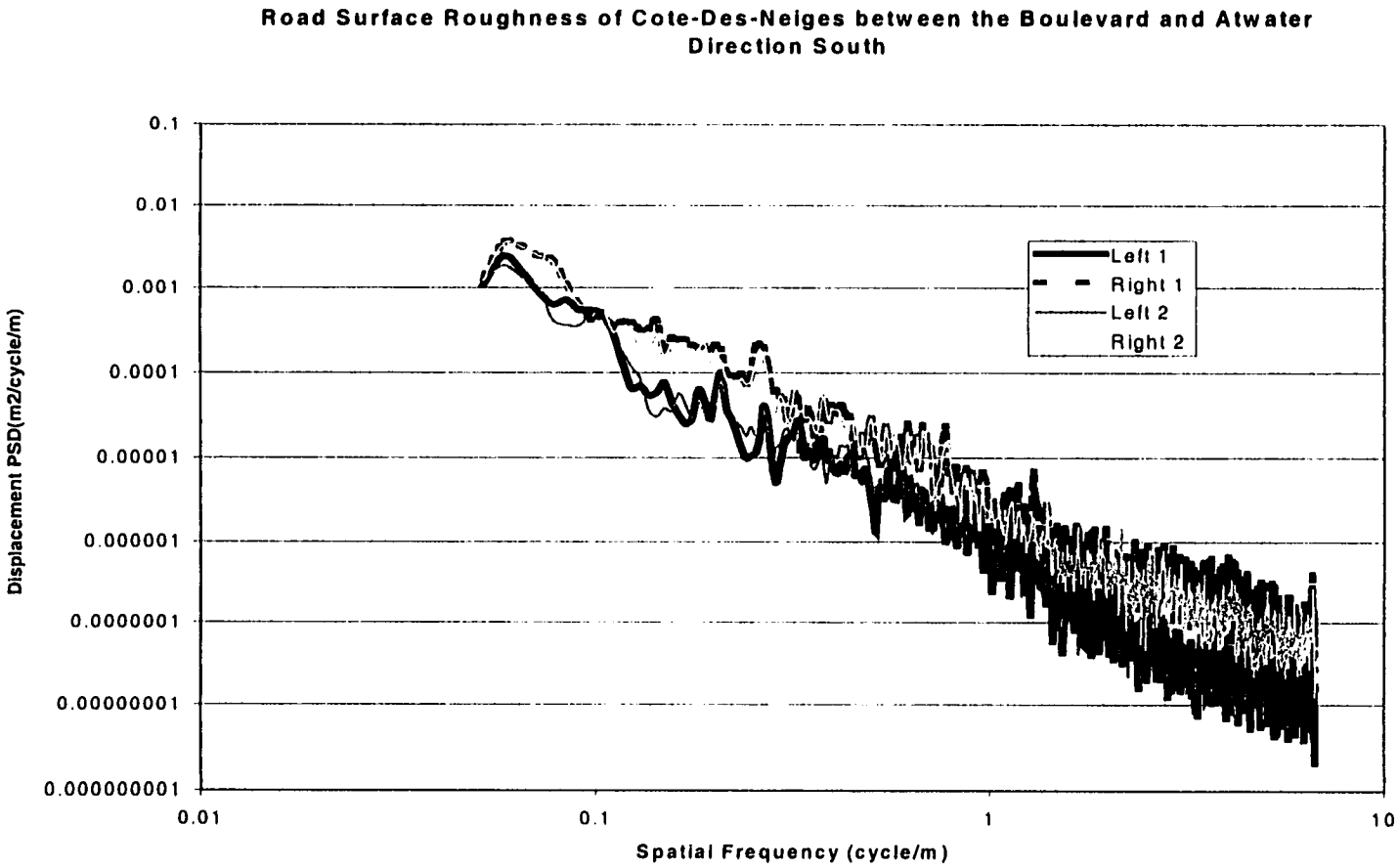

Figure 5.1 Displacement Power Spectral Density of Road Portion of the Cote-des-Neiges in Montreal

5.3 Response of DFC Model to the Random Excitation

Performance analysis through computer simulation on analytical model requires accurate characterization of the model parameters, component characterization and input description. The analytical model developed for this investigation consists of a number of simplifying assumption including simplified model---the quarter vehicle modeling and dynamic friction force modeling, as is described in chapter 3. The excitation used in the simulation is that the road profile of "Cote-des-Neiges" Road described previously. Figure 5.2 illustrated the PSD of bounce acceleration of sprung mass. This clearly indicates two resonance frequencies, one in the lower frequency and the other in the higher frequency, ranged corresponding to the natural frequencies of the suspension and tire respectively, as investigated in Chapter 3. This proves that the vehicle model proposed in previous chapter can yield consistent results under the random road excitation. Figure 5.3 illustrates the PSD of the simulated pattern of the friction force between the cargo and surface of the deck. This figure clearly indicates two peaks in the same position ranged as in the acceleration PSD. The peak in the lower frequency range is higher than the one in the higher frequency range. This states that the largest friction force level is at the bounce resonance frequency of the suspension, which validates the assumption made in previous chapter.

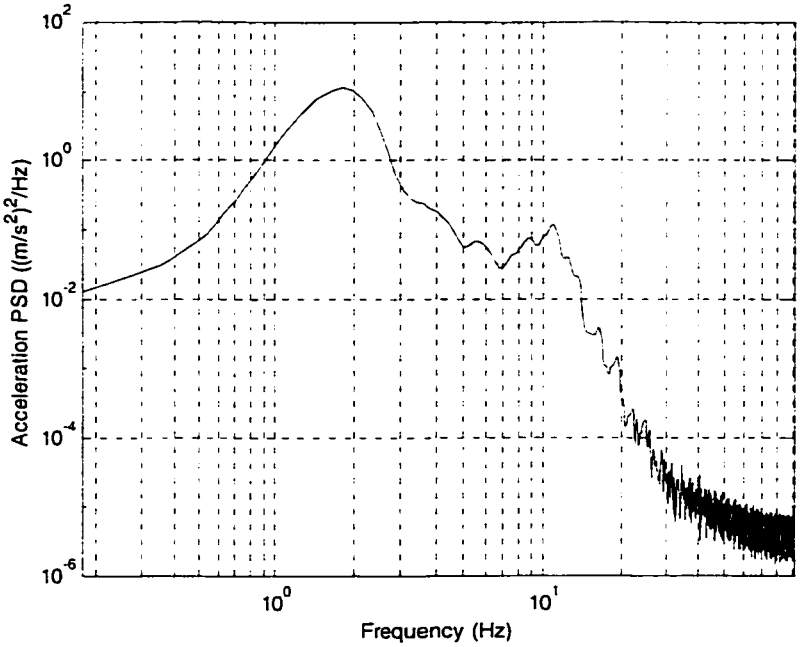

Figure 5.2 Analytical Plot of Frequency vs PSD of Vertical Acceleration at the Trailer Deck Surface for the Quarter Vehicle Model on a Rough Road at a Speed of 50 km/h

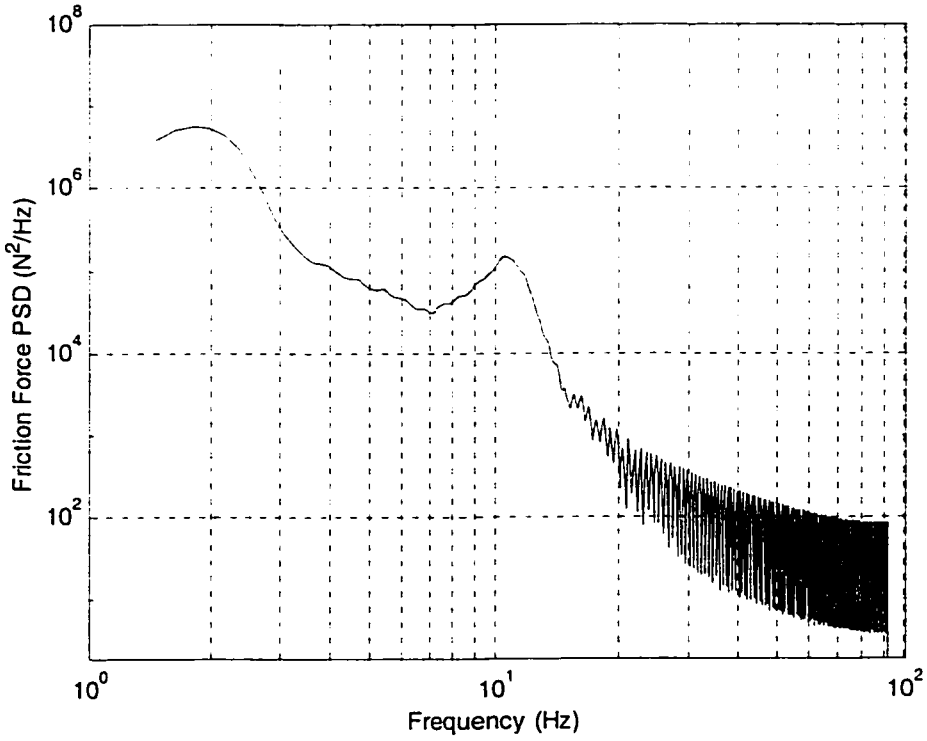

Figure 5.3 Analytical Plot of Frequency vs PSD of Friction Force between the Load and Trailer Deck Surface for the Quarter Vehicle Model on a Rough Road at a Speed of 50 km/h

5.4 Braking Performance of the DFC Model under Random Road Excitation

In Chapter 4, the study of the braking performance was carried out using the quarter-vehicle DFC model under the sinusoidal road profile. The conclusion was drawn from the simulation. Similar simulation will be performed in this section using a random road excitation. Usually, the random vibration analysis is mostly carried out in frequency domain, while it has little meaning in the time domain. The random function is such that its instantaneous value cannot be predicted of a deterministic manner. In the view of road roughness, any time domain resulting from a specific road can only represent the specific characteristic of that road. However, the study of the braking performance of heavy trucks on specific roads can provide useful foundation data for the traffic standard on that type of road, such as speed limitation, deceleration limitation, etc.

The selected road profile is same as in the previous section: "Cote-des-Neiges" Road. The quarter-vehicle model is used for simulations. Assuming that the vehicle travels on this road with a uniform speed of 50 Km/h first, then perform a constant decelerationwheel-lock braking with different deceleration rate ranging from 0.1g to 0.5g.

Figure 5.4 illustrate the time history of the road profile input with 0.1g-deceleration rate braking. The braking time is about 14 seconds. The simulated results show that the cargo has no sliding on the deck, because the maximum inertia force would not exceed the limit of the developed friction force. 0.2g-deceleration braking yields the same result. When the deceleration exceeds 0.3g, the calculation yields different results.

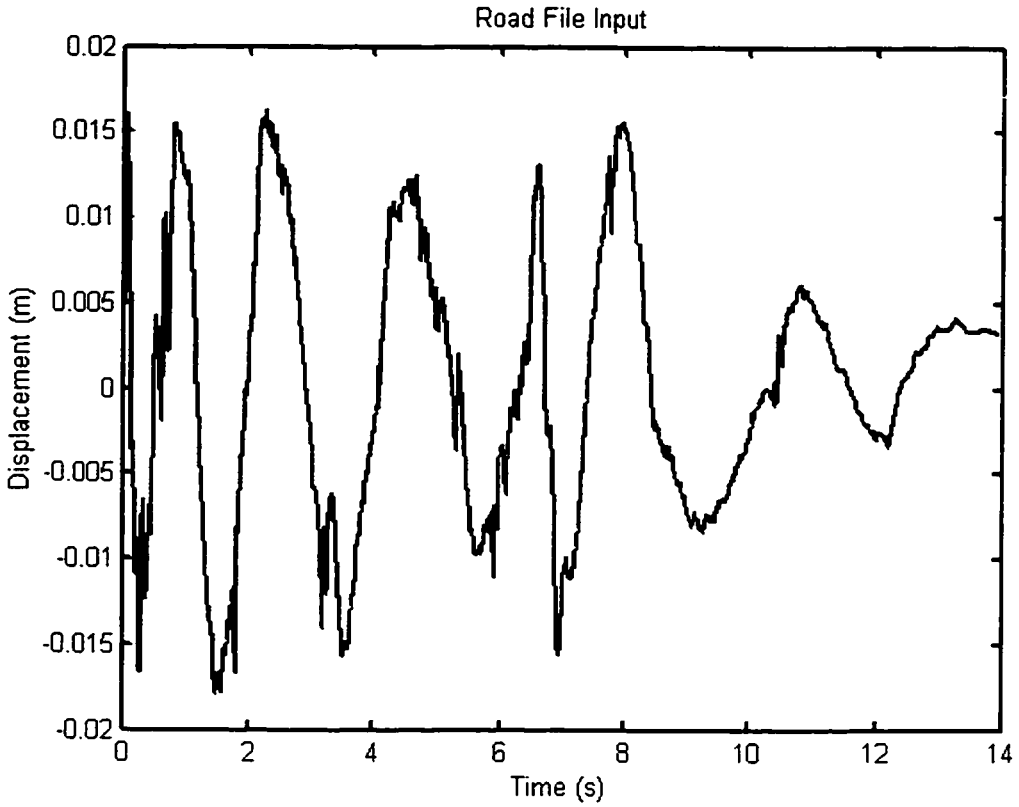

Figure 5.4 Time History of Road Profile under 0.1g-Deceleration Braking Maneuver

Figure 5.5 illustrates the time history of the DFC in the case of 0.3g-braking deceleration. Under 0.3g deceleration at the interface of the cargo and the deck, significant oscillation of the DFC occurs, and the minimum value of the friction coefficient had dropped to 50% of that corresponding to the static friction coefficient. Calculation revealed that in this case, the cargo would slide for a distance of 12cm, and the largest impact force that the cargo may apply to the anchor point or any other working load limit is 1980.4 N. All different simulation results data are listed in Table 5.1.

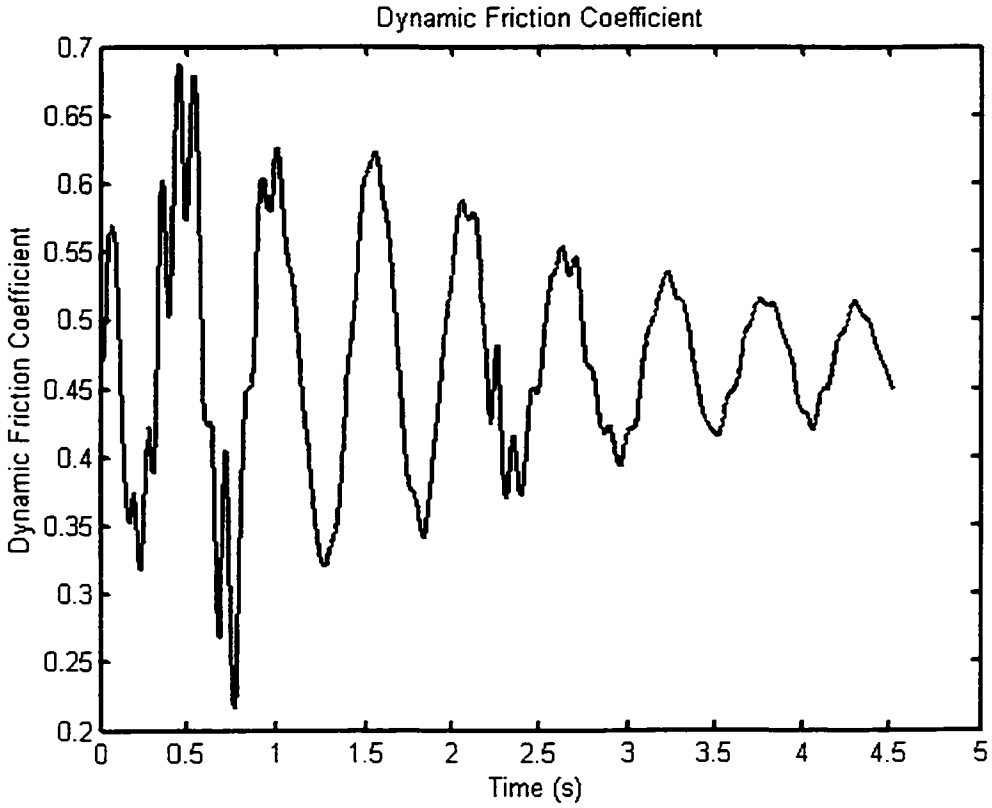

Figure 5.5 Time History of Dynamic Friction Coefficient under 0.3g-Deceleration Braking Maneuver

Figure 5.6 illustrates the comparison of dynamic friction force and braking force under 0.4g-deceleration braking maneuver. From the figure, there are instants for which the instantaneous friction forces are less than the braking forces. The sum of these durations in this case is about 26% of the whole braking process. The cargo would slide over a distance of 87.8cm and the largest impact force is 4056.6 N. This kind of value already implies the dangerous to the cargo and the vehicle itself.

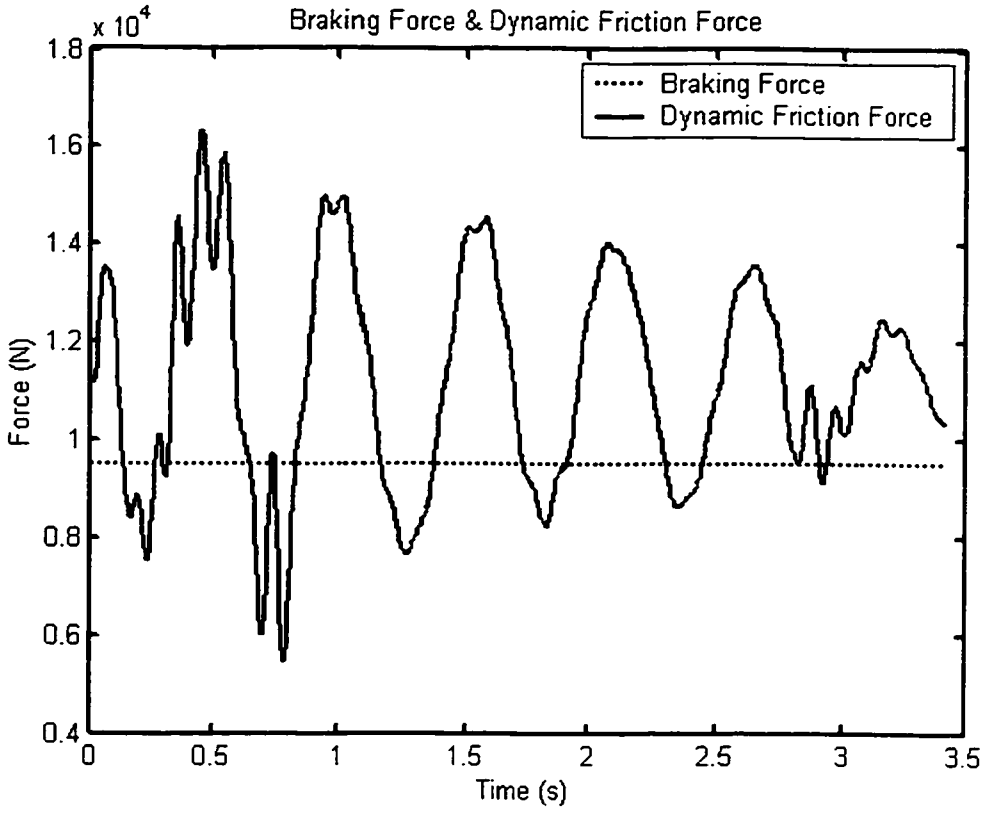

Figure 5.6 Comparison of the Braking Force and Dynamic Friction Force under 0.4g-Deceleration Braking Maneuver

As mentioned in the braking performance analysis, the friction force in Figure 5.6 does not represent the real friction force, but the possible trend. All the parts in the figure that friction showed larger than braking force is not true in practical situation, the real friction force value in these period are equal to the braking force. Figure 5.7 illustrates the real resultant force in the case of 0.5g-deceleration braking maneuver. In this case, the duration that the friction force is less than braking force reaches 55.2% of the whole braking process, and the sliding distance of the cargo reaches 232cm, while the maximum impact force that the cargo apply to the workload limit is 5914.5 N. If no other security apparatus is applied to the cargo, the load loss is quite certain under the circumstances.

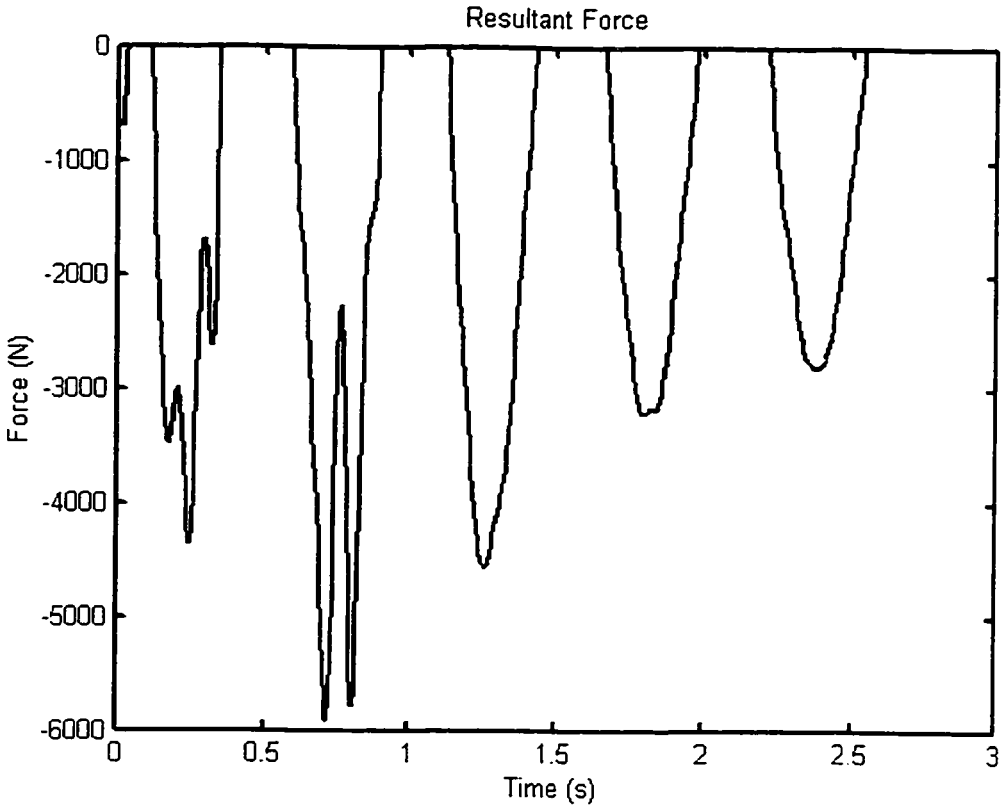

Figure 5.7 Time History of Resultant Force Applied to the Cargo under 0.5g-Deceleration Braking Maneuver

Table 5.1 Simulated Braking Results under Different Deceleration

Deceleration Rate	Sliding Distance (cm)	Maximum Impact Force (N)
0.1g	0	0
0.2g	0	0
0.3g	12	1980.4
0.4g	87.8	4056.6
0.5g	232	5914.5

5.5 Summary

Attempts are made to study the response of the quarter-vehicle DFC model under random road excitation and the braking performance on a specific road condition. Acceleration and PSD of the friction force response validate the model as well as the assumptions proposed in previous chapter. In the study of the braking performance under the road condition of "Cote-des-Neiges", simulation result indicated that the braking maneuver at deceleration rates larger than 0.3g would yield the sliding of the cargo sliding, and braking with 0.5g deceleration would yield to the load loss from the vehicle.

CHAPTER 6

CONCLUSION AND RECOMMENDATION FOR FUTURE WORK

6.1 General

Security of loads on vehicles is a matter of public safety. Load securement system is a complex system, which includes many factors. Although there are secured tiredown means and method that are commonly used to provide security to the load in trucks, there may be tendency to rely on the friction to provide part of the security. Friction itself is a highly complex phenomenon and is dependent on numerous factors. In vehicle application further complexity is introduced due to vibration environment with wide excitation amplitude and frequencies.

In this study, an attempt is made to model the dynamic friction in vibration environment for heavy vehicle load security, based on many experiments conducted at CONCAVE research center. Since the friction force is not an object that can be measured directly, most tests and measurement are created based on the quantity of the balanced force. The model proposed in this dissertation is also based on such measuring process. Furthermore, another essential concept in this dissertation is the correlation between the horizontal acceleration and vertical acceleration, and the link between the two issues is the normal load.

The model can be used as a tool for investigation on the friction characteristics between the load and trailer deck of the vehicle under the dynamic environment, and can be used to make prediction on the availability of friction force for load security, given a specific vehicle and certain road. Moreover, The results generated using a validated model can be used to generate data for the requirement of Government safety code for the standard on load securement.

6.2 Major Highlights

The study presented in this thesis is an investigation on the modeling of dynamic friction under vertical vibration environment. Starting from the simple load-platform friction model, the study explored the idea of modeling the dynamic friction with the vehicle model. The major highlights of the thesis are summarized as follows:

1) Proposed a load-platform friction model, studied the relationship between horizontal friction force and vertical vibration through the simulation of the sliding process. Results were validated with the measurements of the experiments conducted in CONCAVE research center, and it reveal that the dynamic friction force is a function of magnitude of vertical vibration.

2) Proposed friction model was further developed with different vehicle model to study the dynamic friction response under different road profile input. Sinusoidal excitation analysis shows that the dynamic friction coefficient of the vehicle is also a function of the vibration

frequency, and this is connected to the characteristics of the vehicle vibration system.

3) Proposed model also was simulated with random vibration. Results verified the conclusion drawn in sinusoidal excitation analysis.

4) Based on the responses of dynamic friction Coefficients to the road profile input, a braking performance study was carried out through simulating the braking process. Results indicated that braking process froma given velocity causes a sweep in excitation frequency, which in turn leads to variation in DFC.

5) Braking performance was further studied to examine the influence of the vehicle parameters. It is found that the stiffness of the suspension and tire have more influence on the dynamic friction force than the damping does.

6.3 Major Conclusion

1). Although friction is a complex phenomenon, a simple model can predict the dynamic friction behaviour in vibration environment.

2). The model can reliably reproduce the influence of vibration amplitude and frequency with limitations on surface finish, and flexibility of platform.

3). The vertical acceleration experienced by the load on truck deck is maximum when excitation are at the sprungmass natural frequency and is also high at unsprung mass natural frequency.

4). The variation in DFC in vibration environment is maximum at the sprung mass natural frequency and is linked to the previous conclusion.

5). When braking is applied from a constant velocity on rough road, the excitation frequency decreases to zero at the stop. The DFC variation is found to increase as the resonance frequency approaches.

6). DFC could be low enough at certain deceleration leads to introduce dangerous load shift. At 0.5g deceleration on a road with amplitude 0.01m leads to over 1m shift of the load.

7). An increase in suspension stiffness leads to increased proneness to load shift in a significant manner. An increase in tire stiffness show same trend with the significance.

8). Damping in both suspension and tire has negligible effect.

9). The trend under random excitation is same as that under sinusoidal excitation.

6.4 Recommendation for Further Study

In view of the DFC model potential in load security study, a list of future work recommended are as following:

1. Further laboratory experiments regarding to DFC and flexible platform could be conducted to obtain more through validation for the proposed analytical model.
2. More comprehensive vehicle model, including roll, yaw and pitch, could be combined together with DFC model, to have a more reliable model.

3. Other vehicle maneuver, such as turning, changing lane, obstacle avoidance, or above maneuver combination, applied to the simulation of DFC model, could extend the usefulness of the model.
4. DFC model can be developed with tiredown assembly to study the dynamic friction between the load and deck under secured condition
5. DFC model between the load and different layer of cargo should be incorporated for the study of load security.
6. DFC model response to ABS system should be evaluated to study the impact of intermittent brake forces on the potential load shift.

REFERENCES

[1]. Road Safety and Motor Vehicle Regulation Directorate, "Heavy Truck Collisions 1994-1998", December 2001

[2]. David John Matthew Sampson, "Active Roll Control of Articulated Heavy Vehicles", pp1-2

[3]. L. J. J. Kusters. Increasing roll-over safety of commercial vehicles by appli-cation of electronic systems. In J. P. Pauwelussen and H. B. Pacejka, editors, *Smart Vehicles*, pp 362–377. Swets and Zeitlinger, Lisse, The Netherlands,1995.

[4]. S.Rakheja, P.Sauvé and D.Juras "Experimental Evaluation of Friction Coefficients of Typical Loads and Trailer Decks under Vertical Vibration"

[5]. J.R.Billing "Need fro Evaluation of Friction between a Load and a Truck Deck Subject to Vibration"

[6]. Gillespie T.D., "Engineering Analysis of Cargo Restraint on Commercial Highway Trucks", *University of Michigan Transportation Research Institute, Report UMTRI-87-28*, August 1987

[7]. Andrew Gemant, "Frictional Phenomena", pp3-8

[8]. I V Kragelsky, M N Dobychin and V S Kombalov, " Friction and Wear Calculation Methods", pp1-7

[9]. I.V. Kragelsky, "Friction of unlubricated surface". *In All-Union Conference on Friction and Wear in Machines*, Vol.1 pp543-561

[10]. B. Armstrong-Helouvry. "Control of Machines with Friction", Kluwer Academic Publishers, Bonston, Ma., 1991

[11]. B. Armstrong-Helouvry, P. Dupont, and C.Canudas de Wit. "A Survey of Models, Analysis Tools and Compensation Methods for the Control of Machines with Friction" *Automation*, Vol.30(7): pp1083-1138, 1994

[12]. H.Olsson, K.J.Aström, C.Canudas de Wit, M.Gäfvert, P.Lischinsky"Friction Models and Friction Compensation"

[13]. F. P. Bowden and D.Tabor, "The Friction and Lubrication of Solids", Oxford University Press, Oxford, 1950

[14]. O.Reynolds, "On the Theory of Lubrication and its Application to Mr. Beauchamp Tower's Experiments, including an Experimental Determination of the Viscosity of Olive Oil", *Phil Trans. Royal Soc.*, 177, pp157-234, 1886

[15]. SKF. General Catalogue, 1970

[16]. A.J.Morin, "New Friction Experiments Carried Out at Metz in 1831-1833", In *Proceedings of the French Royal Academy of Sciences*, Volume 4, pp1-128, 1833

[17]. R.Stribeck. " The Key Qualities of Sliding and Roller Bearings", *Zeitschrift des Vereines Seutscher Ingenieure*, 46(38,39): pp 1342-48, 1432-37, 1902

[18]. P.Dahl, "A Solid Friction Model", Technical Report Tor-0158(3107-18)-1, The Aerospace Corporation, El Segundo, Ca,1968

[19]. D.A.Haessig and B. Friedland. "On the modeling and simulation of friction" *J Dyn Syst Meas Control Trans ASME*, 113(3), pp354-362, September 1991

[20]. Andreas A.Polycarpou, Andres Soom, "Boundary and Mixed Friction in the Presence of Dynamic Normal Loads: Part I ---System Model", *Journal of Tribology*, Vol. 117, pp255-260, April 1995

[21]. Andreas A.Polycarpou, Andres Soom, "Boundary and Mixed Friction in the Presence of Dynamic Normal Loads: Part II ---Friction Transients", *Journal of Tribology*, Vol. 117, pp261-266, April 1995

[22]. D.M.Tolstoi, " Significance of the Normal Degree of Freedom and Natural Normal Vinrations in Contact Friction", *Wear* Vol. 10, pp199-213, 1967

[23]. D.Godfrey, "Vibration Reduces Metal to Metal Contact and Causes an Apparent Reduction in Friction", *ASLE Transaction* Vol. 10, pp183-192, 1967

[24]. T.Sakamoto, "Normal Displacement and Dynamic Friction Characteristics in a Stick-Slip Process", *Tribology International* Vol. 20, pp25-31, 1987

[25]. Tohru Sakamoto, Masayoshi Abo and Satoshi Kakunai, "Friction Reduction in a Stick Slip Process under Vibratory Load: Friction Change with Low Frequency Load", *Japanese Journal of Tribology*, Vol. 36, pp1395-1407, 1990

[26]. Tohru Sakamoto, Masayoshi Abo and Satoshi Kakunai, "Friction Reduction in a Stick Slip Process under Vibratory Load", *Japanese Journal of Tribology*, Vol. 36, No.1, pp71-82, 1991

[27]. P.R.Nayak, "Contact Vibration", *Journal of Sound and Vibration* Vol. 22, pp297-322, 1972

[28]. D.P. Hess and A.Soom, "Normal Vibrations and Friction under Harmonic Loads: Part I ---Hertzian Contacts", *ASME, Journal of Tribology* Vol.113, pp80-86, 1991

[29]. D.P. Hess and A.Soom, "Normal Vibrations and Friction under Harmonic Loads: Part II ---Rough Planar Contacts", *ASME, Journal of Tribology* Vol.113, pp87-92, 1991

[30]. D.P. Hess, A.Soom and C.H.Kim, "Normal Vibrations and Friction at a Hertzian Contact under Random Excitation: Theory and Experiments", *Journal of Sound and Vibration* Vol.153, pp491-508, 1992

[31]. J.R.Billing, W.R.J.Mercer, W.Cann, "A Proposal for Research to provide Technical Basis for a Revised National Standard on Load Security for Heavy Trucks", pp7-13

[32]. J.R. Billing and C. P. Lam, "Friction Between Typical Beds and Loads, CCMTA Load Security Research Project, Section 10.2", *Ontario Ministry of Transportation Draft Report*, March 19, 1996

[33]. Leonard Segel, "Research in the Fundamentals of Automobile Control and Stability", *SAE Transactions*, Vol. 65, pp527-540, 1957

[34]. Okada, T. et al., "Evaluation of Vehicle Handling and Stability by Computer Simulation at the first Stage of Vehicle Planning", *SAE Transaction Paper* No. 730525, pp1683-1707, 1973

[35]. Ellis J.R., "Vehicle Dynamics", London Business Book Limited. 1969

[36]. J. Y. Wong, "Theory of Ground Vehicles, Second Edition", pp353-370

[37].Newton K., Steeds W. and Garrett T.K., " The Motor Vehicle", eleventh edition, Butterworth International Edition, 1989

[38]. Rakheja, S. and Ahmed, A. K. W., " An Algorithm for Simulation of nonlinear mechanical system with symmetric and Asymmetric Dissipative and Restoring Elements", Computational Methods in Engineering, Vol. 2, pp 915-920, 1992

[39]. Venu Muluka, "Optimal Suspension Damping and Axle Vibration Absorber for Reduction of Dynamic Tire Loads" pp23-27

[40].Cebon, D, "Vehicle Generated Road Damage; A Review:, *Vehicle system dynamics* Vol 18, 1989, pp107-150

[41]. Thomas D. Gillespie, " Fundamentals of Vehicle Dynamics", pp172-181

[42]. David Cebon, "Handbook of Vehicle-Road Interaction", pp84-107

[43]. Cole, D. J., Cebon, D., "Simulation and measurement of Dynamic Tire Forces" Presented at the second international symposium of heavy vehicle weights and dimensions Vol. 2, June 18-22, 1989

[44]. Joel W. Eastman, "Styling Vs. Safety", pp9-35

[45]. W. R. J. Mercer and J. R. Billing, "Bending Strength of Trailer Stakes", CCMTA Load Security Research Project Report No.13, 1998

[46]. FHWA Docket, "Development of a North American Standard for Protection Against Shifting or Falling Cargo: Advance Notice of Proposed Rulemaking, 61 FR 54142 sea, October 17, 1996"

[47]. J.A.Romero, S. Rakheja, A.K.W.Ahmed and A.Lozano, "Restrained Cargo Dynamics in Road Transportation: indirect tiedowns", *Heavy Vehicle System, A Series of the Int. J. of Vehicle Design*, Vol.9, No.2, pp.93-114

[48]. Bo N.J.Persson, "Sliding Friction – Physical Principles and Applications, Second Edition", pp5-pp21

[49]. S.Rakheja and S.Sankar "Response of a Sequential Damper to Shock Inputs", The Shock and Vibration Bulletin, Jan. 1987, Part 3, pp12-13

[50]. G.Amontons "De la Resistance Causée dans les Machines", 1699

[51]. Lin, Wen Kan et al., "Dynamic wheel/pavement force sensitivity to variations in heavy vehicle parameters, speed and road roughness", *Heavy Vehicle System, Int. J. of vehicle design*, 1(2), 1994, pp139-155

[52]. J.Y.Wong, "Theory of Ground Vehicle", Second Edition, pp353-359

[53].Anil Dhir, "Ride Dynamics of Heavy Vehicles Using Local Equivalent Linearization Technique", pp38-39

[54]Dodds, C.J., and Robson, J.D., "The Description of Road Surface Roughness", Journal of Sound and Vibration, 1973, Vol.31, No. 2, pp.175-184

[55].Robson, J.D., "Road Surface Description and Vehicle Response", *International Journal of Vehicle Design*, 1979, Vol.1, No.1. pp25-35

[56].Owais Mustafa Siddiqui, "Dynamic Analysis of a Modern Urban Bus for Assessment of Ride Quality and Dynamic Wheel Loads" , pp65-66

[57].Damien, T.M.et.al., "Pavement profiling various pavements: Ottawa/Smith Falls". John Emery Geotechnical Engineering Report, 1992

[58]. D.Karnopp. "Computer simulation of stick-slip friction in mechanical dynamic system". *Journal of Dynamic System, Measurement, and Control*. 107(1): 100-103,1985

[59]. Kragelskii, I.V. and Mikhin, N.M., "Hankbook of friction unites of machines"

[60]. Harris, C.M. and Crete, C.E., "Shock and vibration handbook"

[61]. Yufeng Li, Aric Kumaran Menon, " A Theoretical Analysis of Breakaway Friction Measurement" *Journal of Tribology*, Vol.118, Apr.1996

[62]. Ernest Rabinowicz "The Nature of the Static and Kinetic Coefficients of Friction" *Al of Applied Physics*, Vol. 22, No.11

[63]. W.R. Chang, I Etsion, D.B. Bogy, "Static Friction Coefficient Model for Metallic Rough Surfaces", *Jornal of Tribology*, January 1988

[64]. R.S.H. Richardson, H. Nolle, "Surface Friction under Time-Dependent Loads", *Wear, Vol 37*, 1976, pp87-101